

NOVEL APPROACHES TO TARGETED ANTIMALARIAL DEVELOPMENT

by

BRIANA FLAHERTY

(Under the Direction of David S. Peterson and Julie M. Moore)

ABSTRACT

Malaria is an ancient disease that has likely plagued mankind for our entire existence. Today, malaria continues to be a leading cause of morbidity and mortality in the developing world, leading to nearly 200 million cases and greater than half a million deaths annually. Although five parasite species are known to infect humans, *Plasmodium falciparum* is the most pathogenic and is the leading cause of malaria-attributable mortality worldwide. Pathogenesis of *P. falciparum* is mediated by cytoadherence of infected red blood cells (iRBC) to the endothelium in the host microvasculature or to the fetal-derived syncytiotrophoblast in the placenta. Although parasite binding and sequestration has long been recognized as a key mediator of pathogenesis in severe malaria, limited tools for *in vitro* analysis of cytoadherent iRBC have considerably hindered our ability to better understand this important parasite mechanism. Current malaria control measures rely heavily on extensive vector control, effective diagnostic testing, and efficacious antimalarial drugs. However, rising parasite resistance to first-line antimalarials places existing control measures in serious jeopardy. All existing antimalarials are small molecule inhibitors and are, therefore, highly vulnerable to the development of drug resistance. Future malaria control efforts will rely on the development of new antimalarials that target essential *Plasmodium* processes and utilize novel mechanisms of action that are uniquely

resilient to parasite mechanisms of drug resistance. In this dissertation, we explore new approaches to targeted antimalarial development that seek to both improve the tools available for *in vitro* malaria research and provide groundwork for future antimalarial peptide therapeutics. We begin by examining a panel of existing antimalarial and antimicrobial drugs with the overarching goal of identifying a cytostatic agent that will arrest late-stage, adherent iRBC for *in vitro* adhesion studies. We then proceed into the rapidly growing field of stapled peptide therapeutics as we explore the permeability and activity of these novel targeted antimalarial agents in *P. falciparum*-iRBC. The results herein provide exciting support for the use of targeted antimalarial therapies both in the control of this widespread global disease and in the understanding of this ancient biological organism.

INDEX WORDS: *Plasmodium falciparum*; malaria; placental malaria; antimalarial; cytoadherence; PfEMP1; CSA; VAR2CSA; peptide therapeutics; stapled peptides; protein kinase A; STAD-2; calcium dependent protein kinase-1; JDD

NOVEL APPROACHES TO TARGETED ANTIMALARIAL DEVELOPMENT

by

BRIANA FLAHERTY

B.S., Boise State University, 2008

A Dissertation Submitted to the Graduate Faculty of The University of Georgia in Partial
Fulfillment of the Requirements for the Degree

DOCTOR OF PHILOSOPHY

ATHENS, GEORGIA

2015

© 2015

Briana Flaherty

All Rights Reserved

NOVEL DRUG TREATMENTS AND NEW TECHNOLOGIES IN PLACENTAL MALARIA

by

BRIANA FLAHERTY

Major Professors: David S. Peterson
Julie M. Moore

Committee: Donald Harn
Robert Jeffrey Hogan
Eileen J. Kennedy

Electronic Version Approved:

Suzanne Barbour
Dean of the Graduate School
The University of Georgia
December 2015

DEDICATION

To my family: Mom, Dad, Shaun, Aletia, Grandma and Papa, aunts and uncles, and all of my many cousins.

Thank you for always being my closest friends and my strongest supporters throughout every stage of my life.

I love you.

ACKNOWLEDGEMENTS

There are so many people that I want to thank for loving and supporting me throughout this journey. First, to my mentors, David Peterson and Julie Moore, and to the rest of my committee. Thank you for challenging and shaping me, and thank you so much for supporting my interests and my unconventional PhD journey as it took me out of the lab and into the classroom or across the globe. Thank you to Dan Colley for sending me to Kenya, for always inspiring me, and for providing guidance as I navigate my winding career path. I am so grateful to have chosen mentors who are invested in both my personal and professional development, and I am fortunate to count you all as my mentors, my colleagues, and my friends.

Next, to my family, without whom I would be completely lost. To my mother and father: thank you for always loving me, supporting me, and believing in me... even when my pursuits carried me across the U.S. or out of the country. You always prioritized my education, pushed me to excel in all things, encouraged me to follow my heart, and loved me unconditionally. Your guidance and values shaped who I am today and who I aspire to be. I am so proud to be your daughter.

To Shaun, Aletia, and Sookie: Shaun, you have been my closest friend and my favorite person since day one. I can't believe how lucky I am to have you as a brother. We have that unique type of relationship that is only found in family – the type that weathers any distance and every stage of life. Thank you for always loving me, even when I probably didn't deserve it, and for always supporting me, even when the work I was doing seemed like gibberish to your ears. And thank you for choosing Aletia as your partner in crime and my sister-in-law; I could not

have asked for a more loving, caring, or understanding person to share you with. I love you both so much, and I look forward to building our futures together.

To Grandma Jo and Grandpa Jack: thank you for giving me so much love, so many prayers, such an amazing family, and a second home that will always be filled with your love and memories. We miss you both so much.

To Grandma and Papa: I don't quite have the words to convey how grateful I am to have you in my life. You two have been my role models, my mentors, my refuge, and the most genuine example of love in my life. Thank you for always supporting me and loving me wholeheartedly and unconditionally. I love you both so very much and am truly blessed to be your granddaughter.

To my undergraduate mentor and the person who encouraged me to go into research, Henry Charlier. Thank you for making my undergraduate research experience so positive and for supporting me throughout my PhD journey. You always challenged and inspired me, and I would not have gotten to where I am today without your mentorship and guidance. I am so lucky to have you as a mentor, a role model, and a friend.

Thank you to my friends and students in Honduras, without whom I would not have developed a passion to focus on global health inequalities. My time in Honduras was a life-changing experience, and I have no idea what direction my life would have taken without it. Thank you for letting me into your lives, allowing me to experience your beautiful culture, and inspiring me to seek a greater purpose with my career pursuits.

To Jake, George, and my Dani: Dani, you have been my best friend since birth. Over any distance and every awkward stage of our lives, our love and friendship has held strong. I am so grateful to have you and Jake in my life. Thank you for your continual love and support. I am so

proud of the people you have become, and I can't wait to see George flourish under your love and guidance.

To the rest of my amazing family: Kelsie and Katrina, I'm so proud of you both – your heart for people is truly inspiring. Thank you for always finding time for a cousins' night whenever I come home. You are two of my closest friends, and I love you both so much. Pat and Janet, thank you for always finding time to see me when I come home, for taking such a genuine interest in my passions and research, and for providing me with so much love and guidance. Chad and Agnes, I miss visiting you every spring break, but I continue to feel your love and support even from the opposite corner of the country. Bruce and Richelle, thank you for always believing in me and inspiring me. And to all the rest of my family that I am so very grateful for – aunts, uncles, and cousins – you are such a blessing to me.

Thank you to Athens for attracting such an incredible group of individuals. I've met so many amazing people during my time here, and I look forward to the life-long friendships that took root in this town. To Maria, you were my closest friend and my local family for my first four years in Athens. I don't know what I would have done without you. I am so grateful for our friendship that has proven to endure any distance, and I look forward to our future adventures in random corners of the globe. Tara, I can't believe how quickly our friendship has grown. From casual labmates to Statler and Waldorf to zouk partners, Dominican adventures, and poop conversations, yours has quickly become the closest friendship I've ever had. Thank you for bringing so much joy and laughter into my life and for sharing your family with me. And thank you to the Brackens for allowing me to be part of your family – I am so grateful for all of your love and support. Melody, thank you for being an amazing friend and roommate over the past few years. Your endless support and positivity have been a light through the dreariness that can

be graduate school. I love you and was so honored to share in your nuptials to an incredible man and the only guy in Athens who can compete with my Chewbacca call. I wish you and Steven the happiest of futures together. I love you guys!

And to all of my other incredible friends, both in Athens and afar. Jesse, thank you for always being a true friend, for helping me align my priorities in life, for many late-night gchat sessions, and for welcoming me into your Psynjir family. Teresa and Natalie, my Costa Rica dirty birds, favorite travel buddies, and life-long friends. I love you both and look forward to more exotic trips, sweaty salsa nights, hilarious inside jokes, and incomparable friendship. Tim and Lilach, I have so many unbelievable memories with you two, and I look forward to creating many more. Thank you for being such good friends and truly genuine people. Nicky and Shiraz, you are two of the most caring and goodhearted people I know. I am so grateful for your friendship and for all of the wonderful memories we have made together; and I can't wait to share in your wedding in December. Buddy, thank you for always listening to me, supporting me, and helping me find clarity during murky times. Leo, thank you for supporting and believing in me and for always being so excited about my work. I truly cherish the memories we made together. Finally, to all of the "biochem kids": DJ, Rob, Izzy, Kausar, Farah, Ryan, Brittany, Tony, and many more. Thank you all for making my time in Athens so much sweeter.

TABLE OF CONTENTS

	Page
ACKNOWLEDGEMENTS	v
LIST OF TABLES	xii
LIST OF FIGURES	xiii
CHAPTER	
1 INTRODUCTION	1
Specific aims	6
References	7
2 LITERATURE REVIEW	9
Malaria Overview	9
Early History of Malaria Research	10
Life Cycle of <i>Plasmodium</i>	11
Malaria – The Disease	15
Current Epidemiology and Progress toward Malaria Elimination.....	16
Placental Malaria	20
Antimalarial Drugs.....	25
Chemically Stabilized Peptides.....	33
Protein Kinases in <i>Plasmodium</i>	35
Protein Kinase A	37
<i>Plasmodium falciparum</i> Calcium-Dependent Protein Kinase-1	38

Summary	39
References	40
Figures.....	52
3 LATE-STAGE ARREST OF CYTOADHERENT <i>PLASMODIUM FALCIPARUM</i> FOR <i>IN VITRO</i> CHRONIC ADHESION STUDIES	59
Abstract	60
Introduction.....	61
Materials and Methods.....	64
Results.....	68
Discussion	72
Conclusions.....	74
References	75
Figures.....	79
Tables	86
4 THE STAPLED AKAP DISRUPTOR PEPTIDE STAD-2 DISPLAYS ANTIMALARIAL ACTIVITY THROUGH A PKA-INDEPENDENT MECHANISM	87
Abstract	88
Introduction.....	89
Materials and Methods.....	93
Results.....	100
Discussion	107
Conclusions.....	110

References	111
Figures	116
Tables	130
5 TARGETED INHIBITION OF <i>PLASMODIUM FALCIPARUM</i> CALCIUM DEPENDENT PROTEIN KINASE-1 WITH A STAPLED J DOMAIN DISRUPTOR PEPTIDE.....	135
Abstract	136
Introduction.....	137
Materials and Methods.....	143
Results	147
Discussion	153
Conclusions	155
References	156
Figures.....	160

LIST OF TABLES

	Page
Table 3.1: Antimalarial Agents.....	86
Table 4.1: Stapled Peptides.....	130
Table S4.1: Top Hits from Host Supernatant.....	131
Table S4.2: Top Hits from Parasite Supernatant	133

LIST OF FIGURES

	Page
Figure 2.1: <i>Plasmodium</i> life cycle	52
Figure 2.2: <i>Plasmodium falciparum</i> blood-stage life cycle	54
Figure 2.3: Synthesis of chemically stapled peptides	55
Figure 2.4: Chemically stabilized peptides block AKAP binding and localization	56
Figure 2.5: The PfCDPK1 J domain regulates enzyme activity	58
Figure 3.1: Complications with <i>in vitro</i> analyses using cytoadherent <i>P. falciparum</i> -iRBC.....	79
Figure 3.2: Methotrexate and vinblastine induce late-stage arrest of intracellular <i>P. falciparum</i>	80
Figure 3.3: Methotrexate, sodium azide, vinblastine, and cycloheximide are promising cytostatic agents	81
Figure 3.4: Sodium azide and methotrexate arrest parasite growth.....	82
Figure 3.5: High concentrations of sodium azide are required to universally arrest parasite growth	83
Figure S3.1: Late-stage iRBC degrade following treatment with high concentrations of sodium azide	84
Figure 4.1: STAD-2 synthesis and function	116
Figure 4.2: STAD-2 peptides are selectively permeable to <i>Plasmodium</i> -infected red blood cells	117
Figure 4.3: STAD-2 reduces viability of <i>P. falciparum in vitro</i>	118

Figure 4.4: STAD-2 rapidly localizes within the parasitophorous vacuole.....	120
Figure 4.5: STAD-2 does not associate with PKA	121
Figure 4.6: STAD-2 uptake is largely independent of the PSAC.....	122
Figure 4.7: STAD-2 is uniquely permeable to iRBC.....	123
Figure 4.8: STAD-2 activity is elevated at the erythrocyte membrane	124
Figure S4.1: STAD-2 is permeable to <i>P. falciparum</i> strains <i>in vitro</i>	125
Figure S4.2: STAD-2 permeability increases with time.....	126
Figure S4.3: STAD-2 reduces viability of <i>P. falciparum</i> strains <i>in vitro</i>	127
Figure S4.4: STAD-2 reduces parasitemia 6 hours post-treatment	128
Figure S4.5: H89 Dose Response Curve.....	129
Figure 5.1: JDD Synthesis and Function	160
Figure 5.2: JDD is selectively permeable to schizonts	161
Figure 5.3: JDD colocalizes with late, segmented schizonts	163
Figure 5.4: JDD is not hemolytic.....	164
Figure 5.5: JDD displays robust antimalarial activity	165

CHAPTER 1

INTRODUCTION

Malaria is a tremendous public health problem affecting 97 countries and 3.2 billion people worldwide [1]. Despite intensified efforts to control and eliminate the global malaria burden, ongoing transmission resulted in nearly 200 million cases and 600,000 deaths in 2013 alone. The overwhelming majority of this burden falls to young children and pregnant women, who are uniquely susceptible to severe malaria due to both a lack of protective immunity and parasite patterns of pathogenicity.

Pathogenesis of the most virulent malaria parasite, *Plasmodium falciparum*, is mediated by cytoadherence of infected red blood cells (iRBC) to the endothelium in the microvasculature or to the fetal-derived syncytiotrophoblast (ST) in the placenta. A wide variety of endothelial cell receptors functionally mediate this adhesion such as CD36, intercellular adhesion molecule-1 (ICAM-1), E-selectin, platelet/endothelial cell adhesion molecule-1 (PECAM-1), and chondroitin sulfate A (CSA). Varying patterns of cytoadherence are frequently shown to correlate with different manifestations of disease. For example, parasite binding to ICAM-1, E-selectin, and/or the endothelial protein C receptor (EPCR) is thought to correlate with the development of cerebral malaria [2,3] while binding to low-sulfated placental CSA mediates parasite sequestration in the placenta and the subsequent development of placental malaria (PM) [4,5].

P. falciparum-iRBC binding to host endothelial receptors is mediated by members of a family of parasite-encoded adhesins known as *P. falciparum* erythrocyte membrane protein-1

(*PfEMP1*). *PfEMP1* is encoded by the *var* genes, of which ~60 are present in each parasite genome. These proteins are increasingly expressed by the parasite on the erythrocyte surface beginning at ~16 hours post-invasion [6]. Monoallelic expression of *PfEMP1* proteins facilitates parasite endothelial sequestration, which prevents splenic clearance, as well as antigenic variation, which enables parasite evasion of the host immune response.

In pregnant women, parasite sequestration within the placenta can lead to significant pathology and a range of outcomes including placental insufficiency, intrauterine growth restriction, pre-term delivery, and infant low birth weight. Characterization of parasites isolated from malaria-infected pregnant women has identified a single member of the *PfEMP1* family, VAR2CSA, to be the principal mediator of parasite binding in the placenta [7]. VAR2CSA binds with high affinity to a unique, low-sulfated form of CSA that decorates the surface of the fetal ST that coat the villous trees within the placenta [8]. Since VAR2CSA expression is post-transcriptionally suppressed in hosts lacking a placenta [9,10], even women in malaria-endemic regions who have been repeatedly exposed to malaria since infancy are unable to acquire protective immunity to this unique *PfEMP1* variant. As a result, women in their first and second pregnancies are often those at highest risk of suffering the detrimental outcomes of PM.

Maternal immune responses to placental parasite sequestration are incompletely understood but are known to involve combined input from both the immunosuppressed pregnant host and the fetal-derived syncytiotrophoblast. Our lab has developed an effective *in vitro* model that explores the contribution of the fetal ST to PM immunopathology [11]. The primary goal of our studies, thus far, has been to assess how exposure to malaria induces functional changes in ST that may influence the overall immune response in the placenta. Preliminary studies with this model have found that primary ST upregulate mRNA expression of TGF β and IL-8 in response

to stimulation with cytoadherent iRBC [12]. These stimulated ST also secrete chemotactic chemokines, such as macrophage migration inhibitory factor (MIF) and macrophage inflammatory protein-1 alpha (MIP-1 α), and effectively recruit peripheral blood mononuclear cells. Studies with this model have, similarly, demonstrated that stimulation of primary ST with the parasite byproduct, hemozoin, induces secretion of inflammatory cytokines and chemokines as well as the recruitment of mononuclear cells [13]. These data, together, clearly demonstrate a role for an immunoactive ST in the response to PM.

Many questions remain to be answered regarding the contribution of this unique cell type to the maternofetal immunological crosstalk that is likely to be a key contributor to immunopathological outcomes in PM. Ongoing studies in our lab seek to utilize this *in vitro* model to fully characterize the interaction between malaria and ST. In doing so, we intend to explore the influence of individual components of malaria infection – iRBC binding, parasite GPI, and parasite hemozoin – on ST function. This is where my dissertation research began.

Initial work, discussed in Chapter 3, sought to identify a cytostatic agent to arrest late-stage, adherent iRBC and facilitate *in vitro* studies of chronic PM. The blood-stage life cycle of *P. falciparum* lasts ~44 – 48 hours, wherein the parasite expresses cytoadherent PfEMP1 during the latter half of this cycle. Throughout its intraerythrocytic lifetime, the intracellular parasite digests 60 – 80% of its host erythrocyte's hemoglobin and packages the toxic heme moieties into a crystal known as hemozoin [14]. Although these crystals are inert to the parasite, hemozoin has been shown to be both immune-activating and immunosuppressive to the human host [15]. At the conclusion of the 48-hour life cycle, the parasite bursts out of the infected cell, releasing hemozoin and other toxic by-products into the host circulation. *In vitro* efforts to assess the effect of iRBC binding to host endothelium are significantly hindered by the relatively short duration of

parasite cytoadherence. Long-term immunological studies, in particular, are largely infeasible as the completion of the parasite life cycle signals the release of toxic byproducts and the introduction of many confounding factors into the experiment. As a result, studies discussed in Chapter 3 sought to identify a cytostatic antimalarial agent that arrests late-stage, adherent iRBC while maintaining native binding and *PfEMP1* expression.

Studies examining the influence of various antimalarial agents on iRBC *in vitro* led us to a collaboration that is the topic of Chapters 4 and 5 of this dissertation. Dr. Eileen Kennedy of the University of Georgia College of Pharmacy specializes in designing carefully targeted chemically stabilized peptides that disrupt protein-protein interactions. Given that all existing antimalarials are small molecule inhibitors, we decided to explore the antimalarial potential of this novel class of peptide therapeutic.

Permeability of iRBC is carefully regulated and largely mediated by the *Plasmodium* surface anion channel (PSAC). The PSAC is expressed by the parasite on the erythrocyte membrane and mediates the transport of, primarily, low molecular weight solutes, like sugars and amino acids [16]. Given the relatively large size of stapled peptides, initial studies, discussed in Chapter 4, began by exploring iRBC permeability to an existing synthetic peptide that was the current focus of research in the Kennedy lab. The Stapled AKAP Disruptor-2, or STAD-2, had been designed to interact with the regulatory subunit of human PKA and occlude binding of the PKA regulator, A Kinase Anchoring Protein (AKAP). Previous studies with STAD-2 found the compound to be highly specific for and effective at inhibiting PKA-RII in a mammalian cell line [17]. Chapter 4 of this dissertation describes our efforts to explore the permeability and activity of this compound in *P. falciparum*-iRBC *in vitro*.

Promising results with STAD-2 encouraged us to design a new chemically stabilized peptide targeting a novel *Plasmodium* kinase found in plants and apicomplexan parasites but not in the human host. Calcium Dependent Protein Kinase-1 (CDPK1) is an essential *Plasmodium* protein that has been shown to play a key role in parasite motility, egress, and invasion [18,19]. The J Domain Disruptor peptide, JDD, was designed to mimic the autoinhibitory J domain of *Pf*CDPK1 and lock this essential kinase into an inactivate state. Chapter 5 describes the design and study of this carefully targeted antimalarial peptide therapeutic.

This dissertation has been formed around the Specific Aims listed below. Following these aims, Chapter 2 provides readers with a short review of the current literature in the malaria field. Therein, readers will find an overview of the early history and beginnings of malaria research, a description of the manifestations of severe disease, a discussion of current malaria epidemiology, and a foundation for the topics to be discussed in chapters 3-5 of this dissertation.

Specific Aims

Aim 1: Develop a method for arresting late-stage *P. falciparum*-infected red blood cells for use in *in vitro* chronic adhesion studies.

The temporal nature of parasite cytoadherence presents a considerable challenge to *in vitro* studies in malaria, since researchers wishing to examine the effects of parasite binding, particularly in an immunological context, are inhibited to a relatively short time frame. Aim 1 seeks to overcome this obstacle by identifying an antimalarial agent that will arrest late-stage *P. falciparum*-iRBC. We hypothesize that this agent will arrest intracellular parasites in a stage-specific manner while maintaining the erythrocyte membrane composition and PfEMP1 presentation intact. This work will establish a new tool for use in future *in vitro* studies that seek to understand, for example, how parasite cytoadherence influences immunopathology in malaria.

Aim 2: Explore the use of chemically stabilized peptides in *P. falciparum* *in vitro*.

Despite considerable research, no new class of antimalarial drug has been introduced into clinical practice since the introduction of the artemisinins in 1996. To date, all antimalarials fall under the class of small molecule inhibitors. Aim 2 seeks to explore the use of a novel peptide therapeutic – hydrocarbon stapled peptides – as a new class of antimalarial agent. These peptides target protein-protein interfaces and can be specifically designed to bind and disrupt critical inter- or intramolecular protein-protein interactions. Our research aims to establish chemically stabilized peptides as a novel class of antimalarial drugs and set the groundwork for future studies utilizing this unique class of inhibitors for malaria research and control.

References

1. WHO (2014) World Malaria Report 2014.
2. Turner GDH, Morrison H, Jones M, Davis TME, Looareesuwan S, et al. (1994) An Immunohistochemical Study of the Pathology of Fatal Malaria. Evidence for Widespread Endothelial Activation and a Potential Role for Intercellular Adhesion Molecule-1 in Cerebral Sequestration. *Am J Pathol* 145: 1057–1069.
3. Aird WC, Mosnier LO, Fairhurst RM (2014) *Plasmodium falciparum* picks (on) EPCR. *Blood* 123: 163–167. doi:10.1182/blood-2013-09-521005.
4. Doritchamou J, Sossou-tchatcha S, Cottrell G, Moussiliou A, Hounton Hounbeme C, et al. (2014) Dynamics in the cytoadherence phenotypes of *Plasmodium falciparum* infected erythrocytes isolated during pregnancy. *PLoS One* 9. doi:10.1371/journal.pone.0098577.
5. Fried M, Duffy PE (1996) Adherence of *Plasmodium falciparum* to chondroitin sulfate A in the human placenta. *Science* 272: 1502–1504. doi:10.1126/science.272.5267.1502.
6. McMillan PJ, Millet C, Batinovic S, Maiorca M, Hanssen E, et al. (2013) Spatial and temporal mapping of the PfEMP1 export pathway in *Plasmodium falciparum*. *Cell Microbiol* 15: 1401–1418. doi:10.1111/cmi.12125.
7. Magistrado P, Salanti A, Tuikue Ndam NG, Mwakalinga SB, Resende M, et al. (2008) VAR2CSA expression on the surface of placenta-derived *Plasmodium falciparum*-infected erythrocytes. *J Infect Dis* 198: 1071–1074. doi:10.1086/591502.
8. Srivastava A, Gangnard S, Round A, Dechavanne S, Juillerat A, et al. (2010) Full-length extracellular region of the var2CSA variant of PfEMP1 is required for specific, high-affinity binding to CSA. *Proc Natl Acad Sci U S A* 107: 4884–4889. doi:10.1073/pnas.1000951107.
9. Amulic B, Salanti A, Lavstsen T, Nielsen M a, Deitsch KW (2009) An upstream open reading frame controls translation of var2csa, a gene implicated in placental malaria. *PLoS Pathog* 5: e1000256. doi:10.1371/journal.ppat.1000256.
10. Mok BW, Ribacke U, Rasti N, Kironde F, Chen Q, et al. (2008) Default Pathway of var2csa switching and translational repression in *Plasmodium falciparum*. *PLoS One* 3: e1982. doi:10.1371/journal.pone.0001982.
11. Lucchi NW, Koopman R, Peterson DS, Moore JM (2006) *Plasmodium falciparum*-infected red blood cells selected for binding to cultured syncytiotrophoblast bind to chondroitin sulfate A and induce tyrosine phosphorylation in the syncytiotrophoblast. *Placenta* 27: 384–394. doi:10.1016/j.placenta.2005.04.009.

12. Lucchi NW, Peterson DS, Moore JM (2008) Immunologic activation of human syncytiotrophoblast by *Plasmodium falciparum*. *Malar J* 7: 42. doi:10.1186/1475-2875-7-42.
13. Lucchi NW, Sarr D, Owino SO, Mwalimu SM, Peterson DS, et al. (2011) Natural hemozoin stimulates syncytiotrophoblast to secrete chemokines and recruit peripheral blood mononuclear cells. *Placenta* 32: 579–585. doi:10.1016/j.placenta.2011.05.003.
14. Francis SE, Sullivan DJ, Goldberg DE (1997) Hemoglobin metabolism in the malaria parasite *Plasmodium falciparum*. *Annu Rev Microbiol* 51: 97–123. doi:10.1146/annurev.micro.51.1.97.
15. Boura M, Frita R, Góis A, Carvalho T, Hänscheid T (2013) The hemozoin conundrum: is malaria pigment immune-activating, inhibiting, or simply a bystander? *Trends Parasitol* 29: 469–476. doi:10.1016/j.pt.2013.07.005.
16. Desai S (2014) Why do malaria parasites increase host erythrocyte permeability? *Trends Parasitol* 30: 151–159. doi:10.1016/j.pt.2014.01.003.
17. Wang Y, Ho TG, Bertinetti D, Neddermann M, Franz E, et al. (2014) Isoform-Selective Disruption of AKAP-Localized PKA Using Hydrocarbon Stapled Peptides. *ACS Chem Biol* 9: 635–642. doi:10.1021/cb500329z.
18. Azevedo, Mauro F., Sanders, Paul R., Krejany, Efrosinia, Nie, Catherine Q., Fu, Ping, Bach, Leon A., Wunderlich, Gerhard, Crabb, Brendan S., Gilson PR (2013) Inhibition of *Plasmodium falciparum* CDPK1 by conditional expression of its J-domain demonstrates a key role in schizont development. *Biochem J*.
19. Bansal A, Singh S, More KR, Hans D, Nangalia K, et al. (2013) Characterization of *Plasmodium falciparum* calcium-dependent protein kinase 1 (PfCDPK1) and its role in microneme secretion during erythrocyte invasion. *J Biol Chem* 288: 1590–1602. doi:10.1074/jbc.M112.411934.

CHAPTER 2

LITERATURE REVIEW

Malaria Overview

Malaria is an enormous global public health problem affecting 97 countries and territories across the globe. Ongoing transmission places 3.2 billion individuals at risk of malaria infection and lead to an estimated 198 million cases and 584,000 deaths in 2013 alone [1]. Of these, the overwhelming majority of deaths (90%) occurred in Africa, and 78% of total deaths were in children under 5 years of age.

Malaria is a mosquito-borne infectious disease caused by protozoan parasites belonging to the genus *Plasmodium*. Disease is transmitted to human hosts via the bite of an infective female *Anopheles* mosquito carrying *Plasmodium* sporozoites [2]. There are five species of *Plasmodium* that are known to infect humans: *P. falciparum*, *P. vivax*, *P. ovale*, *P. malariae*, and *P. knowlesi*. While *P. falciparum* is the most pathogenic of the five species, *P. vivax* has a wider distribution owing to its ability to develop within the *Anopheles* vector at lower temperatures, which enables parasite persistence at higher altitudes and cooler climates [3]. *P. knowlesi* is the species of *Plasmodium* most recently shown to infect humans; while originally thought to solely infect primates, it is now recognized that *P. knowlesi* is a zoonosis prevalent in Southeast Asia involving macaque and leaf monkeys as reservoir hosts [4].

Over recent years, the science and public health communities have achieved significant advances in understanding the complex biology and epidemiology of this ancient parasite. Nevertheless, malaria elimination still seems a lofty, and even unattainable, goal to many in the

field given the tools currently available. Although, over the past 50 years, multiple highly effective antimalarial drugs have been placed on the market, high parasite recombination rates and suboptimal drug treatment conditions have, consistently, led to the development of drug-resistant parasites [5]. As a result, *Plasmodium* continues to evade elimination efforts and malaria remains an ongoing threat to millions across the globe.

Early History of Malaria Research

While likely references to malaria can be found in ancient Chinese, Indian, and Egyptian medical texts dating as far back as 2700 BC, the ancient Greek physician, Hippocrates, is recognized as being the first physician to describe, in detail, the clinical picture of malaria [4,6]. However, despite a thorough understanding of the clinical symptoms of malaria, it wasn't until thousands of years later, in the late 1800s, that the details behind the cause and parasitic nature of the disease began to emerge.

In 1880, a French army surgeon working in Algeria named Charles Laveran was the first to identify parasites in the blood of malaria infected humans. He carried out meticulous analyses of 200 human blood samples and convincingly demonstrated the presence of protozoan parasites in the blood of patients infected with malaria [4]. Over the following 20 years, researchers across the globe would succeed in elucidating nearly the entire *Plasmodium* life cycle. While Laveran's work was conducted using unstained blood and a dry microscope, the discovery of Dimitri Romanowsky's methylene blue stain in 1891 and the invention of the immersion microscope objective by Carl Zeiss Company in 1882 ushered in an era of great discovery in the forming malaria field. By the turn of the century, researchers had confirmed the protozoan nature of *Plasmodium*; worked out the asexual life cycle of the parasite, including details of the

pathogenesis and periodicity of benign tertian (*P. vivax*), malignant tertian (*P. falciparum*), and quartan (*P. malariae*) malarias; identified mosquitoes as the vector responsible for transmitting infection between humans; delineated the sexual life cycle of the parasite within the definitive host; identified successful control measures to block malaria transmission; and even correlated characteristics of the parasite life cycle with observed disease pathogenesis [4,6].

By the beginning of the 20th century, only one gap remained to be filled in our understanding of the *Plasmodium* life cycle. Following transmission of parasites from an infective mosquito to a susceptible human, there is a span of 10-14 days during which the parasite cannot be detected in the blood – the parasite’s residence during this time was a mystery. In 1937, it was shown that chickens infected with *P. gallinaceum* go through a developmental stage of infection wherein the parasites take up residence and multiply within the reticuloendothelial system [4]. In 1947, researchers in London, building upon previous work demonstrating exo-erythrocytic parasites in the parenchyma cells of the liver, inoculated rhesus macaques with a massive dose of *P. cynomolgi* and identified the exo-erythrocytic parasites in the liver seven days later. By 1954, such exoerythrocytic forms had been identified in the livers of human volunteers infected with *P. falciparum*, *P. vivax*, and *P. ovale*. Thus, some 70 years after Laveran’s initial discovery, the complete life cycle of *Plasmodium* had been resolved.

Life Cycle of *Plasmodium*

Plasmodium is an obligate intracellular parasite belonging to the phylum Apicomplexa [7]. Female mosquitoes of the genus *Anopheles* are the definitive hosts for *Plasmodium* parasites. *Plasmodium* can infect a plethora of intermediate hosts, ranging from birds and rodents to primates and humans, in a species-specific manner. All human *Plasmodium* parasites share the

same overall life cycle (Figure 2.1). Infection in the human host begins when an infective *Anopholes* mosquito bites a susceptible host, simultaneously passing *Plasmodium* sporozoites from the mosquito salivary glands into the host dermis [8,9]. Unlike many of its Apicomplexan relatives, *Plasmodium* sporozoites are inoculated a considerable distance from the cells in which they first begin to replicate; sporozoites must, therefore, transverse the dermis and enter the circulatory system to gain passage to their intended target cell and successfully infect their host [7].

Post-inoculation, *Plasmodium* sporozoites migrate to the liver where they invade and replicate asexually within host hepatocytes. Approximately 8 days post-invasion, hepatic schizonts burst, releasing 10,000 to 30,000 daughter merozoites into the host bloodstream [10]. Once in the bloodstream, merozoites invade circulating red blood cells wherein they, again, replicate asexually for a duration which varies according to parasite species. The asexual blood cycle lasts roughly 48 hours for *P. falciparum*, *P. vivax*, and *P. ovale*; 72 hours for *P. malariae*; and 24 hours for *P. knowlesi*.

The blood-stage cycle of *Plasmodium* can be easily seen by light microscopy in Giemsa-stained thin smears of infected red blood cells (Figure 2.2, *P. falciparum*). This cycle begins with the invasion of a circulating red blood cell by a merozoite. The merozoite attaches to the surface of the red blood cell via proteins expressed on the merozoite surface. These proteins, which include the vaccine candidate merozoite surface protein-1 (MSP-1), are cleaved during invasion but are critical to merozoite attachment to the circulating erythrocyte [11].

Once attached to the red blood cell via the apical end of the merozoite, a tight junction forms and a cluster of merozoite proteins discharge their contents into the red blood cell to begin the invasion process [11,12]. As the merozoite migrates across the erythrocyte membrane, an

invasion pit begins to form, eventually sealing at the posterior end of the parasite and forming a vacuole wherein the parasite will live for the duration of its residency within the red blood cell. Within the confines of the red blood cell, *Plasmodium* development begins with the ring stage, so named because of its appearance in Giemsa-stained blood smears (Figure 2.2). The ring-stage parasite begins to feed on hemoglobin from the surrounding red blood cell via a ring-like structure called the cytostome, packaging and storing the toxic heme component in one of a few small vacuoles that will later fuse to form a single digestive vacuole [11]. As the parasite grows, its ribosomes multiply, the endoplasmic reticulum enlarges, and the parasite takes on a more rounded shape called a trophozoite. The trophozoite continues to grow and expand until it reaches a point of nuclear division, or schizogony. Here, the intraerythrocytic parasite, now called a schizont, carries out a process of repeated, asexual nuclear divisions to form between 6 and 30 daughter cells [10]. Finally, the mature schizont, which is still contained within the parasitophorous vacuole, bursts out of both the erythrocyte and parasitophorous vacuole membranes, releasing free daughter merozoites into the bloodstream and re-initiating the blood-stage life cycle.

During the blood-stage cycle, some parasites differentiate into male and female gametocytes. Although it has been established that commitment to both gametocyte differentiation and sex is made before schizogony of the generation immediately preceding gametocyte formation, the exact triggers for differentiation are still poorly understood [13–15]. Gametocyte development in *Plasmodium falciparum* is considerably delayed relative to other human-infective *Plasmodium* species, reaching peak gametocytemia 7-10 days after the peak of asexual parasitemia [10,16]. Unlike the cyclical existence of asexual bloodforms, mature

gametocytes enter into cell-cycle arrest and will subsequently die within the human host if not taken up by a mosquito vector [13].

After being taken up with a mosquito bloodmeal, female gametocytes (macrogametocytes) immediately emerge from the erythrocyte while male gametocytes (microgametocytes) go through a process of rapid division and exflagellation before emerging to fuse with macrogametes [13]. The male and female gametes quickly fuse to form a diploid zygote that subsequently develops into a mature, motile ookinete. The ookinete first traverses the peritrophic matrix surrounding the ingested bloodmeal and then the midgut epithelium before taking up residence on the outside of the midgut epithelium where it develops into a vegetative oocyst [13,17]. Over a period of 10-14 days, the oocyst undergoes multiple rounds of nuclear division. At the completion of sporogony, the oocyst ruptures releasing hundreds of infective sporozoites into the haemocoel. These sporozoites migrate to the mosquito salivary glands where they will be injected into a new host during a subsequent bloodmeal to complete the *Plasmodium* life cycle.

While the general structure of the *Plasmodium* life cycle is consistent between the many species that infect humans, some noteworthy differences do exist. Although some such differences, like incubation period and blood-stage life cycle length, are relatively benign, others represent massive obstacles to malaria elimination efforts, particularly in the case *P. vivax*. For example, *P. vivax* and *P. ovale* development can be delayed in the liver when a proportion of the population falls dormant within hepatocytes. These hypnozoites can remain dormant for as little as two weeks up to several years before reawakening to cause relapse infections [10,18,19]. At present, the only drug effective against this latent form requires a radical 14-day regimen of

primaquine, a drug that dates back to the 1950's and is known to cause acute hemolysis in individuals with glucose-6-phosphate dehydrogenase (G6PD) deficiencies [19–22].

Also unique to the *P. vivax* life cycle is a preference for immature red blood cells, or reticulocytes [23]. This preference effectively keeps host parasitemias at lower levels than in *P. falciparum* infections and, perhaps, contributes to the perceived reduced disease severity and consequent underreporting of *P. vivax* infections. These and other factors that will be further discussed later in this review make *P. vivax* a massive obstacle to malaria elimination efforts worldwide.

Malaria – The Disease

Infection with malaria can manifest itself, broadly, in two ways – uncomplicated or severe. Especially in areas of moderate to high transmission where host immunity to infection is more stable, uncomplicated malaria (UM) is quite common. UM symptoms are initially non-specific, presenting as a flu-like syndrome. Over the course of infection, host blood parasitemia levels increase and the asexual blood-stage parasites become synchronous, leading to the cyclical fevers that are highly characteristic of malaria. In addition to fever, UM symptoms can include anorexia, dyspepsia, nausea, vomiting, and watery diarrhea, all of which can easily be misdiagnosed as gastrointestinal infection [24]. Given such non-specific symptoms, malaria infection should be conclusively diagnosed via peripheral blood smear, antigen-based rapid diagnostic tests (RDTs), or polymerase chain reaction (PCR). In the case of infection, blood smears should show evidence of ring-form parasites and, occasionally, gametocytes, while late trophozoites and schizonts are seldom observed. Presence of these late-stage parasites is often associated with heavy infection and poor prognosis [24].

Severe malaria more commonly affects non-immune individuals, as evidenced by its higher frequency in young children. Pregnant women represent a uniquely susceptible class of individuals due to the presence of a new organ, the placenta. Lack of immunity also places travelers and military personnel at an increased risk of severe malaria. Severe malaria can encompass a wide range of symptoms including, but not limited to, cerebral malaria, severe anemia, pulmonary edema, and acute renal failure [24–26]. Although parasitemia levels can directly correlate with severity of infection, in many cases downstream inflammatory processes seem to play a greater role in development of severe malaria [27].

Current Epidemiology and Progress toward Elimination

Over the past 15 years, remarkable progress has been made toward the reduction of the global malaria burden. Between 2000 and 2014, the estimated worldwide malaria mortality rates fell by 47% overall and by 53% in children under 5 years of age [1]. Such progress placed 55 of the 106 countries with ongoing malaria transmission on track for achieving the Roll Back Malaria (RBM) and World Health Assembly target of 75% reduction in malaria case incidence rates by 2015.

The successes in malaria elimination efforts can be attributed to a wide variety of influences including increased funding, improved health systems, better case management with more effective treatment regimens, and improved case reporting and surveillance [28]. Perhaps one of the most influential public health control measures has been vector control via insecticide-treated bednets (ITNs) and indoor residual spraying (IRS). As of 2014, a total of 97 countries with ongoing malaria transmission were distributing ITNs free of charge [1]. Use of ITNs is focused, primarily, on vulnerable individuals – children under 5 and pregnant women; however,

the practice of universal distribution is gaining traction, and 83 countries are currently distributing ITNs to all age groups.

A growing concern for vector-control measures is insecticide resistance in the mosquito population. To date, mosquito resistance to at least one commonly used insecticide has been reported in nearly two-thirds of malaria-endemic countries worldwide [29]. A recent mathematical model published by Blayneh and Mohammed-Awel demonstrated that, in a large mosquito population, even a small number of insecticide-resistant mosquitoes could represent a fatal threat to insecticide-based control efforts [30]. Thus, in an effort to manage this rising threat, WHO and RBM have created the Global Plan for Insecticide Resistance Management (GPIRM) in malaria vectors, a five-pillar strategy that considers country-specific entomological, ecological, epidemiological, and operational factors in its efforts to slow and counteract the development of insecticide resistance [3,29].

Another public health measure that has been critical to malaria control efforts is drug treatment, both in the form of chemoprevention and treatment post-infection. As previously discussed, pregnant women and children under 5 represent those at greatest risk of severe malaria. Given that there are an estimated 35 million pregnant women living and 26 million infants born each year in sub-Saharan Africa, significant efforts are ongoing to prevent infection in these highly vulnerable populations [3]. Over recent years, pregnant women and infants have received increased rates of intermittent preventative therapy (IPT), most often in the form of sulfadoxine-pyrimethamine (SP), while children 3-59 months have been targeted for seasonal malaria chemoprevention (SMC) in select areas since 2013 [1]. By the year 2014, 37 of the sub-Saharan African countries with moderate-to-high malaria transmission had adopted IPT for pregnant women (IPTp) as national policy; however, a large discrepancy between the number of

women attending antenatal care and the number receiving even one dose of IPTp persists, suggesting many opportunities for IPTp are missed in the antenatal clinics [1]. Research indicates that, despite a marked increase in IPTp administration between 2000 and 2007, these rates have slowed considerably, leaving this population unnecessarily vulnerable to disease.

To date, only Burkina Faso has implemented a national policy for IPT in infants (IPTi) despite the fact that WHO recommends that those areas with moderate-to-high malaria transmission and low levels of parasite drug resistance implement IPTi at defined intervals throughout infant vaccination schedules [3,1]. In addition, although Burkina Faso adopted IPTi as national policy following the WHO policy recommendation in 2011, the country is yet to begin implementation, further demonstrating the slow progress of IPTi in malaria endemic regions.

Of the chemopreventive policies in place to protect highly vulnerable populations, SMC is the most recently endorsed. Beginning in 2012, WHO began to recommend SMC for children 3-59 months of age, and, by 2013, six of the 16 countries deemed appropriate for SMC had adopted the practice as national policy [1]. SMC is only recommended in regions with highly seasonal transmission and involves maintaining therapeutic levels of antimalarial drug in the blood. SMC protocol recommends children are treated with amodiaquine plus sulfadoxine-pyrimethamine during periods of high malaria transmission. The greatest hindrance to SMC malaria control efforts, to date, has been lack of drug supply and proper training. However, the most recent World Malaria Report indicates that the financial resources needed to support SMC implementation in more countries have recently been mobilized [1].

Improvements in malaria treatment post-infection can be attributed, primarily, to increased availability of both RDTs and artemisinin-based drugs. As of 2012, malaria diagnostic

testing was being offered free of charge in the public sector in 85 countries around the world [3]. This increased availability of RDTs has led to an encouraging trend: in 2013, for the first time, the number of diagnostic tests distributed exceeded the number of artemisinin combination therapies (ACTs) administered in the public sector of the WHO Africa Region [1]. Unfortunately, neither RDTs nor microscopy perform well when detecting low level infections. Thus, as malaria prevalence continues to drop, future elimination efforts will require more sensitive diagnostic methods.

Since 2012, 79 countries and territories have maintained ACTs as first-line treatment for malaria [3]. Given mounting evidence of artemisinin resistance in Southeast Asia, efforts to remove artemisinin-based monotherapies from the market have been in effect since 2007 [31–33]. Nevertheless, a recent study published in the New England Journal of Medicine demonstrated well-established resistance throughout mainland Southeast Asia as well as possible evidence for pockets of resistance in Nigeria and the Democratic Republic of the Congo [33]. With the threat of widespread resistance looming, new drugs, or an effective vaccine, are needed to continue the promising trend toward malaria elimination.

In addition to the threat of drug resistance, a variety of other factors pose serious concerns to malaria elimination efforts. One such concern, especially in view of the current world climate, is residual transmission in hard-to-reach populations [28]. These populations usually include ethnic or political minority groups who are forced to live concealed and mobile lifestyles and, therefore, have limited access to medical care. A second concern is the low responsiveness of *P. vivax* to control interventions. While many of the elimination efforts discussed have made considerable progress with *P. falciparum* malaria, a reliable estimate of the burden of *P. vivax* infections is more difficult to achieve. Elimination of *P. vivax* malaria is

certain to prove problematic as *P. vivax* is more widely distributed, more ecologically resilient, and less susceptible to drug interventions than *P. falciparum* [28]. Finally, perhaps the most sizeable barrier to malaria elimination efforts is the prevalence of asymptomatic and submicroscopic infections. Notably, in regions of high transmission, a significant number of infected individuals remain asymptomatic. Given that individuals with asymptomatic and submicroscopic infections remain capable of transmitting disease, they serve as undetected but critical reservoirs of infection [2,34–37]. Hence, although considerable progress has been made in malaria control, these and other factors pose significant obstacles to malaria elimination goals.

In the Moore and Peterson labs, our research focuses largely on understanding and alleviating the burden of malaria during pregnancy. In this uniquely susceptible class of individuals, sequestration of malaria parasites in the placenta can lead to severe complications for both the mother and the developing fetus. Hereafter, I will discuss placental malaria (PM), briefly outline the approaches utilized by our lab to better understand the disease, and provide groundwork for the aims of this dissertation.

Placental Malaria

A 2010 study by Dellicour et al. estimated that over 85 million pregnancies occur in areas with *P. falciparum* transmission every year [38]. While it's generally accepted that repeated infection and persistent exposure to *Plasmodium* parasites in malaria-endemic regions provides hosts with protective immunity to infection, pregnant women, especially those in their first and second pregnancies, represent a uniquely susceptible group of individuals who lack protective immunity to the unique parasite variant that sequesters in the placenta [39]. A recent modeling analysis estimated that, in the absence of IPTp, nearly 45% of the 27.6 million live births in

Africa would be exposed to malaria infection resulting in approximately 900,000 low birth weight (LBW) deliveries annually [40]. Thus, although the overwhelming majority of malaria-attributable deaths occur in children under five, pregnant women and their fetuses bear a huge burden of malaria morbidity. The breakdown of age-associated immunity in pregnant women can be attributed primarily to the presence of the placenta, a unique organ with novel receptors for *P. falciparum* infected red blood cells (iRBC).

In conventional malaria, pathogenesis of *P. falciparum* is mediated by cytoadherence of iRBC to the endothelium in the microvasculature. This adherence is achieved via members of the *P. falciparum* erythrocyte membrane protein 1 (*PfEMP1*) family of variant surface antigens. *PfEMP1* is a clonally variant adhesion protein that is trafficked by the parasite to the host cell membrane and can be found on the surface of an infected erythrocyte by 24 hours post-invasion [41]. *Plasmodium* parasites encode ~60 different *PfEMP1* genes which are expressed in a monoallelic fashion [42,43]. *PfEMP1* proteins can mediate adhesion to a wide variety of endothelial receptors such as CD-36, E-selectin, PECAM-1, ICAM-1 and EPCR, the latter two of which have been shown to correlate with the development of cerebral malaria [44,45].

In the context of PM, expression of a single *PfEMP1* variant, VAR2CSA, mediates adhesion to a low-sulfated form of chondroitin sulfate A (CSA) that is found at high levels in the intervillous space (IVS) of the placenta [46]. This unique proteoglycan decorates the surface of the fetal syncytiotrophoblast (ST) that coat the villous trees and mediate the exchange of nutrients and waste between the mother and the developing fetus [47]. Binding of iRBC to this important cell type can lead to damage of the ST, disruption of the maternofetal exchange, and, ultimately, the severe complications that define PM [48].

Complications in PM are varied and can include maternal anemia, placental insufficiency, intra-uterine growth restriction (IUGR), pre-term delivery, and infant LBW. In highly endemic regions, up to 50% of LBW deliveries can be attributed to PM. In addition, fatality rates in infants born with IUGR are 10- to 20-fold higher than those of infants who undergo normal development. As a result, it's estimated that PM contributes to 363,000 infant deaths in Africa per year [49].

Since PM is defined by sequestration of iRBC in the placenta, the risk of PM in pregnant women is generally non-existent during the early weeks of gestation before maternal blood flows into the IVS [50]. However, recent analyses demonstrate that the greatest risk of infection may exist at the initial point when maternal blood first flows into the placenta, after which a woman remains at risk of developing PM throughout the remainder of her pregnancy [39,51]. The accumulation of iRBC within the placenta triggers the infiltration of maternal immune cells, especially monocytes, into the IVS [52]. These cells act to phagocytose iRBC and hemozoin, the parasite byproduct of hemoglobin degradation. Once activated, fetal ST and maternal immune cells promote a pro-inflammatory environment often characterized by the secretion of type 1 cytokines, like IFN- γ and TNF- α , and chemokines such as monocyte chemotactic protein 1 (MCP-1), macrophage inflammatory protein (MIP)-1 α , MIP-1 β , and IFN- γ inducible protein-10 (IP-10) [53,54]. Although the host response to PM has received enormous attention from researchers seeking to understand how host immune responses and coagulation factors influence the pathology of PM, a clear mechanism for disease pathology is far from elucidated.

Perhaps the best understood aspect of the immune response to PM is the development of VAR2CSA-specific antibodies with successive pregnancies. It has been well established for some time that, in highly malaria endemic regions, primigravid and secundigravid women are at

high risk for PM while the risk of disease in multigravid women is greatly reduced [55].

Research into this phenomenon has demonstrated that multigravid women in highly endemic regions possess VAR2CSA-specific antibodies. These anti-VAR2CSA antibodies effectively block binding of iRBC to placental CSA and are associated with increased birth weight and higher gestational age of newborns [56–58].

During PM, parasites encounter a highly complex immune environment influenced by both the immunosuppressed state of the pregnant host and the presence of the fetal ST. Evidence showing that clearance of infection is insufficient to resolve PM pathology clearly demonstrates the critical influence of the host response to infection and highlights the need to achieve greater understanding of the immunopathology of PM. Research in our lab has focused both on understanding the role of the ST in the response to PM and dissecting the genetic complexity of the variant surface antigen VAR2CSA. Experiments utilizing samples from *P. falciparum*-infected term women, *P. falciparum*-stimulated primary ST, and/or *P. falciparum*-stimulated syncytialized choriocarcinoma cells (BeWoST) have provided further evidence for the presence of a proinflammatory environment in the infected placenta by demonstrating upregulation of macrophage migration inhibitory factor (MIF) [59], CSA-specific tyrosine phosphorylation [60], ERK1/2 phosphorylation, release of TNF- α , secretion of PBMC chemotactic chemokines (CXCL8, CCL3, and CCL4) [61], and upregulation of markers of inflammation such as increased monocyte counts and elevated levels of TNF, IL-10, IL-6, sCD163, and sICAM-1 [62]. In addition, work exploring the influence of coagulation and fibrinolysis in PM found increased markers of activated coagulation and decreased markers of fibrinolysis in the plasma of *P. falciparum*-infected term women and proposed a role for dysregulated homeostasis in the development of PM [62]. Studies using our mouse model of PM have, likewise, demonstrated

the influence of a procoagulant response and a proinflammatory environment on poor pregnancy outcomes [62,63]. This work together with a large body of primary literature has led us to propose a model that delineates the complex immune response and poor outcomes of PM. In this model, *P. falciparum*-iRBC traffic into the IVS with the maternal blood, bind to the fetal ST, and induce the secretion of chemokines and cytokines that recruit and activate maternal lymphocytes and monocytes within the maternal blood space. Once present, maternal immune cells are activated and secrete additional proinflammatory cytokines and chemokines to enhance the response to infection and recruit more maternal immune cells. Monocytes phagocytose iRBC and parasite hemozoin but are, ultimately, ineffective at clearing infection. As the intracellular parasites mature, they burst out of their red blood cell homes and release a variety of proinflammatory stimulants including parasite GPI and hemozoin, which act to further stimulate the ongoing immune response. Over a short time, this exacerbated immune response results in overproduction of soluble proinflammatory signals, over-recruitment of maternal immune cells, deposition of fibrin on the ST, and damage to the ST that inhibits effective maternofetal exchange and ultimately causes PM-associated complications such as LBW.

Clearly, the interaction between *P. falciparum*, ST, and the maternal immune response is highly complex and involves a variety of parasite stimulants and host cell types. Our recent work in the Moore and Peterson labs has sought to dissect the role of the ST in the response to infection by examining functional changes in ST following stimulation with cytoadherent iRBC, hemozoin, and/or parasite GPI. However, the temporal nature of the parasite life cycle has presented a sizeable barrier to these efforts. Given that VAR2CSA is only expressed on the surface of iRBC during the latter half of the *P. falciparum* blood-stage life cycle, parasites are only cytoadherent during a limited time window. In addition, tightly synchronized parasites can

be difficult to achieve as most synchronization methods rely either on changes in density or altered permeability of late- versus early-stage parasites [64,65]. As a result, these techniques succeed only in separating late and early parasites as opposed to achieving a tightly synchronous parasite population. Given that mature iRBC lyse their erythrocyte host and release a variety of stimulants, including hemozoin and GPI, onto the ST, it is essential that we identify a method to arrest late-stage, cytoadherent iRBC *in vitro* in order to successfully carry out these analyses. In chapter 3, we aim to address this dilemma and facilitate our *in vitro* studies by identifying a cytostatic agent from amongst of panel of antimalarial drugs.

Antimalarial Drugs

Given how long malaria has been plaguing mankind, perhaps it's not surprising that the first antimalarial dates back nearly 400 years. The serendipitous discovery of quinine marked the first successful use of a chemical compound in treating an infectious disease [66]. Although more than one story has been attributed to its discovery, quinine, a component of the bark of the cinchona tree, was used by South American Indians to treat malaria as early as the 1600s. Dried bark was ground into a fine powder and mixed into liquid until 1820 when French chemists, Pierre Joseph Pelletier and Joseph Caventou, first extracted quinine from the cinchona bark [66]. In 1856, chemist William Henry Perkins attempted the first reported synthesis of quinine; however, his efforts were unsuccessful, and quinine would not be successfully synthesized until 1944 [67]. By that point, quinine was not the only drug on the market – effective synthetic antimalarials began arriving on the scene 20 years before. Since the 1920s, hundreds of researchers have studied thousands of chemical compounds for antimalarial activity. In chapter 2, we explore many of these compounds for cytostatic potential. Here, I briefly summarize those

compounds as well as others that have played key roles in malaria control efforts of past and present.

Despite its ancient origins, quinine continues to serve as a critical antimalarial today. Quinine belongs to a class of drugs known as arylaminoalcohols [68]. Although this class of drugs is thought to interfere with parasite heme digestion, the mechanism of action of quinine remains largely unsolved. Quinine's rapid schizonticidal activity against intraerythrocytic parasites makes it a common choice for uncomplicated malaria, and its ability to be prepared for intravenous applications makes it one of the only therapeutic option against severe malaria [66–68]. Unfortunately, although parasite susceptibility to quinine is high in Africa and South America, side effects are exceedingly common and often severe in nature [67,68]. As a result, use of quinine is usually reserved for severe cases.

Mefloquine, another arylaminoalcohol, was developed by the Walter Reed Army Institute from analogues of quinine synthesized during World War II [67]. Mefloquine demonstrates high activity against chloroquine-resistant strains of *Plasmodium* and has retained efficacy in most regions, excluding Asia where successful treatment with mefloquine monotherapy has dropped to 40% [68]. Like quinine, the mode of action of mefloquine is unknown, and drug side effects can be serious. Use of mefloquine as a prophylaxis is associated with neuropsychiatric effects including insomnia, depression, and panic attacks [67,68].

Historically, chloroquine has been the most successful single drug for malaria treatment and prophylaxis. Chloroquine is a 4-aminoquinoline that was safe, affordable, and highly effective for decades. Widespread resistance began to appear in the 1960s after chloroquine was used in population-based dosing regimens seeking to accomplish malaria eradication goals [69]. Today, more than 80% of *P. falciparum* field isolates are resistant to chloroquine [68]. Although

the exact details of its mechanism of action are still a matter of debate, it's generally accepted that, like other 4-aminoquinolines, chloroquine forms a complex with hemozoin from digested hemoglobin thereby preventing its polymerization into hemozoin crystals. Free hemozoin then interferes with parasite detoxification processes and causes fatal damage to parasite membranes [67,70].

Chloroquine resistance developed independently in four different regions of the world and subsequently spread over nearly all malaria-endemic regions [67]. The primary mechanism of chloroquine resistance has been shown to involve a mutation in the *P. falciparum* chloroquine resistance transporter (*PfCRT*) protein [67]. *PfCRT* is a transmembrane protein located on the digestive vacuole membrane. Mutations in this protein consistently correlate with reduced chloroquine accumulation in the parasite digestive vacuole and compromised drug efficacy. A recent study comparing experimental results with computational protein modeling argues that mutated *PfCRT* may act as an active protein carrier to pump chloroquine out of the digestive vacuole [70].

Despite widespread *P. falciparum* resistance, chloroquine is still an active player in the antimalarial community. Most strains of *P. vivax*, *P. malariae*, *P. ovale*, and *P. knowlesi* remain susceptible to chloroquine, and treatment with chloroquine, combined with primaquine, has been the standard regimen for the radical cure of *P. vivax* and *P. ovale* malaria since the 1950s [67,71]. In addition, some researchers have succeeded in overcoming chloroquine resistance by applying a variety of molecular modifications to chloroquine [67]. These experiments have resulted in a number of promising drug candidates that are currently in various stages of clinical development [67,72,73]. Finally, there is evidence suggesting that parasites may reacquire susceptibility to chloroquine in regions where drug pressure has been removed for a significant

period of time. A 2006 study in Malawi found that replacement of chloroquine with sulfadoxine-pyrimethamine for 12 years was sufficient to reestablish chloroquine susceptibility in the local parasite population [74].

Another class of drugs utilizing the quinolone base structure is the 8-aminoquinolines, the most well-known of which is primaquine. Primaquine is a peculiar choice as an antimalarial given that its activity against asexual blood-stage parasites is too low to be therapeutically relevant [67,71]. However, primaquine is the only drug currently in use that is active against liver and sexual blood stages of different *Plasmodium* spp.; as a result, primaquine is effective at preventing relapse infections with *P. vivax* and *P. ovale* and can also function as a transmission-blocking drug [19,67,68,71]. Primaquine is most commonly used in combination with other drugs, like chloroquine, to treat *P. vivax* and *P. ovale* malaria. Despite its gametocytocidal activity, primaquine is rarely an option against *P. falciparum* malaria. This is because primaquine can have serious side effects in individuals suffering from glucose-6-phosphate dehydrogenase (G6PD) deficiency, an X-linked disorder that is highly prevalent in many *P. falciparum*-endemic areas [19,67,75]. Primaquine treatment in individuals with certain forms of G6PD deficiency can lead to potentially life-threatening hemolysis. Given that, in many *P. falciparum*-endemic regions, testing for genetic deficiencies is not practical, primaquine is rarely considered a viable option.

In nearly all malaria endemic countries, artemisinin combination therapies (ACT) are now recommended as first-line treatment against uncomplicated *P. falciparum* malaria. The artemisinins are a fast-acting, highly potent class of drugs that demonstrates some degree of activity against all asexual blood stages of parasite development as well as moderate activity against sexual blood stages [67,76]. Parasites are most sensitive to artemisinin treatment during

the trophozoite/schizont stages and also demonstrate hypersensitivity to treatment as very early rings (2-4 hours post-invasion) [76]. Since the active byproduct of artemisinin, dihydroartemisinin, has an incredibly short half-life (<1 hr), artemisinins must be used in combination with a second, longer-lasting drug to reduce the risk of resistance [68]. Often, this second drug takes the form of an arylaminoalcohol such as mefloquine or lumefantrine [32]. Since pure artemisinin is poorly soluble in water and oil, ACTs utilize one of various semisynthetic derivatives of artemisin, artemether or artesunate [67].

The mechanism of action of artemisinin has been widely debated but is unanimously considered to require hemoglobin and, particularly, iron [77]. For some time it was thought that artemisinin activity was concentrated in the digestive vacuole wherein the artemisinin endoperoxide bridge was cleaved in the presence of Fe^{2+} resulting in highly active free radicals that, ultimately, led to parasite death [78]. However, other studies have demonstrated artemisinin binding to an ATP-dependent Ca^{2+} pump, *PfATP6*, located on the parasite endoplasmic reticulum [67,78]. A recent study utilized a computational approach to demonstrate that tight binding of an Fe-artemisinin complex results in strong allosteric inhibition of *PfATP6* [78]. Such a mechanism would satisfy binding to *PfATP6* as well as the need for hemoglobin uptake and a role for iron in artemisinin activity.

Another class of antimalarials is the antifolates. Tetrahydrofolate derivatives are essential cofactors for single carbon transfer reactions in biosynthetic processes such as synthesis of nucleic acids and sulfur-containing amino acids [67,79,80]. While humans rely on dietary intake of preformed dihydrofolic acid, *Plasmodium*, as well as other pathogenic microorganisms, are capable of *de novo* folate biosynthesis from simple precursors. As a result, drugs that target processing and biosynthesis of tetrahydrofolic acid were successfully employed against *P.*

falciparum until resistance was established. The antifolates include a variety of drugs that act by inhibiting one of two enzymes essential to folate processing: dihydropteroate synthase (DHPS) and dihydrofolate reductase (DHFR). These drugs include DHPS inhibitor sulfadoxine and DHFR inhibitors pyrimethamine, proguanil, WR99210, and methotrexate, some of which were designed to overcome *Plasmodium* resistance to previous antifolates [67,68,81,82]. Antifolate resistance has been extensively studied and has been shown to develop through consecutive accumulation of mutations in the *dhfr* gene that result in decreased inhibitor binding affinity [67]. Despite widespread resistance and limited efficacy, low-priced antifolates like sulfadoxine/pyrimethamine are still widely used in Africa in combination with other antimalarials [68].

Atovaquone is the only antimalarial currently in use that targets the *Plasmodium* electron transport chain (ETC). The role of electron transport in *Plasmodium* varies significantly from that found in higher eukaryotes. Although an active ETC still localizes to the mitochondrial membrane, *Plasmodium* asexual blood-stage parasites contain only a single mitochondrion whose activity is coupled solely to ubiquinone generation and not to ATP synthesis [83,84]. Nevertheless, mitochondrial electron transport is essential for parasite survival. Although generation of a proton electrochemical gradient may be important for transport of proteins and metabolites into and out of the mitochondrion, electron transport in *Plasmodium* appears to serve one primary function: regeneration of ubiquinone as an electron acceptor for the essential enzyme that drives pyrimidine biosynthesis, dihydroorotate dehydrogenase [67,84,85]. As *Plasmodium* is unable to salvage pyrimidines from the host erythrocyte, it must make them *de novo*, and the inability to do so is fatal to parasite development. Atovaquone acts to collapse mitochondrial membrane potential and inhibit pyrimidine biosynthesis by binding to and

inhibiting cytochrome bc₁ complex [67,85]. As a monotherapy, resistance to atovaquone develops quickly; however, atovaquone demonstrates strong synergism with proguanil, and the two are commonly prescribed together under the brand name Malarone [67].

In pursuit of my goal of arresting late-stage parasites, I also considered various antimalarial agents that are not currently used in clinical practice. One such set of compounds are microtubule inhibitors. Microtubules are filamentous fibers found in almost all eukaryotic cells that play critical roles in various cell processes including cell division, cell motility, structural integrity, and intracellular transport of vesicles and organelles [86,87]. Various microtubule inhibitors have been shown to have activity against malaria parasites both *in vitro* and *in vivo* [87–91]. Despite highly potent activity against asexual blood-stage parasites, some inhibitors, such as taxol and vinblastine, have limited clinical potential due to high toxicity to mammalian cells while another class of inhibitors, the dinitroanilines, is relatively non-toxic to human cells but demonstrate reduced activity against *Plasmodium* [88]. I chose to examine the effects of an inhibitor from each of the aforementioned categories, vinblastine and oryzalin.

Both vinblastine and oryzalin inhibit parasite schizogony by binding tubulin and inhibiting polymerization of microtubules during mitosis [87–89]. Vinblastine is a potent antimalarial, inhibiting parasite development at nanomolar concentrations [88]. It is also commonly used in cancer chemotherapy to inhibit replication of rapidly dividing cells. Despite its promising activity against *Plasmodium*, its equally potent activity against mammalian cells abolishes its usefulness as an antimalarial. Nonetheless, its potent inhibition of parasite schizogony makes vinblastine an ideal candidate for my *in vitro* studies.

Oryzalin belongs to a family of herbicides known as the dinitroanilines. Like vinblastine, oryzalin achieves antimalarial activity by binding to tubulin and inhibiting mitosis; however,

oryzalin is considerably less potent than vinblastine, arresting parasite development at micromolar concentrations [87]. Its low toxicity against mammalian cells has made it the recipient of considerable attention from the research community. Nevertheless, no dinitroaniline antimalarials have achieved clinical significance.

In addition to the antimalarial compounds discussed, I also consider two common antimicrobial reagents: sodium azide and cycloheximide. As a general biocide, sodium azide binds iron in porphyrin complexes to inhibit the activity of catalase, peroxidases, and cytochrome oxidase [92]. Under microaerophilic conditions, such as those found in *in vitro* culture of *Plasmodium*, catalase and peroxidase activities are generally negligible [93]. Hence, sodium azide activity against parasites *in vitro* is likely to simulate that of atovaquone by inhibiting the mitochondrial electron transport chain.

Cycloheximide, like sodium azide, is a common laboratory reagent and general antimicrobial. Cycloheximide blocks microbial growth by inhibiting protein synthesis [94]. Previous studies have demonstrated sensitivity of *P. falciparum* to treatment with cycloheximide [95–97]. Extensive research has been carried out to delineate the mechanism of cycloheximide inhibition in humans. These studies have shown that cycloheximide binds to eukaryotic elongation factor 2 (eEF2) on the 60S ribosome, thereby stalling translocation and inhibiting protein translation elongation [94].

Although the above is far from a comprehensive list of antimalarials, it provides some details on almost every class of existing antimalarial drug. However, despite the many types of drugs available, some degree of resistance has risen to every clinically relevant antimalarial manufactured thus far. Although measures have been taken to slow the development of resistance to artemisinin, studies continue to demonstrate the gradual spread of resistance to the

defining member of our current first-line treatment. As a result, there is a clear and growing need for new antimalarials to combat this resistance and secure ongoing malaria control efforts. In Specific Aim 2, we aim to address this need by exploring a new method for antimalarial treatment – chemically stabilized peptides.

Chemically Stabilized Peptides

Chemically stabilized, or “stapled”, peptides were first designed 10 years ago in response to limitations in target specificity offered by traditional therapeutic agents [98]. Historically, two structural classes of drugs exist: small molecule inhibitors and protein therapeutics (or biologicals). Small molecule inhibitors generally possess less than 100 atoms and achieve protein inhibition by binding within tight, hydrophobic binding pockets while protein therapeutics are large and bind relatively flat protein surfaces [99,100]. As a result, small molecule inhibitors can bind with high affinity and specificity to the ~10% of human proteins with surface-accessible hydrophobic pockets. Meanwhile, biologicals are limited, by their size, to the <10% of proteins secreted or accessible on the cell surface [99,100]. These restrictions mean that nearly 80% of protein targets are inaccessible by traditional chemotherapeutic techniques. Chemically stapled peptides were, therefore, proposed to help fill this gap by combining the broad surface-recognition properties of biologicals with the permeability and synthetic specificity of small molecule inhibitors.

Stapled peptides are polypeptide sequences that are locked into an α -helical conformation by a hydrocarbon linker. These peptides are generally designed to target protein-protein interfaces and disrupt protein localization and/or activity. α -helix stabilization via an all-hydrocarbon linker was first published by Verdine and colleagues in 2000 [101]. Peptide design

begins with solid phase synthesis of a polypeptide sequence possessing two α -methyl, α -alkenylglycine cross-linking amino acids. These non-natural residues can be spaced in one of three optimized configurations (Figure 2.3) and are induced to form hydrocarbon linkage via ruthenium-mediated olefin metathesis, or Grubb's catalysis [99]. Release of the stabilized helix from the solid resin yields the final stapled peptide. Additional modifications can be incorporated during solid phase synthesis and can include pegylation for increased solubility, biotinylation for immunoprecipitation studies, and FITC-conjugation for fluorescence-based analyses.

Recent structural analyses have shown alpha-helices to be the most common elements of protein secondary structure found at protein-protein interfaces [102]. Chemically stapled peptides seek to target these protein-protein interfaces by mimicking alpha-helix-based interactions. Although peptides are generally accepted to be poor therapeutics, the introduction of the hydrocarbon staple imparts a variety of highly desirable attributes to chemically stapled peptides. For example, stapled peptides can be designed to be extremely specific to their targets, are resistant to degradation by proteases, and are highly cell permeable [103].

Over recent years, stapled peptides have been employed, primarily, in cancer research and have had considerable success at binding and inhibiting targets that were previously considered "undruggable" [98,100,104]. Dr. Eileen Kennedy's lab has successfully designed chemically stabilized peptides to target the AKAP binding site of human PKA [105]. We set out to build upon this work and explore the potential of chemically stapled peptides as novel malaria therapeutics.

To date, all existing antimalarials are small molecule inhibitors. The high specificity and limited surface area of these inhibitors renders them inherently vulnerable to the development of resistance, as even single point mutations within the binding pocket of a target protein may be

sufficient to abrogate binding and eliminate the drug's activity. We propose that stapled peptides may offer a novel class of therapeutic that would boast reduced susceptibility to parasite mechanisms of drug resistance due to the relatively large surface area targeted by these peptides. Herein, we explore the permeability and activity of two kinase-specific stapled peptides in *P. falciparum* infected red blood cells *in vitro*.

Protein Kinases in *Plasmodium*

Regrettably, of 1,223 new drugs developed between 1975 and 1996, only four were antimalarials [106,107]. With mounting evidence for the spread of artemisinin resistance, there is a dire need for new antimalarials that target novel aspects of *Plasmodium* biology. In 2009, a high throughput phenotypic screening of nearly 2 million compounds from a GlaxoSmithKline chemical library identified 13,533 compounds that inhibit parasite growth by greater than 80% at 2 μ M concentration [108]. Of the compounds identified and validated in this study, the grand majority were protein kinase inhibitors.

Protein kinases represent one of the largest families of evolutionarily related proteins known [109]. Although kinases are a relatively understudied field of *Plasmodium* biology, they may represent a previously unexplored class of highly promising drug targets. In general, kinases are involved in all aspects of cellular life, and alterations in kinase structure and function can have strong phenotypic manifestations. For example, a wide variety of human developmental and metabolic disorders have been linked to kinase gene mutations, and multiple kinase inhibitors have been approved for the treatment of certain cancers [109,110]. As a result, the pharmaceutical industry and academic community have invested tremendous effort into understanding all aspects of kinases and their inhibitors, providing a large body of research on

which to build *Plasmodium* kinase studies [111]. In addition, since most existing kinase inhibitors act by binding to conserved ATP-binding sites, kinases are likely to demonstrate high cross-reactivity and, therefore, reduced susceptibility for developing resistance [111].

Various phosphoproteomic studies have demonstrated a clear role for kinases in *Plasmodium* cell signaling [112–114]. Bioinformatic analyses have shown there to be nearly 100 kinases in the *Plasmodium* kinome [111,115]. While some of these share homology with other eukaryotic protein kinases (ePK), many vary significantly, or are entirely absent, from the human host kinome [112,116,117]. One such family, the FIKKs, are unique to *Plasmodium* and are defined by a conserved Phe-Ile-Lys-Lys sequence at the N-terminal region of the kinase domain [111]. A recent study used a reverse genetics approach to show that two FIKK kinases phosphorylate membrane skeletal proteins of the infected erythrocyte in a stage-specific manner [118]. It is hypothesized that other members of the FIKK family, likewise, associate with the erythrocyte membrane and may play a crucial role in trafficking of parasite signaling pathway components [111].

Recent advances in genetic engineering of *Plasmodium* parasites have enabled researchers to identify kinases essential to various stages of the parasite life cycle. One such study took a reverse genetics approach to knock out all 65 ePKs and, in doing so, identified 36 parasite kinases likely to be essential to erythrocyte schizogony [112]. A similar study used *P. berghei* to identify kinases essential during mosquito portions of the parasite life cycle; this study also demonstrated *P. berghei* kinases to be potential targets for therapeutic and transmission-blocking interventions [119].

Specific Aim 2 focuses on targeting kinases with chemically-stabilized polypeptide compounds. These studies focus on two protein kinases: protein kinase A (PKA) and *P. falciparum* calcium-dependent protein kinase 1 (CDPK1).

Protein Kinase A

PKA was the first protein kinase structure to be solved nearly 25 years ago [120]. Since then, a substantial amount of research has been dedicated to understanding the molecular structure and carefully regulated activity of this “molecular switch” [121]. PKA is a cAMP-dependent protein kinase that is responsible for an incredible variety of cellular activities. The PKA holoenzyme is a tetramer composed of two inactive catalytic subunits bound to a dimer of regulatory subunits that can take on a variety of isoforms (RI α , RI β , RII α , RII β) [121]. Protein activity is highly regulated and involves both activation by cAMP and protein localization by an A-kinase anchoring protein (AKAP) [122–124]. AKAPs bind to the docking and dimerization domain located between the PKA-R subunits to recruit PKA to distinct subcellular locations and position the enzyme in the proximity of cAMP production (Figure 2.4A). This careful localization ensures phosphorylation of a restricted number of potential substrates [105,122]. Once localized, two cAMP bind to PKA-R subunits and induce the release of active PKA-C subunits. Dr. Kennedy’s lab successfully inhibited PKA localization and subsequent activity by designing a Stapled AKAP Disruptor peptide, STAD-2. This peptide mimics native AKAP and serves to block AKAP binding within the PKA docking and dimerization domain (Figure 2.4B). Our initial studies with chemically stabilized peptides explore the permeability and activity of STAD-2 in *P. falciparum* infected red blood cells *in vitro* (Chapter 4 and 5).

*Pf*PKA bears some similarities and some differences to *Hs*PKA. Notably, *Pf*PKA holoenzyme is a dimer containing one, single R subunit and one C subunit [125]. Although an ortholog of *P. yoelii* AKAP has been identified in the *P. falciparum* genome, evidence of a *Pf*PKA AKAP-binding domain has not yet surfaced [125,126]. Therefore, it is suggested that *Pf*PKA might utilize a novel mechanism for subcellular localization. Although *Pf*PKA has been shown to be essential for parasite growth, there is considerable debate regarding its purpose and activity in blood-stage parasites [127]. *Pf*PKA has been implicated in a variety of parasite processes ranging from phosphorylation of apical membrane antigen 1 (AMA1) to control of anion channel conductance at the erythrocyte membrane to melatonin-dependent regulation of the parasite cell cycle [128–131].

***Plasmodium falciparum* Calcium-Dependent Protein Kinase-1**

CDPK1 is one of seven members of a multi-gene family of calcium-dependent protein kinases (CDPKs). While the CDPKs are known to be present in plants and alveolates, there are no known human orthologs of this gene family, making the CDPKs ideal candidates for drug targets in *Plasmodium* [111]. *Pf*CDPK1 is composed of an N-terminal kinase domain (KD) and a calmodulin-like domain (CLD) linked by an autoregulatory junction domain (J domain) (Figure 2.5) [132,133]. This J domain, which is the target of our studies in Chapter 6, acts to regulate protein activity and is essential to protein function and parasite survival. Studies with *Pf*CDPK4 suggest that calcium binding to the CLD promotes interaction between the J domain and CLD, dissociation of the autoinhibitory region of the J domain, and activation of the kinase domain of CDPK [134]. Consistent with this model, studies utilizing conditional knockdown of the CDPK1

J domain found that continued binding of the inhibitory J domain to CDPK1 causes an arrest in parasite development during schizogony [135].

Although *Pf*CDPK1 is expressed throughout erythrocyte schizogony, it is most highly expressed in mature schizonts and merozoites and has been linked to an essential role in host cell invasion [133,136]. In addition, *Pf*CDPK1 has been implicated in the phosphorylation of glideosome associated protein 45 (*Pf*GAP45) and merozoite motility [136,137]. Finally, gene knockdown studies of *Pb*CDPK1 demonstrate an essential role for CDPK1 during parasite sexual development and mosquito transmission [138].

Summary

This dissertation explores a variety of novel approaches drug development and application in *Plasmodium falciparum*. Initial studies seek to identify a candidate cytostatic agent to facilitate *in vitro* stimulation studies with both primary and lab-adapted ST cells. Our work with these antimalarial agents, then, led us into the rapidly developing field of chemically stapled peptides as we pioneered experiments exploring the potential of these novel compounds as both antimalarials and novel tools to study the biology of the malaria parasite. The following work provides interesting insight into the biology of *Plasmodium falciparum*, offers brand new tools for the study of malaria, and establishes important groundwork for the use of novel compounds in the treatment of this ancient organism.

References

1. WHO (2014) World Malaria Report 2014.
2. Lindblade KA, Steinhardt L, Samuels A, Kachur SP, Slutsker L (2013) The silent threat: asymptomatic parasitemia and malaria transmission. *Expert Rev Anti Infect Ther* 11: 623–639. doi:10.1586/eri.13.45.
3. Butler D (2013) World Malaria Malaria Report 2013. World Heal Organ. doi:10.1038/nature.2013.13535.
4. Cox FE (2010) History of the discovery of the malaria parasites and their vectors. *Parasit Vectors* 3: 5. doi:10.1186/1756-3305-3-5.
5. Bloland PB (2001) Drug resistance in malaria. World Heal Organ.
6. David A. Warrell HMG, editor (2002) *Essential Malariology*. Fourth Ed. Arnold.
7. Ejigiri I, Sinnis P (2009) Plasmodium sporozoite-host interactions from the dermis to the hepatocyte. *Curr Opin Microbiol* 12: 401–407. doi:10.1016/j.mib.2009.06.006.
8. Amino R, Thiberge S, Martin B, Celli S, Shorte S, et al. (2006) Quantitative imaging of Plasmodium transmission from mosquito to mammal. *Nat Med* 12: 220–224. doi:10.1038/nm1350.
9. Gueirard P, Tavares J, Thiberge S, Bernex F, Ishino T, et al. (2010) Development of the malaria parasite in the skin of the mammalian host. doi:10.1073/pnas.1009346107/-/DCSupplemental.www.pnas.org/cgi/doi/10.1073/pnas.1009346107.
10. White NJ, Pukrittayakamee S, Hien TT, Faiz MA, Mokuolu O a, et al. (2013) Malaria. *Lancet* 6736. doi:10.1016/S0140-6736(13)60024-0.
11. Bannister LH, Hopkins JM, Fowler RE, Krishna S, Mitchell GH (2000) A brief illustrated guide to the ultrastructure of Plasmodium falciparum asexual blood stages. *Parasitol Today* 16: 427–433.
12. Cowman AF, Berry D, Baum J (2012) The cellular and molecular basis for malaria parasite invasion of the human red blood cell. *J Cell Biol* 198: 961–971. doi:10.1083/jcb.201206112.
13. Baton LA, Ranford-Cartwright LC (2005) Spreading the seeds of million-murdering death: metamorphoses of malaria in the mosquito. *Trends Parasitol* 21: 573–580. doi:10.1016/j.pt.2005.09.012.

14. Smith TG, Walliker D, Ranford-Cartwright LC (2002) Sexual differentiation and sex determination in the Apicomplexa. *Trends Parasitol* 18: 315–323.
15. Silvestrini F, Alano P, Williams JL (2000) Commitment to the production of male and female gametocytes in the human malaria parasite *Plasmodium falciparum*. *Parasitology* 121 Pt 5: 465–471.
16. Tibúrcio M, Niang M, Deplaine G, Perrot S, Bischoff E, et al. (2012) A switch in infected erythrocyte deformability at the maturation and blood circulation of *Plasmodium falciparum* transmission stages. *Blood* 119: e172–e180. doi:10.1182/blood-2012-03-414557.
17. Angrisano F, Tan Y-H, Sturm A, McFadden GI, Baum J (2012) Malaria parasite colonisation of the mosquito midgut--placing the *Plasmodium* ookinete centre stage. *Int J Parasitol* 42: 519–527. doi:10.1016/j.ijpara.2012.02.004.
18. Shanks GD, White NJ (2013) The activation of vivax malaria hypnozoites by infectious diseases. *Lancet Infect Dis* 13: 900–906. doi:10.1016/S1473-3099(13)70095-1.
19. Baird JK, Hoffman SL (2004) Primaquine therapy for malaria. *Clin Infect Dis* 39: 1336–1345. doi:10.1086/424663.
20. Carson PE, Flanagan CL, Ickes CE, Alving AS (1956) Enzymatic Deficiency in Primaquine-Sensitive Erythrocytes. *Science* (80-) 124: 484–485.
21. Zeeman A-M, van Amsterdam SM, McNamara CW, Voorberg-van der Wel A, Klooster EJ, et al. (2014) KAI407, a potent non-8-aminoquinoline compound that kills *Plasmodium cynomolgi* early dormant liver stage parasites in vitro. *Antimicrob Agents Chemother* 58: 1586–1595. doi:10.1128/AAC.01927-13.
22. Baird JK (2009) Resistance to therapies for infection by *Plasmodium vivax*. *Clin Microbiol Rev* 22: 508–534. doi:10.1128/CMR.00008-09.
23. Furuya T, Sá JM, Chitnis CE, Wellems TE, Stedman TT (2014) Reticulocytes from cryopreserved erythroblasts support *Plasmodium vivax* infection in vitro. *Parasitol Int* 63: 278–284. doi:10.1016/j.parint.2013.11.011.
24. Bartoloni A, Zammarchi L (2012) Clinical aspects of uncomplicated and severe malaria. *Mediterr J Hematol Infect Dis* 4: e2012026. doi:10.4084/MJHID.2012.026.
25. Trampuz A, Jereb M, Muzlovic I, Prabhu RM (2003) Clinical review: Severe malaria. *Crit Care* 7: 315–323. doi:10.1186/cc2183.
26. WHO (2000) Severe falciparum. *Trans R Soc Trop Med Hyg*.

27. Rogerson SJ, Grau GE, Hunt NH (2004) The microcirculation in severe malaria. *Microcirculation* 11: 559–576. doi:10.1080/10739680490503311.
28. Cotter C, Sturrock HJW, Hsiang MS, Liu J, Phillips AA, et al. (2013) The changing epidemiology of malaria elimination: new strategies for new challenges. *Lancet* 382: 900–911. doi:10.1016/S0140-6736(13)60310-4.
29. WHO (2012) Global Plan for Insecticide Resistance Management.
30. Blayneh KW, Mohammed-Awel J (2014) Insecticide-resistant mosquitoes and malaria control. *Math Biosci* 252: 14–26. doi:10.1016/j.mbs.2014.03.007.
31. Dondrop AM, Nosten F, Yi P, Das D, Phyo AP, et al. (2009) Artemisinin Resistance in *Plasmodium falciparum* Malaria. *N Engl J Med* 361: 455–467.
32. Dondorp AM, Yeung S, White L, Nguon C, Day NPJ, et al. (2010) Artemisinin resistance: current status and scenarios for containment. *Nat Rev Microbiol* 8: 272–280. doi:10.1038/nrmicro2331.
33. Ashley EA, Dhorda M, Fairhurst RM, Amaratunga C, Lim P, et al. (2014) Spread of Artemisinin Resistance in *Plasmodium falciparum* Malaria. *N Engl J Med* 371: 411–423. doi:10.1056/NEJMoa1314981.
34. Griffin JT, Hollingsworth TD, Okell LC, Churcher TS, White M, et al. (2010) Reducing *Plasmodium falciparum* malaria transmission in Africa: a model-based evaluation of intervention strategies. *PLoS Med* 7. doi:10.1371/journal.pmed.1000324.
35. Ouédraogo AL, Bousema T, Schneider P, de Vlas SJ, Ilboudo-Sanogo E, et al. (2009) Substantial contribution of submicroscopical *Plasmodium falciparum* gametocyte carriage to the infectious reservoir in an area of seasonal transmission. *PLoS One* 4: e8410. doi:10.1371/journal.pone.0008410.
36. Tietje K, Hawkins K, Clerk C, Ebels K, McGray S, et al. (2014) The essential role of infection-detection technologies for malaria elimination and eradication. *Trends Parasitol* 30: 259–266. doi:10.1016/j.pt.2014.03.003.
37. Okell LC, Bousema T, Griffin JT, Ouédraogo AL, Ghani AC, et al. (2012) Factors determining the occurrence of submicroscopic malaria infections and their relevance for control. *Nat Commun* 3: 1237. doi:10.1038/ncomms2241.
38. Dellicour S, Tatem AJ, Guerra CA, Snow RW, ter Kuile FO (2010) Quantifying the number of pregnancies at risk of malaria in 2007: a demographic study. *PLoS Med* 7: e1000221. doi:10.1371/journal.pmed.1000221.

39. Walker PGT, Griffin JT, Cairns M, Rogerson SJ, van Eijk AM, et al. (2013) A model of parity-dependent immunity to placental malaria. *Nat Commun* 4: 1609. doi:10.1038/ncomms2605.
40. Walker PGT, ter Kuile FO, Garske T, Menendez C, Ghani AC (2014) Estimated risk of placental infection and low birthweight attributable to *Plasmodium falciparum* malaria in Africa in 2010: A modelling study. *Lancet Glob Heal* 2: e460–e467. doi:10.1016/S2214-109X(14)70256-6.
41. McMillan PJ, Millet C, Batinovic S, Maiorca M, Hanssen E, et al. (2013) Spatial and temporal mapping of the PfEMP1 export pathway in *Plasmodium falciparum*. *Cell Microbiol* 15: 1401–1418. doi:10.1111/cmi.12125.
42. Guizetti J, Scherf A (2013) Silence, activate, poise and switch! Mechanisms of antigenic variation in *Plasmodium falciparum*. *Cell Microbiol* 15: 718–726. doi:10.1111/cmi.12115.
43. Janes JH, Wang CP, Levin-Edens E, Vigan-Womas I, Guillotte M, et al. (2011) Investigating the host binding signature on the *Plasmodium falciparum* PfEMP1 protein family. *PLoS Pathog* 7: e1002032. doi:10.1371/journal.ppat.1002032.
44. Turner GDH, Morrison H, Jones M, Davis TME, Looareesuwan S, et al. (1994) An Immunohistochemical Study of the Pathology of Fatal Malaria. Evidence for Widespread Endothelial Activation and a Potential Role for Intercellular Adhesion Molecule-1 in Cerebral Sequestration. *Am J Pathol* 145: 1057–1069.
45. Aird WC, Mosnier LO, Fairhurst RM (2014) *Plasmodium falciparum* picks (on) EPCR. *Blood* 123: 163–167. doi:10.1182/blood-2013-09-521005.
46. Samak AC (2004) Malaria in Pregnancy : an overview. *McGill J Med*: 66–71.
47. Maubert B, Guilbert LJ, Deloron P, Maubert B, Guilbert LJ (1997) Cytoadherence of *Plasmodium falciparum* to intercellular adhesion molecule 1 and chondroitin-4-sulfate expressed by the syncytiotrophoblast in the human placenta . Cytoadherence of *Plasmodium falciparum* to Intercellular Adhesion Molecule 1 and Chondroitin-. *Infect Immun*.
48. Beeson JG, Reeder JC, Rogerson SJ, Brown G V (2001) Parasite adhesion and immune evasion in placental malaria. *Trends Parasitol* 17: 331–337.
49. Desai M, ter Kuile FO, Nosten F, McGready R, Asamo K, et al. (2007) Epidemiology and burden of malaria in pregnancy. *Lancet Infect Dis* 7: 93–104. doi:10.1016/S1473-3099(07)70021-X.
50. Brabin BJ, Romagosa C, Abdelgalil S, Menéndez C, Verhoeff FH, et al. (2004) The sick placenta-the role of malaria. *Placenta* 25: 359–378. doi:10.1016/j.placenta.2003.10.019.

51. Huynh B-T, Cottrell G, Cot M, Briand V (2014) Burden of Malaria in Early Pregnancy: A Neglected Problem? *Clin Infect Dis* 60: 598–604. doi:10.1093/cid/ciu848.
52. Rogerson SJ, Pollina E, Getachew A, Tadesse E, Lema VM, et al. (2003) Placental monocyte infiltrates in response to *Plasmodium falciparum* malaria infection and their association with adverse pregnancy outcomes. *Am J Trop Med Hyg* 68: 115–119.
53. Suguitan AL, Leke RGF, Fouda G, Zhou A, Thuita L, et al. (2003) Changes in the levels of chemokines and cytokines in the placentas of women with *Plasmodium falciparum* malaria. *J Infect Dis* 188: 1074–1082. doi:10.1086/378500.
54. Fried M, Muga RO, Misore a O, Duffy PE (1998) Malaria elicits type 1 cytokines in the human placenta: IFN-gamma and TNF-alpha associated with pregnancy outcomes. *J Immunol* 160: 2523–2530.
55. Brabin BJ (1983) An analysis of malaria in pregnancy in Africa. *Bull World Health Organ* 61: 1005–1016.
56. Duffy PE, Fried M (2003) Antibodies That Inhibit *Plasmodium falciparum* Adhesion to Chondroitin Sulfate A Are Associated with Increased Birth Weight and the Gestational Age of Newborns Antibodies That Inhibit *Plasmodium falciparum* Adhesion to Chondroitin Sulfate A Are Associated w. 71: 6620–6623. doi:10.1128/IAI.71.11.6620.
57. Ricke CH, Staalsoe T, Koram K, Akanmori BD, Riley EM, et al. (2000) Plasma antibodies from malaria-exposed pregnant women recognize variant surface antigens on *Plasmodium falciparum*-infected erythrocytes in a parity-dependent manner and block parasite adhesion to chondroitin sulfate A. *J Immunol* 165: 3309–3316. doi:ji_v165n6p3309 [pii].
58. Fried M, Nosten F, Brockman A, Brabin B, Duffy P (1998) Maternal antibodies block malaria. *Nature* 395: 851–852. doi:10.1038/27570.
59. Chaisavaneeyakorn S, Lucchi N, Abramowsky C, Othoro C, Chaiyaroj SC, et al. (2005) Immunohistological characterization of macrophage migration inhibitory factor expression in *Plasmodium falciparum*-infected placentas. *Infect Immun* 73: 3287–3293. doi:10.1128/IAI.73.6.3287.
60. Lucchi NW, Koopman R, Peterson DS, Moore JM (2006) *Plasmodium falciparum*-infected red blood cells selected for binding to cultured syncytiotrophoblast bind to chondroitin sulfate A and induce tyrosine phosphorylation in the syncytiotrophoblast. *Placenta* 27: 384–394. doi:10.1016/j.placenta.2005.04.009.
61. Lucchi NW, Sarr D, Owino SO, Mwalimu SM, Peterson DS, et al. (2011) Natural hemozoin stimulates syncytiotrophoblast to secrete chemokines and recruit peripheral blood mononuclear cells. *Placenta* 32: 579–585. doi:10.1016/j.placenta.2011.05.003.

62. Avery JW, Smith GM, Owino SO, Sarr D, Nagy T, et al. (2012) Maternal malaria induces a procoagulant and antifibrinolytic state that is embryotoxic but responsive to anticoagulant therapy. *PLoS One* 7: e31090. doi:10.1371/journal.pone.0031090.
63. Sarr D, Smith GM, Poovassery JS, Nagy T, Moore JM (2012) *Plasmodium chabaudi* AS induces pregnancy loss in association with systemic pro-inflammatory immune responses in A/J and C57BL/6 mice. *Parasite Immunol* 34: 224–235. doi:10.1111/j.1365-3024.2012.01355.x.
64. Lambros C, Vanderberg JP (1979) Synchronization of *Plasmodium falciparum* Erythrocytic Stages in Culture. *J Parasitol* 65: 418–420.
65. Radfar A, Mendez D, Moneriz C, Linares M, Marin-Garcia P, et al. (2009) Synchronous culture of *Plasmodium falciparum* at high parasitemia levels. *Nat Protoc* 4: 1899–1915.
66. Achan J, Talisuna AO, Erhart A, Yeka A, Tibenderana JK, et al. (2011) Quinine, an old anti-malarial drug in a modern world: role in the treatment of malaria. *Malar J* 10: 144. doi:10.1186/1475-2875-10-144.
67. Schlitzer M (2007) Malaria chemotherapeutics part I: History of antimalarial drug development, currently used therapeutics, and drugs in clinical development. *ChemMedChem* 2: 944–986. doi:10.1002/cmdc.200600240.
68. Schlitzer M (2008) Antimalarial drugs - what is in use and what is in the pipeline. *Arch Pharm (Weinheim)* 341: 149–163. doi:10.1002/ardp.200700184.
69. Foley M, Tilley L (1998) Quinoline Antimalarials : Mechanisms of Action and Resistance and Prospects for New Agents MECHANISM THE BASIS OF PARASITES ACCUMULATE. 79: 55–87.
70. Chinappi M, Via A, Marcatili P, Tramontano A (2010) On the mechanism of chloroquine resistance in *Plasmodium falciparum*. *PLoS One* 5: e14064. doi:10.1371/journal.pone.0014064.
71. Pukrittayakamee S, Tarning J, Jittamala P, Charunwatthana P, Lawpoolsri S, et al. (2014) Pharmacokinetic Interactions between Primaquine and Chloroquine. *Antimicrob Agents Chemother* 58: 3354–3359. doi:10.1128/AAC.02794-13.
72. Supan C, Mombo-Ngoma G, Dal-Bianco MP, Ospina Salazar CL, Issifou S, et al. (2012) Pharmacokinetics of ferroquine, a novel 4-aminoquinoline, in asymptomatic carriers of *Plasmodium falciparum* infections. *Antimicrob Agents Chemother* 56: 3165–3173. doi:10.1128/AAC.05359-11.
73. Biot C, Nosten F, Fraisse L, Ter-Minassian D, Khalife J, et al. (2011) The antimalarial ferroquine: from bench to clinic. *Parasite* 18: 207–214.

74. Laufer M, Thesing P, Eddington N, Masonga R, Dzinjalama F, et al. (2006) Return of Chloroquine Antimalarial Efficacy in Malawi. *NEJM*: 1959–1966.
75. Frank JE (2005) Diagnosis and management of G6PD deficiency. *Am Fam Physician* 72: 1277–1282.
76. Klonis N, Xie SC, McCaw JM, Crespo-Ortiz MP, Zaloumis SG, et al. (2013) Altered temporal response of malaria parasites determines differential sensitivity to artemisinin. *Proc Natl Acad Sci U S A* 110: 5157–5162. doi:10.1073/pnas.1217452110.
77. Klonis N, Crespo-Ortiz MP, Bottova I, Abu-Bakar N, Kenny S, et al. (2011) Artemisinin activity against *Plasmodium falciparum* requires hemoglobin uptake and digestion. *Proc Natl Acad Sci U S A* 108: 11405–11410. doi:10.1073/pnas.1104063108.
78. Shandilya A, Chacko S, Jayaram B, Ghosh I (2013) A plausible mechanism for the antimalarial activity of artemisinin: A computational approach. *Sci Rep* 3: 2513. doi:10.1038/srep02513.
79. Salcedo-Sora JE, Ochong E, Beveridge S, Johnson D, Nzila A, et al. (2011) The molecular basis of folate salvage in *Plasmodium falciparum*: characterization of two folate transporters. *J Biol Chem* 286: 44659–44668. doi:10.1074/jbc.M111.286054.
80. Chango A, Abdennebi-Najar L (2011) Folate metabolism pathway and *Plasmodium falciparum* malaria infection in pregnancy. *Nutr Rev* 69: 34–40. doi:10.1111/j.1753-4887.2010.00362.x.
81. Hekmat-nejad M, Rathod PK (1997) *Plasmodium falciparum* : Kinetic Interactions of WR99210 with. 228: 222–228.
82. Imwong M, Russell B, Suwanarusk R, Nzila A, Leimanis ML, et al. (2011) Methotrexate is highly potent against pyrimethamine-resistant *Plasmodium vivax*. *J Infect Dis* 203: 207–210. doi:10.1093/infdis/jiq024.
83. Cassera MB, Zhang Y, Hazleton KZ, Schramm VL (2011) Purine and pyrimidine pathways as targets in *Plasmodium falciparum*. *Curr Top Med Chem* 11: 2103–2115.
84. Painter HJ, Morrissey JM, Mather MW, Vaidya AB (2007) Specific role of mitochondrial electron transport in blood-stage *Plasmodium falciparum*. *Nature* 446: 88–91. doi:10.1038/nature05572.
85. Ke H, Morrissey JM, Ganesan SM, Painter HJ, Mather MW, et al. (2011) Variation among *Plasmodium falciparum* strains in their reliance on mitochondrial electron transport chain function. *Eukaryot Cell* 10: 1053–1061. doi:10.1128/EC.05049-11.
86. Bell A (1998) Microtubule inhibitors as potential antimalarial agents. *Parasitol Today* 14: 234–240.

87. Fennell BJ, Naughton JA, Dempsey E, Bell A (2006) Cellular and molecular actions of dinitroaniline and phosphorothioamidate herbicides on *Plasmodium falciparum*: tubulin as a specific antimalarial target. *Mol Biochem Parasitol* 145: 226–238. doi:10.1016/j.molbiopara.2005.08.020.
88. Naughton JA, Hughes R, Bray P, Bell A (2008) Accumulation of the antimalarial microtubule inhibitors trifluralin and vinblastine by *Plasmodium falciparum*. *Biochem Pharmacol* 75: 1580–1587. doi:10.1016/j.bcp.2008.01.002.
89. Dempsey E, Prudêncio M, Fennell BJ, Gomes-Santos CS, Barlow JW, et al. (2013) Antimitotic herbicides bind to an unidentified site on malarial parasite tubulin and block development of liver-stage *Plasmodium* parasites. *Mol Biochem Parasitol* 188: 116–127. doi:10.1016/j.molbiopara.2013.03.001.
90. Fennell BJ, Carolan S, Pettit GR, Bell a (2003) Effects of the antimitotic natural product dolastatin 10, and related peptides, on the human malarial parasite *Plasmodium falciparum*. *J Antimicrob Chemother* 51: 833–841. doi:10.1093/jac/dkg151.
91. Sinou V, Grellier P, Schrevel J (1996) In vitro and in vivo inhibition of erythrocytic development of malarial parasites by docetaxel. *Antimicrob Agents Chemother* 40: 358–361.
92. Sodium azide (2002). 20: 275–285.
93. Clarebout G, Slomianny C, Delcourt P, Leu B, Masset A, et al. (1998) Status of *Plasmodium falciparum* towards catalase. *Br J Haematol* 103: 52–59.
94. Schneider-poetsch T, Ju J, Eyler DE, Dang Y, Bhat S, et al. (2010) Inhibition of Eukaryotic Translation Elongation by Cycloheximide and Lactimidomycin. 6: 209–217. doi:10.1038/nchembio.304.Inhibition.
95. Babbitt SE, Altenhofen L, Cobbold SA, Istvan ES, Fennell C, et al. (2012) *Plasmodium falciparum* responds to amino acid starvation by entering into a hibernatory state. *Proc Natl Acad Sci U S A* 109: E3278–E3287. doi:10.1073/pnas.1209823109.
96. Martin RE, Kirk K (2007) Transport of the essential nutrient isoleucine in human erythrocytes infected with the malaria parasite *Plasmodium falciparum*. *Blood* 109: 2217–2224. doi:10.1182/blood-2005-11-026963.The.
97. Budimulja AS, Tapchaisri P, Wilairat P, Marzuki S (1997) The sensitivity of *Plasmodium* protein synthesis to prokaryotic ribosomal inhibitors. 84: 137–141.
98. Walensky LD, Kung AL, Escher I, Malia TJ, Barbuto S, et al. (2004) Activation of apoptosis in vivo by a hydrocarbon-stapled BH3 helix. *Science* (80-) 305: 1466–1470. doi:10.1126/science.1099191.

99. Verdine GL, Hilinski GJ (2012) Stapled peptides for intracellular drug targets. 1st ed. Elsevier Inc. 3-33 p. doi:10.1016/B978-0-12-396962-0.00001-X.
100. Verdine GL, Walensky LD (2007) The challenge of drugging undruggable targets in cancer: lessons learned from targeting BCL-2 family members. *Clin cancer Res* 13: 7264–7270. doi:10.1158/1078-0432.CCR-07-2184.
101. Schafmeister CE, Po J, Verdine GL (2000) An All-Hydrocarbon Cross-Linking System for Enhancing the Helicity and Metabolic Stability of Peptides. *J Am Chem Soc* 122: 5891–5892. doi:10.1021/ja000563a.
102. Guharoy M, Chakrabarti P (2007) Secondary structure based analysis and classification of biological interfaces: identification of binding motifs in protein-protein interactions. *Bioinformatics* 23: 1909–1918. doi:10.1093/bioinformatics/btm274.
103. Kritzer JA (2010) Magic bullets in nature's arsenal. *Nat Chem Biol* 6: 1–3.
104. Stewart ML, Fire E, Keating AE, Walensky LD (2010) The MCL-1 BH3 helix is an exclusive MCL-1 inhibitor and apoptosis sensitizer. *Nat Chem Biol* 6: 595–601. doi:10.1038/nchembio.391.
105. Wang Y, Ho TG, Bertinetti D, Neddermann M, Franz E, et al. (2014) Isoform-Selective Disruption of AKAP-Localized PKA Using Hydrocarbon Stapled Peptides. *ACS Chem Biol* 9: 635–642. doi:10.1021/cb500329z.
106. Greenwood B, Mutabingwa T (2002) Malaria in 2002. *Nature* 415: 670–672. doi:10.1038/415670a.
107. Trouiller P, Olliaro PL (1997) Drug development output from 1975 to 1996: what proportion for tropical diseases? *Int J Infect Dis* 3: 61–63.
108. Gamo F-J, Sanz LM, Vidal J, De Cozar C, Alvarez E, et al. (2010) Thousands of chemical starting points for antimalarial lead identification. *Nature* 465: 305–310. doi:10.1038/nature09107.
109. Lahiry P, Torkamani A, Schork NJ, Hegele RA (2010) Kinase mutations in human disease: interpreting genotype-phenotype relationships. *Nat Rev Genet* 11: 60–74. doi:10.1038/nrg2707.
110. Zhang J, Yang PL, Gray NS (2009) Targeting cancer with small molecule kinase inhibitors. *Nat Rev Cancer* 9: 28–39. doi:10.1038/nrc2559.
111. Lucet IS, Tobin A, Drewry D, Wilks AF, Doerig C (2012) Plasmodium kinases as targets for new-generation antimalarials. *Future Med Chem* 4: 2295–2310. doi:10.4155/fmc.12.183.

112. Solyakov L, Halbert J, Alam MM, Semblat J-P, Dorin-Semblat D, et al. (2011) Global kinomic and phospho-proteomic analyses of the human malaria parasite *Plasmodium falciparum*. *Nat Commun* 2: 565. doi:10.1038/ncomms1558.
113. Lasonder E, Green JL, Camarda G, Talabani H, Holder AA, et al. (2012) The *Plasmodium falciparum* schizont phosphoproteome reveals extensive phosphatidylinositol and cAMP-protein kinase A signaling. *J Proteome Res* 11: 5323–5337. doi:10.1021/pr300557m.
114. Treeck M, Sanders JL, Elias JE, Boothroyd JC (2011) The phosphoproteomes of *Plasmodium falciparum* and *Toxoplasma gondii* reveal unusual adaptations within and beyond the parasites' boundaries. *Cell Host Microbe* 10: 410–419. doi:10.1016/j.chom.2011.09.004.
115. Lasonder E, Treeck M, Alam M, Tobin AB (2012) Insights into the *Plasmodium falciparum* schizont phospho-proteome. *Microbes Infect* 14: 811–819. doi:10.1016/j.micinf.2012.04.008.
116. Doerig C (2004) Protein kinases as targets for anti-parasitic chemotherapy. *Biochim Biophys Acta* 1697: 155–168. doi:10.1016/j.bbapap.2003.11.021.
117. Ward P, Equinet L, Packer J, Doerig C (2004) Protein kinases of the human malaria parasite *Plasmodium falciparum* : the kinome of a divergent eukaryote. *BMC Genomics* 19: 1–19. doi:10.1186/1471-2164-5-79.
118. Nunes MC, Okada M, Scheidig-Benatar C, Cooke BM, Scherf A (2010) *Plasmodium falciparum* FIKK kinase members target distinct components of the erythrocyte membrane. *PLoS One* 5: e11747. doi:10.1371/journal.pone.0011747.
119. Tewari R, Straschil U, Bateman A, Böhme U, Cherevach I, et al. (2010) The systematic functional analysis of *Plasmodium* protein kinases identifies essential regulators of mosquito transmission. *Cell Host Microbe* 8: 377–387. doi:10.1016/j.chom.2010.09.006.
120. Knighton DR, Zheng J, Eyck LF Ten, Ashford VA, Xuong N, et al. (1991) Crystal Structure of the Catalytic Subunit of Cyclic Adenosin Monophosphate-Dependent Protein Kinase. 253: 407–414.
121. Taylor SS, Zhang P, Steichen JM, Keshwani MM, Kornev AP (2013) PKA: lessons learned after twenty years. *Biochim Biophys Acta* 1834: 1271–1278. doi:10.1016/j.bbapap.2013.03.007.
122. Wong W, Scott JD (2004) AKAP signalling complexes: focal points in space and time. *Nat Rev Mol Cell Biol* 5: 959–970. doi:10.1038/nrm1527.
123. Edwards AS, Scott JD (2000) A-kinase anchoring proteins: protein kinase A and beyond. *Curr Opin Cell Biol* 12: 217–221.

124. Langeberg LK, Scott JD (2005) A-kinase-anchoring proteins. *J Cell Sci* 118: 3217–3220. doi:10.1242/jcs.02416.
125. Haste NM, Talabani H, Doo A, Merckx A, Langsley G, et al. (2012) Exploring the *Plasmodium falciparum* cyclic-adenosine monophosphate (cAMP)-dependent protein kinase (PfPKA) as a therapeutic target. *Microbes Infect* 14: 838–850. doi:10.1016/j.micinf.2012.05.004.
126. Wurtz N, Chapus C, Desplans J, Parzy D (2011) cAMP-dependent protein kinase from *Plasmodium falciparum*: an update. *Parasitology* 138: 1–25. doi:10.1017/S003118201000096X.
127. Syin C, Parzy D, Traincard F, Boccaccio I, Joshi MB, et al. (2001) The H89 cAMP-dependent protein kinase inhibitor blocks *Plasmodium falciparum* development in infected erythrocytes. *Eur J Biochem* 268: 4842–4849.
128. Gazarini ML, Beraldo FH, Almeida FM, Bootman M, Da Silva AM, et al. (2011) Melatonin triggers PKA activation in the rodent malaria parasite *Plasmodium chabaudi*. *J Pineal Res* 50: 64–70. doi:10.1111/j.1600-079X.2010.00810.x.
129. Beraldo FH, Almeida FM, da Silva AM, Garcia CRS (2005) Cyclic AMP and calcium interplay as second messengers in melatonin-dependent regulation of *Plasmodium falciparum* cell cycle. *J Cell Biol* 170: 551–557. doi:10.1083/jcb.200505117.
130. Merckx A, Nivez M-P, Bouyer G, Alano P, Langsley G, et al. (2008) *Plasmodium falciparum* regulatory subunit of cAMP-dependent PKA and anion channel conductance. *PLoS Pathog* 4: e19. doi:10.1371/journal.ppat.0040019.
131. Leykauf K, Treeck M, Gilson PR, Nebl T, Bräulke T, et al. (2010) Protein kinase a dependent phosphorylation of apical membrane antigen 1 plays an important role in erythrocyte invasion by the malaria parasite. *PLoS Pathog* 6: e1000941. doi:10.1371/journal.ppat.1000941.
132. Ahmed A, Gaadhe K, Sharma GP, Kumar N, Neculai M, et al. (2012) Novel insights into the regulation of malarial calcium-dependent protein kinase 1. *FASEB J* 26: 3212–3221. doi:10.1096/fj.12-203877.
133. Bansal A, Singh S, More KR, Hans D, Nangalia K, et al. (2013) Characterization of *Plasmodium falciparum* calcium-dependent protein kinase 1 (PfCDPK1) and its role in microneme secretion during erythrocyte invasion. *J Biol Chem* 288: 1590–1602. doi:10.1074/jbc.M112.411934.
134. Ranjan R, Ahmed A, Gourinath S, Sharma P (2009) Dissection of mechanisms involved in the regulation of *Plasmodium falciparum* calcium-dependent protein kinase 4. *J Biol Chem* 284: 15267–15276. doi:10.1074/jbc.M900656200.

135. Azevedo, Mauro F., Sanders, Paul R., Krejany, Efrosinia, Nie, Catherine Q., Fu, Ping, Bach, Leon A., Wunderlich, Gerhard, Crabb, Brendan S., Gilson PR (2013) Inhibition of *Plasmodium falciparum* CDPK1 by conditional expression of its J-domain demonstrates a key role in schizont development. *Biochem J*.
136. Green JL, Rees-Channer RR, Howell SA, Martin SR, Knuepfer E, et al. (2008) The motor complex of *Plasmodium falciparum*: phosphorylation by a calcium-dependent protein kinase. *J Biol Chem* 283: 30980–30989. doi:10.1074/jbc.M803129200.
137. Thomas DC, Ahmed A, Gilberger TW, Sharma P (2012) Regulation of *Plasmodium falciparum* glideosome associated protein 45 (PfGAP45) phosphorylation. *PLoS One* 7: e35855. doi:10.1371/journal.pone.0035855.
138. Sebastian S, Brochet M, Collins MO, Schwach F, Jones ML, et al. (2012) A *Plasmodium* calcium-dependent protein kinase controls zygote development and transmission by translationally activating repressed mRNAs. *Cell Host Microbe* 12: 9–19. doi:10.1016/j.chom.2012.05.014.

Figures

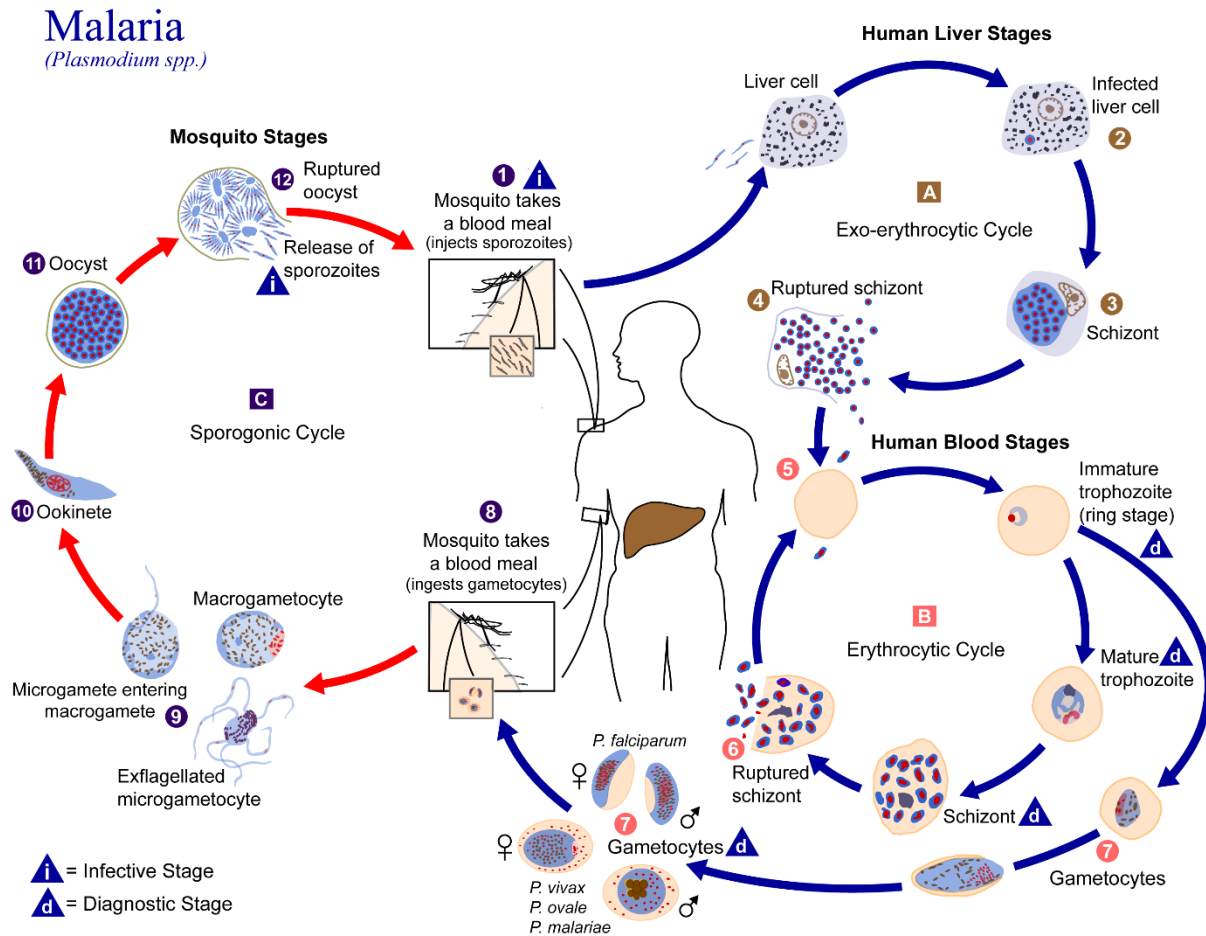


Figure 2.1 Malaria life cycle. Human malaria infection begins with the bite an infective *Anopheles* mosquito wherein *Plasmodium* sporozoites pass from the definitive host's salivary glands into the human dermis (1). Sporozoites then migrate to the liver to initiate the exo-erythrocytic cycle defined by parasite invasion and replication within host hepatocytes followed by hepatocyte rupture, release of merozoites into the host bloodstream, and initiation of the erythrocytic cycle (4). During the erythrocytic cycle, free merozoites invade and replicate within circulating host red blood cells and, sporadically, develop into sexual gametocytes (7). Gametocytes are taken up by the definitive host during a subsequent bloodmeal to initiate the

sporogonic cycle. Sporogenesis within the mosquito lasts approximately two weeks after which the *Plasmodium* life cycle reinitiates with a subsequent mosquito bloodmeal.

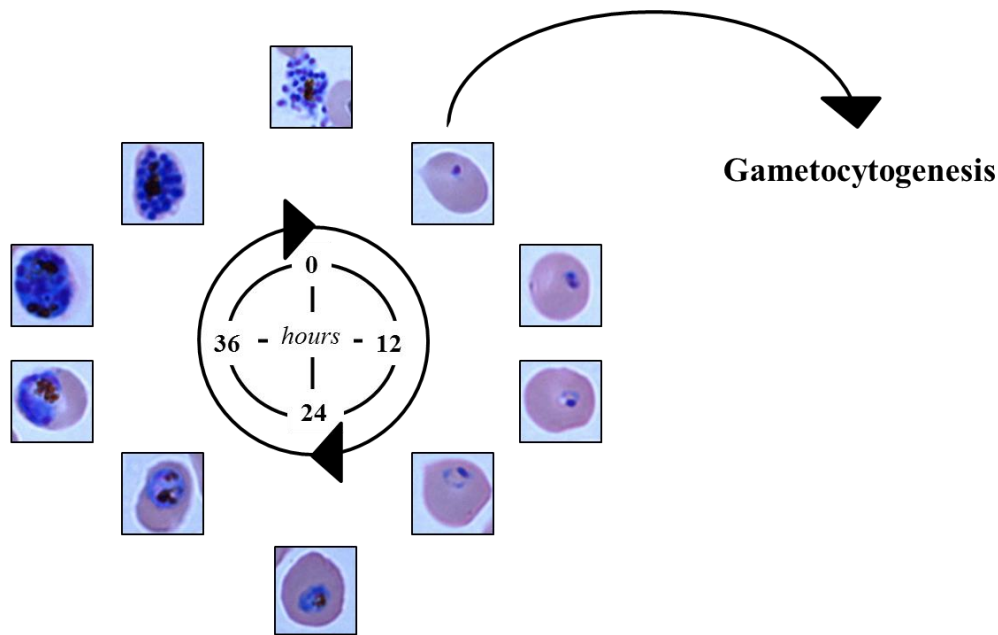


Figure 2.2 *Plasmodium falciparum* blood-stage life cycle. The intraerythrocytic life cycle of *Plasmodium falciparum* begins with merozoite invasion of a circulating red blood cell. Post-invasion, the intracellular parasite progresses from a ring-stage form into a late-stage trophozoite which, subsequently, divides into daughter cells to produce an intraerythrocytic schizont. The schizont bursts out of the infected cell, releasing merozoites back into the bloodstream to invade circulating uninfected red blood cells. This cycle lasts roughly 48 hours. Select parasites deviate from this developmental cycle and enter into gametocytogenesis. Gametocyte-infected red blood cells are taken up by feeding mosquitoes to perpetuate the full life cycle of *Plasmodium falciparum*.

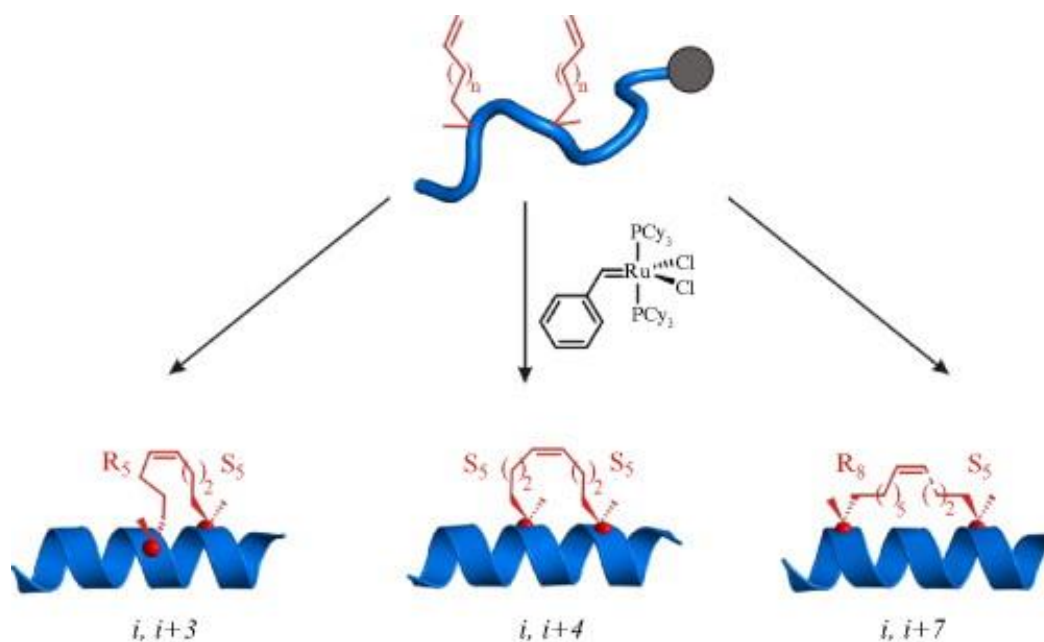


Figure 2.3. Synthesis of chemically stapled peptides. Stapled peptides can be designed in three possible confirmations based on where the non-natural, cross-linking amino acids are incorporated. Peptide synthesis takes place on a solid resin substrate wherein two α -methyl, α -alkenylglycine cross-linking amino acids are incorporated into the polypeptides strand. These non-natural amino acids are then cross-linked with an all-hydrocarbon staple via ruthenium-based ring-closing metathesis. The final stapled peptides are then removed from the resin and dissolved in an appropriate solute, such as DMSO.

Reprinted from Methods in Enzymology, Vol 503, Gregory L. Verdine and Gerard J. Hilinski, Stapled peptides for intracellular drug targets, page 7, Copyright (2012), with permission from Elsevier.

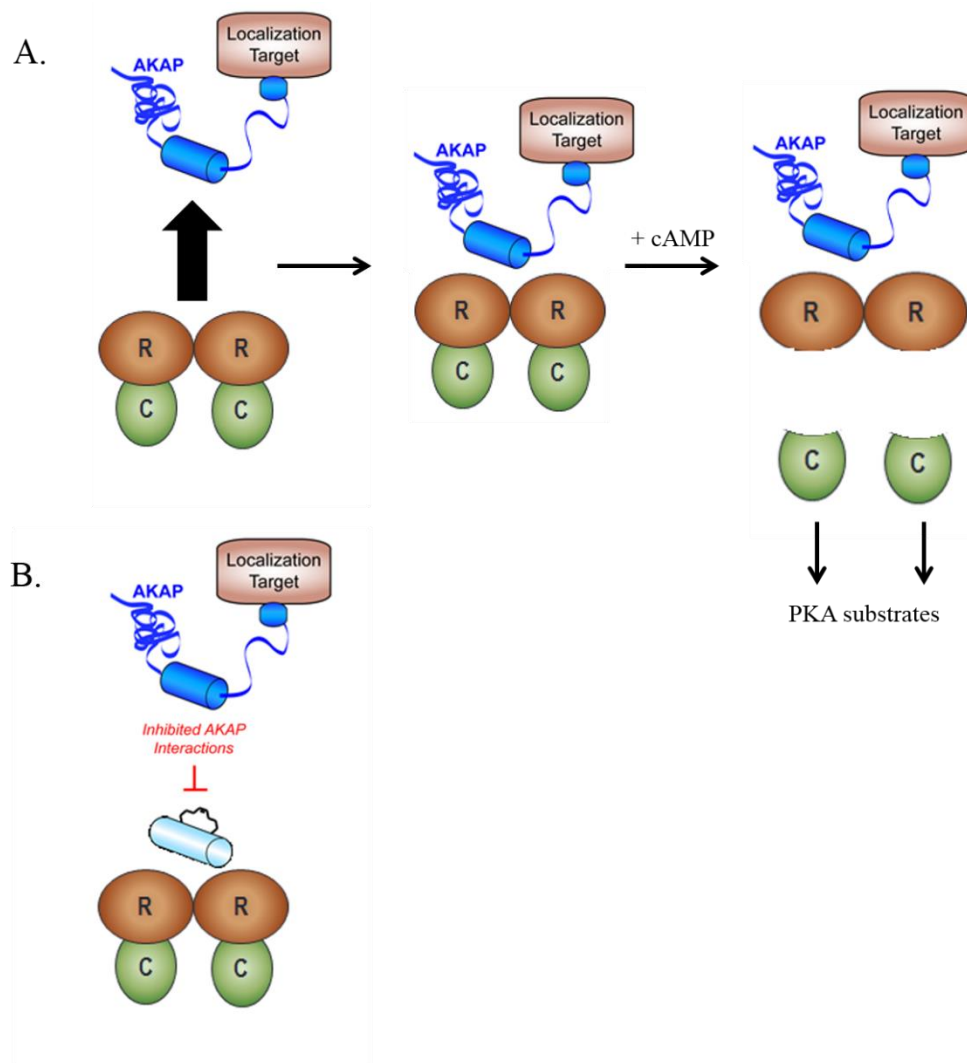


Figure 2.4. Chemically stabilized peptides block AKAP binding and localization. (A) *Hs*PKA activity is regulated by the binding an A Kinase Anchoring Protein (AKAP) to the docking and dimerization domain located between two regulatory subunits (R) of the PKA dimer. AKAPs are expressed in a tissue-specific manner and serve to localize PKA to an appropriate subregion of the cell. Upon addition of cAMP, PKA catalytic subunits dissociate from the regulatory subunits and proceed to act upon relevant PKA substrates. (B) Stapled peptides designed to mimic AKAP bind to the docking and dimerization domain formed at the

PKA-R dimer interface thereby blocking binding of AKAP and inhibiting protein localization and activity.

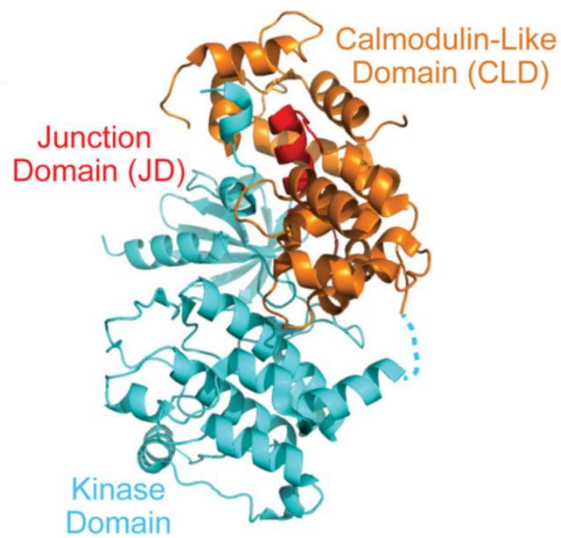


Figure 2.5. The *Pf*CDPK1 J domain regulates enzyme activity. *Pf*CDPK1 is a calcium-dependent protein kinase with an N-terminal kinase domain (blue) and a calmodulin-like domain (orange) containing two calcium-binding EF hands. The kinase domain and calmodulin-like domain are separated by a junction domain (J domain, red) that is critical to regulating protein activity. Binding of the J domain results in autoinhibition of CDPK1 while release of the J domain promotes kinase activity.

CHAPTER 3

LATE-STAGE ARREST OF CYTOADHERENT *PLASMODIUM FALCIPARUM* FOR *IN VITRO* CHRONIC ADHESION STUDIES ¹

¹ Flaherty, B.R., Moore, J.M., and Peterson, D.S. To be submitted to Experimental Parasitology.

Abstract

Extended *in vitro* adhesion studies with *Plasmodium falciparum* infected red blood cells (iRBC) are largely infeasible due to the limited duration of parasite cytoadherence and the finite length of the blood-stage life cycle. Here, we explore methods by which to isolate late-stage, cytoadherent iRBC for *in vitro* chronic adhesion studies. A wide panel of antimalarial agents was tested to determine the stage of parasite arrest following chemical treatment, and top candidates were further assessed for duration of arrest, cellular integrity, and receptor binding. Although treatment with sodium azide yielded promising results, further analysis is required to identify an effective cytostatic agent.

Introduction

Cytoadherence of *Plasmodium falciparum* infected red blood cells (iRBC) to host tissues is a critical parasite mechanism that mediates malaria pathology. In addition to preventing clearance of blood-stage parasites by the spleen, parasite sequestration is responsible for the organ-specific manifestations characteristic of severe disease. The ability of iRBC to bind to endothelium within the microvasculature and become sequestered from the peripheral blood was first discovered by Marchiafava and Bignami in the 1890's [1]. However, despite being the focus of much research since that time, many important questions remain to be answered regarding the effects of parasite binding and sequestration on malaria pathology.

iRBC cytoadherence is mediated by a family of immunovariant adhesive proteins known as *Plasmodium falciparum* erythrocyte membrane protein-1 (*PfEMP1*). *PfEMP1* is encoded by the *var* genes, of which there are ~60 in each parasite genome. In order to evade the host immune response to infection, parasites express only one *PfEMP1* variant at a time and periodically switch variants in a process called antigenic variation. Different *PfEMP1* subtypes have been shown to bind to specific host cell receptors [2] and have been correlated with varying manifestations of severe disease [3–6]. For example, severe childhood malaria has been associated with *PfEMP1* subtypes containing domain cassettes (DC) 8 and 13 [5], and *in vitro* analyses of DC8-expressing parasites demonstrated binding to brain-derived endothelial cells via the endothelial protein C receptor (EPCR) [4]. In addition, binding of the *PfEMP1* variant VAR2CSA to placental chondroitin sulfate A has been repeatedly shown to mediate iRBC sequestration in the intervillous space and the development of placental malaria [3,7–9].

PfEMP1-mediated binding of iRBC to vascular endothelium induces critical changes to host endothelial cell structure and function. Under physiological flow conditions, iRBC have

been shown to interact synergistically with various host cells receptors on the microvascular endothelium in a shear-dependent manner [10,11]. iRBC rolling and tethering on intercellular adhesion molecule 1 (ICAM-1), vascular cell adhesion molecule 1 (VCAM-1), CD36, and P-selectin induces cytoskeletal restructuring, increased expression of CD36 and VCAM-1, and enhanced adhesion of iRBC [10,12,13]. In addition, cross-linking of CD36 and ICAM-1 has been shown to upregulate various signaling pathways as evidenced by increased expression of Src-related kinases, mitogen activated protein (MAP) kinases, and extracellular signal regulated (ERK-1) kinases [12,14]. Studies in our lab have demonstrated enhanced tyrosine phosphorylation and C-Jun N-terminal kinase 1 (JNK 1) activation in iRBC-stimulated primary syncytiotrophoblast [8,15]. However, more in depth analyses of the influence of iRBC adhesion to host tissues, and particularly the impact of extended iRBC binding, are limited by the duration of the parasite's intraerythrocytic life cycle and the laboratory tools available to isolate late-stage, adherent iRBC.

P. falciparum has a blood-stage life cycle of ~44-48 hours wherein the parasite expresses PfEMP1 on the erythrocyte membrane during the latter portion of this cycle (Figure 3.1). In many *P. falciparum* variants, PfEMP1 expression is associated with the development of surface protrusions, or knobs, on the surface of the erythrocyte membrane, which assist in mediating iRBC cytoadherence [16]. During its intraerythrocytic lifetime, the intracellular parasite digests 60 – 80% of its host cell's hemoglobin and packages the toxic heme moieties into a paramagnetic crystal known as hemozoin [17]. As the parasite matures and consumes the majority of hemoglobin in the cell, the iRBC density decreases. Current methods to isolate late-stage, adherent iRBC for *in vitro* studies rely on (a) density gradients that exploit this change in parasite density [18,19], (b) gradients that utilize changes in buoyancy brought about by knob formation

[20], or (c) dipole magnets that select for cells containing paramagnetic hemozoin crystals [21]. However, all of these methods select for late-stage parasites that are undergoing or nearing schizogony (Figure 3.1). As a result, *in vitro* analyses looking to study late, adherent iRBC are limited to the finite time remaining in the parasite's intraerythrocytic life. Particularly in the case of studies examining the effect of iRBC binding on host cell activation and/or immune signaling, this short time window of iRBC cytoadherence is nearly insurmountable.

In the following work, we explore methods by which to extend the lifetime of late, adherent iRBC. A wide variety of antimalarial agents was tested with the aim of identifying antimalarials that induce late-stage arrest of parasite growth. Top candidates from preliminary drug screens were further tested to determine the duration of late-stage arrest, maintained cellular integrity of drug-treated cells, and prolonged binding of arrested iRBC. These studies utilize the VAR2CSA-expressing parasite line CS2, a VAR2CSA knockout control, and the CSA-expressing BeWo choriocarcinoma cell line. Although treatment with sodium azide yielded promising results, further analysis will be required to optimize the treatment conditions of this general microbicide and/or identify a more effective cytostatic agent.

Materials and Methods

Blood and Reagents

Human O⁺ red blood cells were either purchased from Interstate Blood Bank, Inc. or donated by healthy volunteers. This research was approved by the Institutional Review Board (IRB) at the University of Georgia (no. 2013102100); all donors signed consent forms. Unless otherwise noted, all chemicals and reagents for this study were either purchased from Sigma Aldrich or Fisher Scientific.

Parasite Culture and Synchronization

Plasmodium falciparum CS2 and VAR2CSA KO parasites were maintained in continuous culture according to routine methods. VAR2CSA KO parasites were generated and generously donated by Artur Scherf (Institut Pasteur) [22]. Parasites were cultured at 4% hematocrit in O⁺ red blood cells. Cultures were maintained in 25 cm² or 75 cm² tissue culture flasks at 37°C under a gas mixture of 90% nitrogen/5% oxygen/5% carbon dioxide and in complete culture medium made up of RPMI containing 25 mM HEPES, 0.05 mg/mL hypoxanthine, 2.2 mg/mL NaHCO₃ (J.T. Baker), 0.5% Albumax (Gibco), 2 g/L glucose, and 0.01 mg/mL gentamicin. Primarily ring-stage cultures were treated routinely with 5% D-Sorbitol to achieve synchronous cultures.

Choriocarcinoma Cell Culture

The human choriocarcinoma cell line, BeWo, was obtained from American Type Tissue Culture (ATCC) and maintained as previously described [8]. For experiments, 1 mL of cells at a density of 100,000 cells/mL were seeded in a 24-well tissue culture plate. Single mononuclear

cytotrophoblast cells were induced to form a syncytium by addition of 40 μ M forskolin to the culture medium for 48 hours beginning at 24 hours post-seeding. Medium was changed daily. On the third day, medium was replaced with forskolin-free medium for 24 hours. By day four of culture, cells had formed a syncytium (BeWoST), at which point they were used for experiments.

Preliminary Drug Screen

Synchronous ring-stage CS2 and VAR2CSA KO iRBC were brought up to 4% hematocrit in complete culture medium and transferred to a 96-well tissue culture plate in 100 μ L aliquots. Cells were then treated with one of the following for 24 hours beginning at assay initiation, 2 hours beginning at assay initiation, or 2 hours beginning at 18 hours post-assay initiation: 790 nM artemisinin, 10 nM atovaquone, 200 nM chloroquine, 30 nM methotrexate hydrate (CS2), 800 nM methotrexate hydrate (KO), 50 μ M oryzalin, 10 μ M vinblastine, or 30 nM WR99210 (control). At 24, 2, or 20 hours post-assay initiation, drugged media were aspirated from their respective conditions, and cells were resuspended in 100 μ L complete culture medium for 24 additional hours. At 48 hour post-assay initiation, Giemsa-stained thin blood smears were prepared and analyzed by light microscopy. Images were acquired using a Nikon Eclipse E400 microscope fitted with a Nikon Digital Sight DS-5M-L1 camera (Nikon Instruments Inc.).

Optimized Drug Screen

Synchronous late-stage CS2 or VAR2CSA KO iRBC were brought up to 4% hematocrit in complete culture medium and transferred to a 96-well tissue culture plate in 100 μ L aliquots. Cells were subsequently treated with 5 μ M cycloheximide, 30 nM methotrexate hydrate (CS2),

800 nM methotrexate hydrate (KO), 15.4 mM (0.1% w/v) sodium azide, 10 μ M vinblastine, or 30 nM WR99210 (control) for 2 hours. Following 2-hour treatment, drugged media were aspirated, and cells were resuspended in complete culture medium and placed at 37°C under standard gas conditions. Giemsa-stained thin blood smears were prepared at 24, 48, and 72 hours post-assay initiation for analysis by light microscopy.

Parasitemia Analysis

Synchronous late-stage CS2 or VAR2CSA KO iRBC were brought up to 4% hematocrit in complete culture medium and transferred to a 24-well tissue culture plate in 1 ml aliquots. Cells were then treated as above and subsequently stored at 37°C under standard gas conditions. At 0, 10, 20, 30, 40, and 50 hours post-assay initiation, 25 μ L were removed from each well and stained with 2 μ g/mL Hoechst 33342 for 10 minutes at 37°C. Cells were subsequently washed three times with 1X PBS, resuspended in 300 μ L 1X PBS, and analyzed for Hoechst staining on a Beckman Coulter CyAn flow cytometer. 500,000 events were collected at a rate of 15,000 – 20,000 events per second. Data was analyzed using FlowJo single cell analysis software (FlowJo LLC).

BeWo Binding Analysis

Synchronous late-stage CS2 and VAR2CSA KO iRBC were brought up to 4% hematocrit in complete culture medium and transferred to a 6-well tissue culture plate at 5 mL per well. Cells were subsequently treated with 0.1% sodium azide for 2 hours, washed twice in RPMI, and resuspended in complete culture medium. Thereafter, 2 million cells were removed from each well every 8 hours and stained with 2 μ g/ml Hoechst 33342 for 10 minutes at room temperature.

Cells were then washed once with 1 mL RPMI and resuspended in 1 mL binding buffer composed of RPMI-1640 (HyClone) containing 25 mM HEPES and 10% human serum. BeWoST were rinsed once in RPMI after which iRBCs were overlaid on the syncytium and incubated for 1 hour at room temperature with gentle, continuous rocking. BeWoST were then washed three times with RPMI to remove unbound iRBC and uRBC. The number of bound iRBC was then determined via analysis using an Evos all-in-one digital inverted microscope (AMG Advanced Microscopy Group).

Statistical Analysis

Graphing and statistical analyses were done using GraphPad Prism 5 (GraphPad Software, Inc.).

Results

Methotrexate and vinblastine induce late-stage parasite arrest

In an effort to identify an antimalarial agent that induces late-stage parasite arrest, a wide panel of antimalarials with varying mechanisms of action was tested under three different treatment conditions. All antimalarial agents were applied at approximately 10 times their literature IC₅₀ values (Table 3.1). Since VAR2CSA KO mutants possess a human dihydrofolate reductase (hDHFR) expression cassette and can be selected using WR99210, WR99210 was included as a control in all drug screens. For the initial drug screen, synchronous ring-stage CS2 and VAR2CSA KO *P. falciparum*-iRBC were treated for 24 hours, 2 hours beginning at assay initiation, or 2 hours beginning at 18 hours post-assay initiation with 790 nM artemisinin, 10 nM atovaquone, 200 nM chloroquine, 30 nM methotrexate hydrate (CS2), 800 nM methotrexate hydrate (KO), 50 μ M oryzalin, 10 μ M vinblastine, 30 nM WR99210, or complete culture medium. Since methotrexate, like WR99210, is a DHFR inhibitor, VAR2CSA KO parasites were treated at 10 times the literature *h*sDHFR IC₅₀ value for methotrexate [23]. Cells were subsequently cultured in complete culture medium for 24 additional hours and analyzed by Giemsa-stained thin blood smear at 48 hours post-assay initiation. Of all antimalarials tested, only methotrexate and vinblastine induced late-stage arrest in both CS2 and VAR2CSA KO parasite strains (Figure 3.2).

Methotrexate and sodium azide induce late-stage parasite arrest following 2 hour treatment

Since methotrexate and vinblastine were the only antimalarial agents in our initial screen that achieved late-stage parasite arrest, we next decided to explore the antiparasitodal activity of the more general antimicrobials, cycloheximide and sodium azide. Cycloheximide is an

antimicrobial that inhibits translation elongation and protein synthesis in eukaryotes [24]. Furthermore, previous studies have demonstrated *P. falciparum* sensitivity to cycloheximide [25–27]. Meanwhile, sodium azide is a common biocide that is frequently used as a preservative in aqueous laboratory solutions, such as stock solutions and buffers. Although the mechanism of action of sodium azide has not been fully established, evidence suggests that this compound binds to cytochrome oxidase and inhibits cellular respiration and the mitochondrial electron transport chain [28]. Few studies have used sodium azide in the treatment of *P. falciparum*; however, those that have successfully induced parasite death following treatment with 0.1% sodium azide (Table 3.1) [29].

Since two hour treatment was sufficient to induce late-stage arrest with methotrexate and vinblastine, cycloheximide and sodium azide were applied under the same conditions. Synchronous late-stage CS2 and VAR2CSA KO iRBC were treated for 2 hours with 5 μ M cycloheximide, 30 nM methotrexate hydrate (CS2), 800 nM methotrexate hydrate (KO), 0.1% sodium azide, 10 μ M vinblastine, 30 nM WR99210, or complete culture medium. Cells were then cultured for 24 hours at 37°C under standard gas conditions and analyzed by Giemsa-stained thin blood smear at 24 hours post-treatment. All applied treatments induced late-stage arrest of both CS2 and VAR2CSA KO iRBC (Figure 3.3).

In order to confirm complete arrest of CS2 and VAR2CSA KO iRBC, cells were again treated for 2 hours as above, and parasitemia was determined by flow cytometry at 24 hours post-treatment. Although analysis by Giemsa-stained blood smears had shown clear evidence of late-stage arrest following all treatments, more careful analysis by flow cytometry demonstrated that only methotrexate and sodium azide induced thorough arrest of parasite growth (Figure 3.4).

Methotrexate and sodium azide are suboptimal candidates for in vitro parasite adhesion studies

Although methotrexate was a strong candidate for late-stage arrest of *P. falciparum*-iRBC, a variety of factors complicate the use of this DHFR-targeting drug. For example, genetic transformation of *Plasmodium* parasites via transfection with the WR99210-selectable hDHFR is one of the few genetic tools available for stable transfection of *Plasmodium* parasites [30]. As a result, hDHFR-possessing parasites, which demonstrate >1000-fold resistance to WR99210 relative to their parental controls [31], are relatively common in malaria research. Methotrexate-mediated arrest of such transfected parasites would require drastically different treatment conditions relative to wild type parasites. In addition, methotrexate hydrate is a rather expensive drug that sells for \$1 - \$4 per mg. It is also relatively unstable, lasting only ~1 month in solution at -20°C, and is entirely insoluble in water. Since our aim was to develop a simple laboratory technique that could be widely applied throughout the field, we chose to focus our efforts on sodium azide, which is a common and inexpensive laboratory reagent that is stable in solution indefinitely at 4°C.

To examine the effect of sodium azide treatment on iRBC cytoadherence and *Pf*EMP1 expression, late-stage CS2 and VAR2CSA KO iRBC were treated for 2 hours with 0.1% sodium azide and subsequently stained with 2 µg/mL Hoechst 33342. Fluorescent iRBC were then overlaid on BeWoST at a cell density of 2 million iRBC per mL. Cells were then allowed to bind for 1 hour with gentle rocking, washed three times with RPMI, and examined by fluorescence microscopy every 8 hours. Surprisingly, treated CS2 iRBC did not demonstrate prolonged binding to BeWoST relative to untreated CS2 controls (data not shown). More careful analysis of sodium azide-treated iRBC demonstrated that, although 0.1% sodium azide has robust cytostatic activity against iRBC, 0.1% is not sufficient to universally arrest neither CS2 nor VAR2CSA KO

parasites. Analysis of higher concentrations of sodium azide indicated that concentrations $\geq 0.4\%$ sodium azide were required to achieve universal arrest of iRBC (Figure 3.5). However, examination of Giemsa-stained thin blood smears following treatment with such concentrations of sodium azide showed that concentrations $\geq 0.3\%$ cause degradation of treated cells (Figure S3.1). As a result, we conclude that sodium azide may not be an optimal choice for cytostatic arrest of *P. falciparum*-iRBC.

Discussion

The limited laboratory tools available to isolate and maintain late-stage iRBC significantly inhibit the feasibility of prolonged *in vitro* studies of cytoadherent iRBC. A more in depth appreciation of the influence of parasite cytoadherence to host endothelial tissues is critical to our understanding of the immunopathogenesis of this ancient disease. Herein, we examined the cytostatic potential of a wide panel of antimalarial agents with the aim of arresting late-stage iRBC for use in *in vitro* adherence studies. Our careful analysis of eight different antimalarial and antimicrobial agents has identified only two compounds capable of inducing late-stage arrest of both wild type and mutant *P. falciparum*-iRBC. Although sodium azide showed considerable potential as a new laboratory tool that might prolong the lifetime of late, adherent iRBC, further analysis demonstrated drug-induced toxicity at concentrations required to achieve universal arrest of parasite growth.

Although results with sodium azide were ultimately problematic, our lab will continue to pursue the identification of a cytostatic agent and the development of this critical tool for malaria research. Despite the complications associated with using methotrexate, future studies will seek to further explore the cytostatic potential of this DHFR inhibitor. Some steps can be taken to improve the working conditions of this highly insoluble compound. For example, although diluted stocks are only stable for ~1 month at -20°C, storage of methotrexate hydrate in neat 1M NaOH would increase the shelf life of this compound up to three years at -20°C. Further characterization of methotrexate-induced parasite arrest in both wild type and mutant *P. falciparum* will be necessary to fully define the practicality of this compound as a laboratory tool for drug-induced parasite arrest.

In addition to methotrexate, other compounds will be considered as potential cytostatic agents. For example, various parasite protease inhibitors have been demonstrated to block egress of mature schizonts from the infected erythrocyte [32,33]. Studies carefully delineating the role of parasite proteases in this process have shown that treatment with the cysteine protease inhibitor E64 prevents rupture of the parasitophorous vacuole membrane while treatment with leupeptin and antipain inhibit lysis of the erythrocyte membrane. Therefore, treatment of late-stage iRBC with such protease inhibitors would prevent iRBC rupture and prolong the lifetime of late, cytoadherent iRBC. However, careful analysis will be required to probe the duration of parasite arrest following removal of protease inhibitors from the culture medium.

Conclusions

New laboratory methods that prolong the lifetime of late, adherent *P. falciparum*-iRBC would provide a critical tool to understanding the influence of parasite cytoadherence on host cell function and the immunopathogenesis of malaria. This study carefully examined the cytostatic potential of eight antimalarial and antimicrobial agents in wild type and mutant iRBC *in vitro*. A thorough analysis of sodium azide demonstrated this compound to be an inadequate mediator of universal arrest of late, cytoadherent iRBC. Future studies will further examine the cytostatic potential of methotrexate and consider other promising candidates that may induce late-stage arrest of cytoadherent iRBC for *in vitro* chronic adhesion studies.

References

1. White NJ, Turner GDH, Day NPJ, Dondorp AM (2013) Lethal Malaria: Marchiafava and Bignami Were Right. *J Infect Dis* 208: 192–198. doi:10.1093/infdis/jit116.
2. Rowe JA, Claessens A, Corrigan R a, Arman M (2009) Adhesion of *Plasmodium falciparum*-infected erythrocytes to human cells: molecular mechanisms and therapeutic implications. *Expert Rev Mol Med* 11: e16. doi:10.1017/S1462399409001082.
3. Magistrado P, Salanti A, Tuikue Ndam NG, Mwakalinga SB, Resende M, et al. (2008) VAR2CSA expression on the surface of placenta-derived *Plasmodium falciparum*-infected erythrocytes. *J Infect Dis* 198: 1071–1074. doi:10.1086/591502.
4. Turner L, Lavstsen T, Berger SS, Wang CW, Petersen JE V, et al. (2013) Severe malaria is associated with parasite binding to endothelial protein C receptor. *Nature* 498: 502–505. doi:10.1038/nature12216.
5. Lavstsen T, Turner L, Saguti F, Magistrado P, Rask TS, et al. (2012) *Plasmodium falciparum* erythrocyte membrane protein 1 domain cassettes 8 and 13 are associated with severe malaria in children. *Proc Natl Acad Sci* 109: E1791–E1800. doi:10.1073/pnas.1120455109.
6. Almelli T, Ndam NT, Ezimegnon S, Alao MJ, Ahouansou C, et al. (2014) Cytoadherence phenotype of *Plasmodium falciparum*-infected erythrocytes is associated with specific pfemp-1 expression in parasites from children with cerebral malaria. *Malar J* 13: 333. doi:10.1186/1475-2875-13-333.
7. Fried M, Duffy PE (1996) Adherence of *Plasmodium falciparum* to chondroitin sulfate A in the human placenta. *Science* 272: 1502–1504. doi:10.1126/science.272.5267.1502.
8. Lucchi NW, Koopman R, Peterson DS, Moore JM (2006) *Plasmodium falciparum*-infected red blood cells selected for binding to cultured syncytiotrophoblast bind to chondroitin sulfate A and induce tyrosine phosphorylation in the syncytiotrophoblast. *Placenta* 27: 384–394. doi:10.1016/j.placenta.2005.04.009.
9. Yosaatmadja F, Andrews KT, Duffy MF, Brown G V, Beeson JG, et al. (2008) Characterization of VAR2CSA-deficient *Plasmodium falciparum*-infected erythrocytes selected for adhesion to the BeWo placental cell line. *Malar J* 7: 51. doi:10.1186/1475-2875-7-51.
10. Yipp BG, Anand S, Schollaardt T, Patel KD, Looareesuwan S, et al. (2000) Synergism of multiple adhesion molecules in mediating cytoadherence of *Plasmodium falciparum*-infected erythrocytes to microvascular endothelial cells under flow. *Blood* 96: 2292–2298.

11. Cells RED, Rieger H, Yoshikawa HY, Quadt K, Nielsen M a, et al. (2015) Cytoadhesion of *Plasmodium falciparum* – infected erythrocytes to chondroitin-4-sulfate is cooperative and shear enhanced. 125: 12–15. doi:10.1182/blood-2014-03-561019.The.
12. Lawson C, Ainsworth M, Yacoub M, Rose M (1999) Ligation of ICAM-1 on endothelial cells leads to expression of VCAM-1 via a nuclear factor-kappaB-independent mechanism. *J Immunol* 162: 2990–2996.
13. Davis SP, Lee K, Gillrie MR, Roa L, Amrein M, et al. (2013) CD36 Recruits $\alpha 5\beta 1$ Integrin to Promote Cytoadherence of *P. falciparum*-Infected Erythrocytes. *PLoS Pathog* 9. doi:10.1371/journal.ppat.1003590.
14. Yipp BG, Robbins SM, Resek ME, Baruch DI, Looareesuwan S, et al. (2003) Src-family kinase signaling modulates the adhesion of *Plasmodium falciparum* on human microvascular endothelium under flow. *Blood* 101: 2850–2857. doi:10.1182/blood-2002-09-2841.
15. Lucchi NW, Peterson DS, Moore JM (2008) Immunologic activation of human syncytiotrophoblast by *Plasmodium falciparum*. *Malar J* 7: 42. doi:10.1186/1475-2875-7-42.
16. Quadt K a, Barfod L, Andersen D, Bruun J, Gyan B, et al. (2012) The density of knobs on *Plasmodium falciparum*-infected erythrocytes depends on developmental age and varies among isolates. *PLoS One* 7: e45658. doi:10.1371/journal.pone.0045658.
17. Francis SE, Sullivan DJ, Goldberg DE (1997) Hemoglobin metabolism in the malaria parasite *Plasmodium falciparum*. *Annu Rev Microbiol* 51: 97–123. doi:10.1146/annurev.micro.51.1.97.
18. Rivadeneira E, Wasserman M, Espinal C (1983) Separation and concentration of schizonts of *Plasmodium falciparum* by Percoll gradients. *J Protozool* 30: 367–370.
19. Eling W (1977) Ficoll fractionation for the separation of parasitized erythrocytes. 55.
20. Goodyer I, Johnson J, Eisenthal R, Hayes D (1984) Purification of mature-stage *Plasmodium falciparum* by gelatine flotation. *Ann Trop Med Parasitol* 88: 209–211.
21. Bhakdi SC, Ottinger A, Somsri S, Sratongno P, Pannadaporn P, et al. (2010) Optimized high gradient magnetic separation for isolation of *Plasmodium*-infected red blood cells. *Malar J* 9: 38. doi:10.1186/1475-2875-9-38.
22. Viebig NK, Gamain B, Scheidig C, Lépolard C, Przyborski J, et al. (2005) A single member of the *Plasmodium falciparum* var multigene family determines cytoadhesion to the placental receptor chondroitin sulphate A. *EMBO Rep* 6: 775–781. doi:10.1038/sj.embor.7400466.

23. Norris RE, Adamson PC (2010) Clinical potency of methotrexate, aminopterin, talotrexin and pemetrexed in childhood leukemias. *Cancer Chemother Pharmacol* 65: 1125–1130. doi:10.1007/s00280-009-1120-8.
24. Schneider-poetsch T, Ju J, Eyler DE, Dang Y, Bhat S, et al. (2010) Inhibition of Eukaryotic Translation Elongation by Cycloheximide and Lactimidomycin. 6: 209–217. doi:10.1038/nchembio.304.Inhibition.
25. Babbitt SE, Altenhofen L, Cobbold SA, Istvan ES, Fennell C, et al. (2012) *Plasmodium falciparum* responds to amino acid starvation by entering into a hibernatory state. *Proc Natl Acad Sci U S A* 109: E3278–E3287. doi:10.1073/pnas.1209823109.
26. Martin RE, Kirk K (2007) Transport of the essential nutrient isoleucine in human erythrocytes infected with the malaria parasite *Plasmodium falciparum*. *Blood* 109: 2217–2224. doi:10.1182/blood-2005-11-026963.The.
27. Budimulja AS, Tapchaisri P, Wilairat P, Marzuki S (1997) The sensitivity of *Plasmodium* protein synthesis to prokaryotic ribosomal inhibitors. 84: 137–141.
28. Ishikawa T, Zhu B-L, Maeda H (2006) Effect of sodium azide on the metabolic activity of cultured fetal cells. *Toxicol Ind Health* 22: 337–341. doi:10.1177/0748233706071737.
29. Ch'ng J-H, Kotturi SR, Chong a G-L, Lear MJ, Tan KS-W (2010) A programmed cell death pathway in the malaria parasite *Plasmodium falciparum* has general features of mammalian apoptosis but is mediated by clan CA cysteine proteases. *Cell Death Dis* 1: e26. doi:10.1038/cddis.2010.2.
30. Carvalho TG, Ménard R (2005) Manipulating the *Plasmodium* genome. *Curr Issues Mol Biol* 7: 39–55.
31. Koning-ward TF De, Fidock D a, Thathy V, Menard R, Spaendonk RML Van, et al. (2000) The selectable marker human dihydrofolate reductase. *Mol Biochem Parasitol* 106: 199–212.
32. Wickham ME, Culvenor JG, Cowman AF (2003) Selective inhibition of a two-step egress of malaria parasites from the host erythrocyte. *J Biol Chem* 278: 37658–37663. doi:10.1074/jbc.M305252200.
33. Salmon BL, Oksman a, Goldberg DE (2001) Malaria parasite exit from the host erythrocyte: a two-step process requiring extraerythrocytic proteolysis. *Proc Natl Acad Sci U S A* 98: 271–276. doi:10.1073/pnas.98.1.271.
34. Uhlemann AC, Wittlin S, Matile H, Bustamante LY, Krishna S (2007) Mechanism of antimalarial action of the synthetic trioxolane RBX11160 (OZ277). *Antimicrob Agents Chemother* 51: 667–672. doi:10.1128/AAC.01064-06.

35. Moneriz C, Marín-García P, García-Granados A, Bautista JM, Diez A, et al. (2011) Parasitostatic effect of maslinic acid. I. Growth arrest of *Plasmodium falciparum* intraerythrocytic stages. *Malar J* 10: 82. doi:10.1186/1475-2875-10-82.
36. Vivas L, Rattray L, Stewart LB, Robinson BL, Fugmann B, et al. (2007) Antimalarial efficacy and drug interactions of the novel semi-synthetic endoperoxide artemisone in vitro and in vivo. *J Antimicrob Chemother* 59: 658–665. doi:10.1093/jac/dkl563.
37. Imwong M, Russell B, Suwanarusk R, Nzila A, Leimanis ML, et al. (2011) Methotrexate is highly potent against pyrimethamine-resistant *Plasmodium vivax*. *J Infect Dis* 203: 207–210. doi:10.1093/infdis/jiq024.
38. Fennell BJ, Naughton JA, Dempsey E, Bell A (2006) Cellular and molecular actions of dinitroaniline and phosphorothioamidate herbicides on *Plasmodium falciparum*: tubulin as a specific antimalarial target. *Mol Biochem Parasitol* 145: 226–238. doi:10.1016/j.molbiopara.2005.08.020.
39. Ommeh S, Nduati E, Mberu E, Kokwaro G, Marsh K, et al. (2004) In Vitro Activities of 2 , 4-Diaminoquinazoline and 2 , 4-Diaminopteridine Derivatives against *Plasmodium falciparum*. *Society* 48: 3711–3714. doi:10.1128/AAC.48.10.3711.

Figures

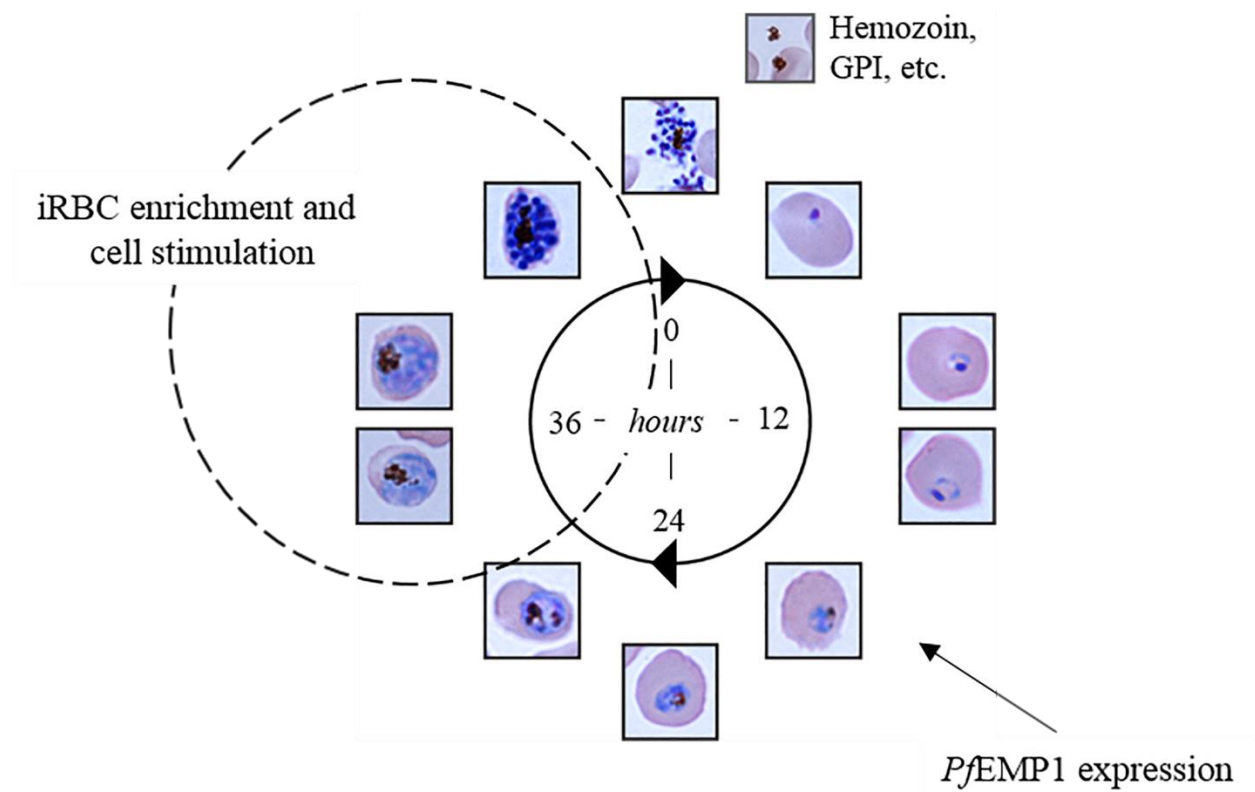


Figure 3.1. Complications with *in vitro* analyses using cytoadherent *P. falciparum*-iRBC. *P. falciparum* has a blood-stage life cycle of ~44-48 hours wherein the parasite begins expressing cytoadherent PfEMP1 at the erythrocyte membrane beginning at ~16 hours post-invasion. Existing iRBC isolation methods select for late-stage parasites that are undergoing or nearing schizogony. As a result, *in vitro* analyses with cytoadherent iRBC are limited to the short time window preceding the termination of the parasite life cycle and the release of parasite by-products, such as hemozoin and parasite GPI.

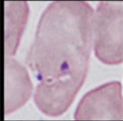
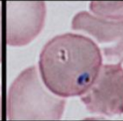
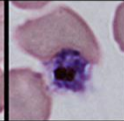
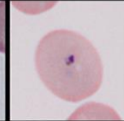
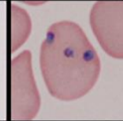
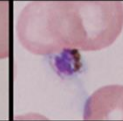
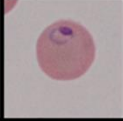
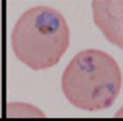
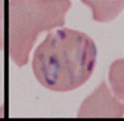
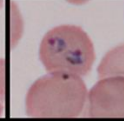
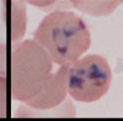
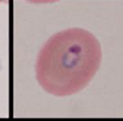
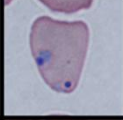
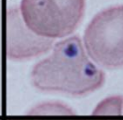
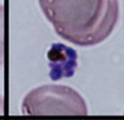
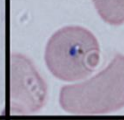
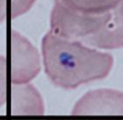
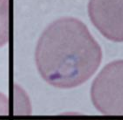
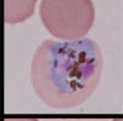

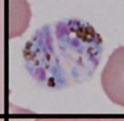
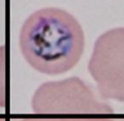
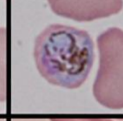
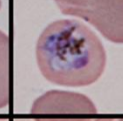
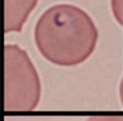


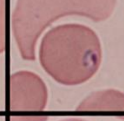
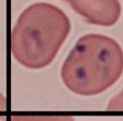
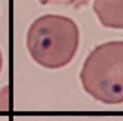
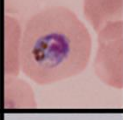
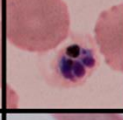
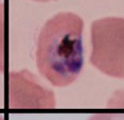
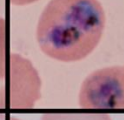
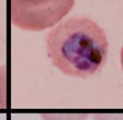

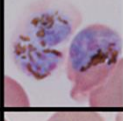
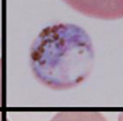
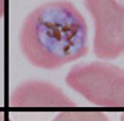
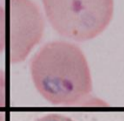

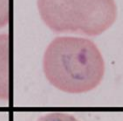
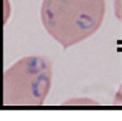
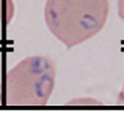
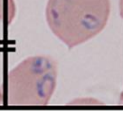
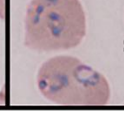
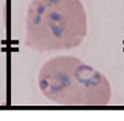
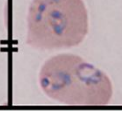
Drug	WT 24 hours	WT 2 ₀ hours	WT 2 ₁₈ hours	KO 24 hours	KO 2 ₀ hours	KO 2 ₁₈ hours	Late-stage arrest?
Artemisinin							No
Atovaquone							No
Chloroquine							No
Methotrexate							Yes
Oryzalin							No
Vinblastine							Partial
WR99210							WT, yes KO, no
Negative Control							

Figure 3.2. Methotrexate and vinblastine induce late-stage arrest of intracellular *P.*

falciparum. Synchronous ring-stage CS2 and VAR2CSA KO iRBC were treated with antimalarial agents for 24 hours, 2 hours beginning at assay initiation, or 2 hours beginning at 18 hours post-assay initiation (trophozoite stage) and examined for late-stage arrest via Giemsa-stained thin blood smear at 48 hours post-assay initiation. Only methotrexate and vinblastine induced late-stage arrest of iRBC.

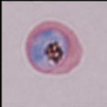
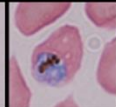
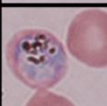
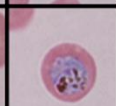
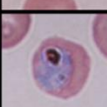

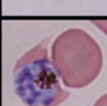

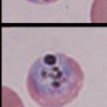
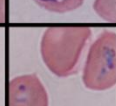
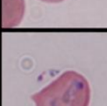

Drug	WT CS2	var2csa KO
Cycloheximide		
Methotrexate		
Sodium Azide		
Vinblastine		
WR99210 Control		
Negative Control		

Figure 3.3. Cycloheximide, methotrexate, sodium azide, and vinblastine are promising cytostatic agents. Synchronous late-stage CS2 and VAR2CSA KO iRBC were treated for two hours and analyzed by Giemsa-stained thin blood smear at 24 hours post-treatment. Methotrexate, sodium azide, vinblastine, and cycloheximide induced late-stage arrest of iRBC.

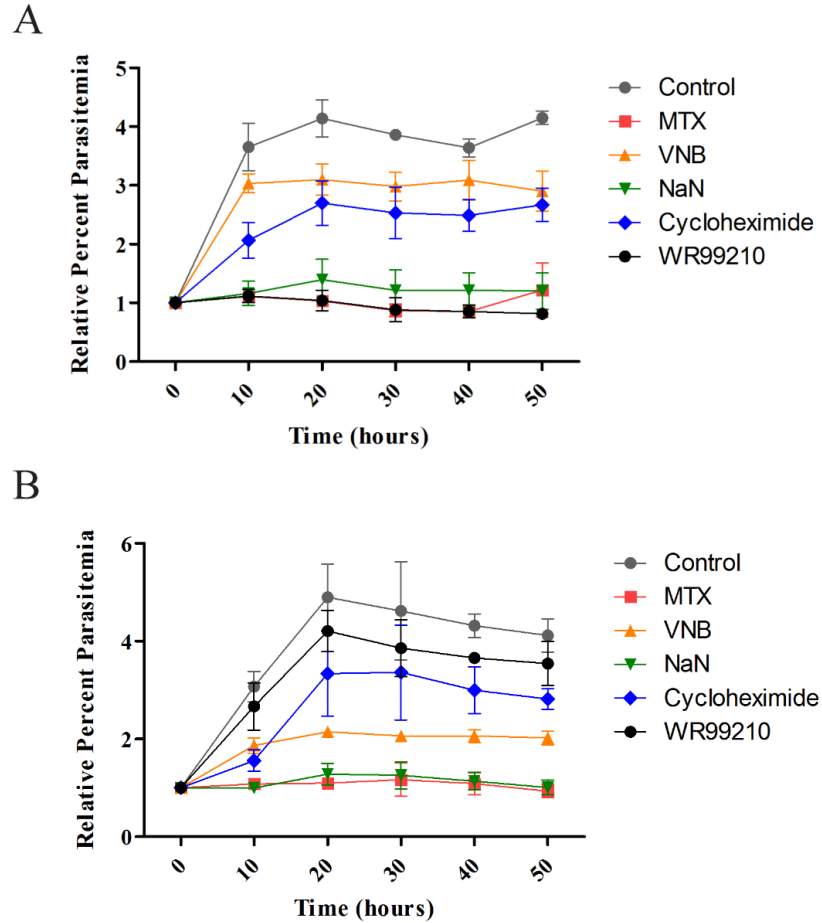


Figure 3.4. Sodium azide and methotrexate arrest parasite growth. Synchronous late-stage CS2 (**A**) and VAR2CSA KO (**B**) iRBC were treated with complete culture medium (grey), vinblastine (orange), cycloheximide (blue), sodium azide (green), methotrexate (red) or WR99210 (black) for 2 hours, and parasitemia was analyzed by flow cytometry at 24 hours post-treatment. Parasitemias are reported as change relative to initial parasitemia. Sodium azide and methotrexate induced a clear arrest in parasite growth in both CS2 and VAR2CSA KO parasite strains.

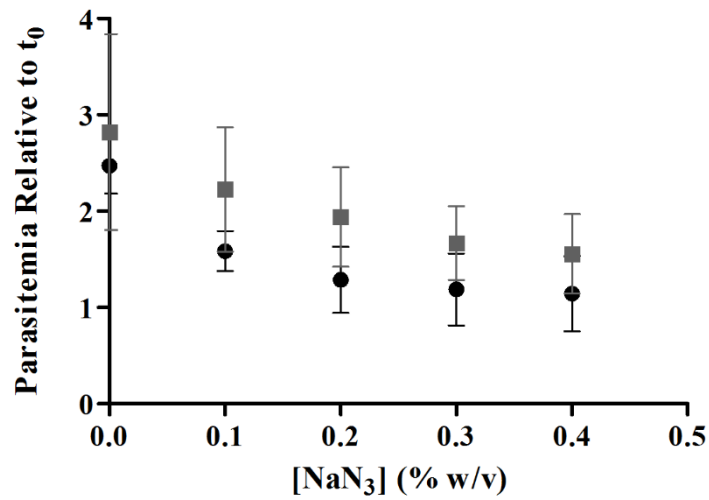


Figure 3.5. High concentrations of sodium azide are required to universally arrest parasite growth. Synchronous late-stage CS2 (black) and VAR2CSA KO (grey) iRBC were treated with increasing concentrations of sodium azide for 2 hours, and parasitemia was analyzed by flow cytometry at 24 hours post-treatment. Data is presented as parasitemia relative to that at assay initiation. $\geq 0.4\%$ sodium azide was required to achieve universal arrest of both CS2 and VAR2CSA KO parasite strains.

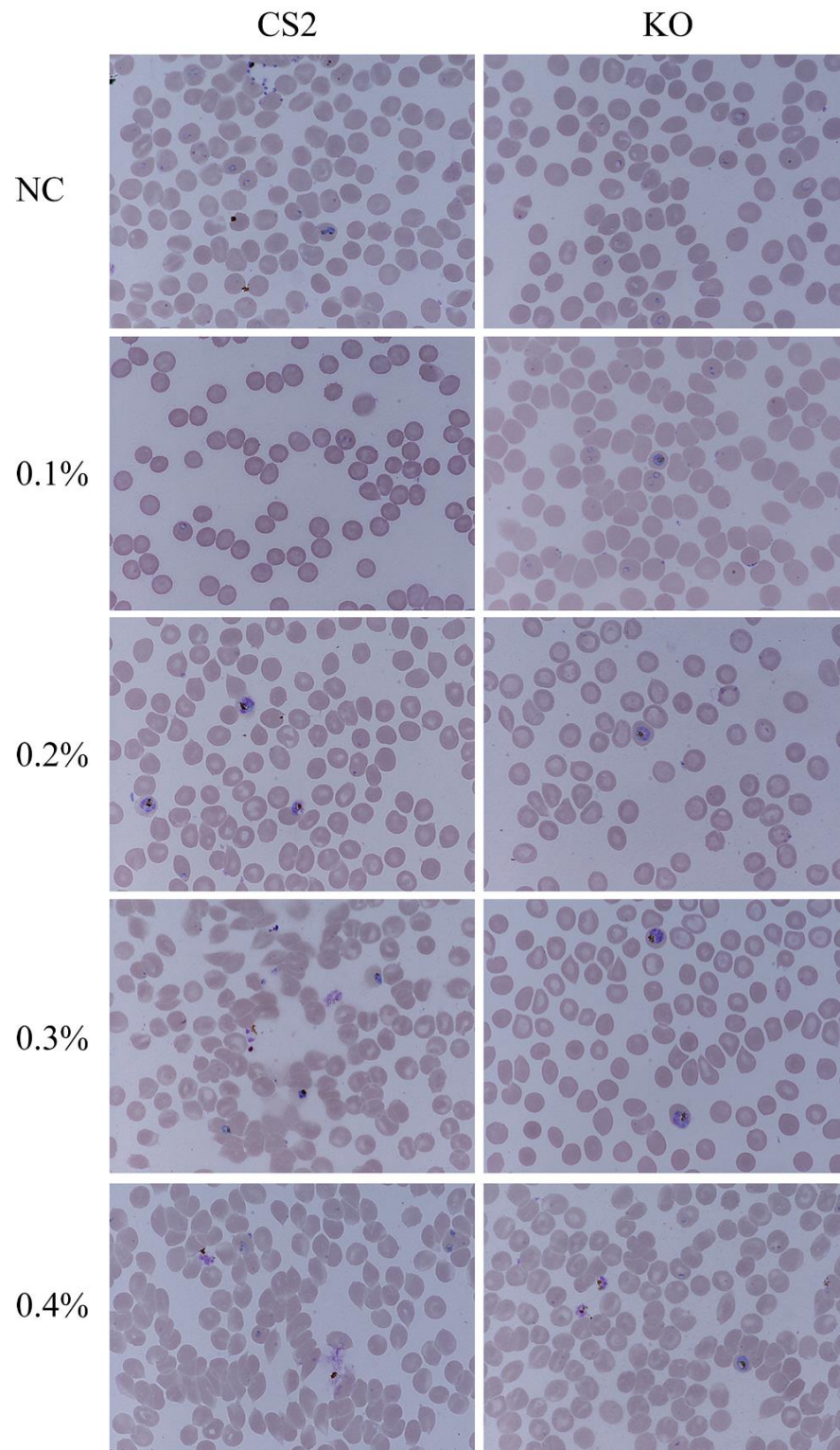


Figure S3.1. Late-stage iRBC degrade following treatment with high concentrations of sodium azide. Synchronous late-stage CS2 (black) and VAR2CSA KO (grey) iRBC were

treated with increasing concentrations of sodium azide for 2 hours and analyzed by Giemsa-stained thin blood smear at 24 hours post-treatment. $<0.2\%$ sodium azide fails to induce universal parasite arrest, and $\geq 0.3\%$ sodium azide induces parasite degradation.

Tables

Table 3.1. Antimalarial Agents

<i>Antimalarial</i>	<i>Concentration Used</i>	<i>IC₅₀</i>	<i>Mechanism of Action</i>	<i>Literature</i>
<i>Artemisinin</i>	790 nM	79 nM	Undefined	[34]
<i>Atovaquone</i>	10 nM	0.8 – 1.1 nM	Electron transport chain inhibition	[35,36]
<i>Chloroquine</i>	200 nM	9.73 – 19 nM	Inhibition of heme polymerization	[36]
<i>Cycloheximide</i>	5 µM	0.5 µM	Inhibition of translation elongation	[27]
<i>Methotrexate</i>	30 nM, 800 nM	2.6 nM, 78 nM	DHFR inhibition	[37,23]
<i>Oryzalin</i>	50 µM	4.3 µM	Inhibition of microtubule polymerization	[38]
<i>Sodium Azide</i>	15.4 mM (0.1%)		Electron transport chain inhibition	[29]
<i>Vinblastine</i>	10 µM	0.028 – 1.7 µM	Inhibition of microtubule polymerization	[38]
<i>WR99210</i>	30 nM	2.7 nM	DHFR inhibition	[39]

CHAPTER 4

THE STAPLED AKAP DISRUPTOR PEPTIDE STAD-2 DISPLAYS ANTIMALARIAL ACTIVITY THROUGH A PKA-INDEPENDENT MECHANISM²

² Flaherty, B.R., Wang, Y., Trope, E.C., Ho, T.G., Muralidharan, V., Kennedy, E.J., and Peterson, D.S. 2015. PLoS ONE 10(5): e0129239. Reprinted here with permission of publisher.

Abstract

Drug resistance poses a significant threat to ongoing malaria control efforts. Coupled with lack of a malaria vaccine, there is an urgent need for the development of new antimalarials with novel mechanisms of action and low susceptibility to parasite drug resistance. Protein Kinase A (PKA) has been implicated as a critical regulator of pathogenesis in malaria. Therefore, we sought to investigate the effects of disrupted PKA signaling as a possible strategy for inhibition of parasite replication. Host PKA activity is partly regulated by a class of proteins called A Kinase Anchoring Proteins (AKAPs), and interaction between *Hs*PKA and AKAP can be inhibited by the stapled peptide Stapled AKAP Disruptor 2 (STAD-2). STAD-2 was tested for permeability to and activity against *Plasmodium falciparum* blood stage parasites *in vitro*. The compound was selectively permeable only to infected red blood cells (iRBC) and demonstrated rapid antiplasmodial activity, possibly via iRBC lysis ($IC_{50} \approx 1 \mu M$). STAD-2 localized within the parasite almost immediately post-treatment but showed no evidence of direct association with PKA, indicating that STAD-2 acts via a PKA-independent mechanism. Furosemide-insensitive parasite permeability pathways in the iRBC were largely responsible for uptake of STAD-2. Further, peptide import was highly specific to STAD-2 as evidenced by low permeability of control stapled peptides. Selective uptake and antiplasmodial activity of STAD-2 provides important groundwork for the development of stapled peptides as potential antimalarials. Such peptides may also offer an alternative strategy for studying protein-protein interactions critical to parasite development and pathogenesis.

Introduction

Malaria, caused by haemoprotezoan parasites of the genus *Plasmodium*, is endemic to nearly 100 countries, placing the lives of an estimated 3.2 billion people at risk each year. Despite widespread endemicity, intensified control efforts have reduced annual malaria-attributable deaths by approximately 47% from nearly 1 million in 2000 to 584 000 in 2013 [1]. Such advances in malaria control are critically dependent on effective disease diagnosis and efficacious drugs. Of the five species of *Plasmodium* currently known to infect humans, *P. falciparum* is the most pathogenic, accounting for the majority of malaria-related deaths, while *P. vivax* has a wider geographic distribution owing to its ability to survive in higher altitudes and cooler climates [1]. Since 2002, artemisinin combination therapy (ACT) has been the recommended first line treatment for uncomplicated *P. falciparum* malaria [2], and chloroquine is recommended for *P. vivax* in regions where it remains efficacious [1]. However, extensive resistance to all existing antimalarials, including growing resistance to artemisinin in the Greater Mekong Subregion, threatens to place control efforts, and millions of lives, in jeopardy [3–5].

As the threat of widespread artemisinin resistance looms, there is a growing need for antimalarials that are less vulnerable to parasite mechanisms of drug resistance. To date, all existing antimalarials, as well as most of those being pursued as potential candidates [6–10], are small molecule inhibitors. These drugs typically act by binding within tight, hydrophobic pockets of target proteins. Although many factors contribute to the development of drug resistant parasites, the binding restrictions of these small molecule inhibitors render them inherently vulnerable to loss of activity via random genetic mutations in the parasite. Most existing antimalarials have lost efficacy as a result of protein mutations that inhibit binding either to their target protein or to parasite transporters [11]. For example, mutations of residues within the

binding pocket of the parasite's dihydrofolate reductase led to resistance towards cycloguanil and pyrimethamine [12,13]; single mutations within the binding pocket of cytochrome b generated resistance to atovaquone [14–16]; mutations within the binding pockets of parasite transporters *PfCRT* and *PfMDR1* eliminated activity of chloroquine and many ACT partner drugs (such as mefloquine and lumefantrine) [17,18]; and new evidence suggests mutations in the *PfKelch13* propeller domain may be responsible for rising resistance to artemisinin [19–21]. As the search for the next antimalarial intensifies, there is an urgent need for new classes of inhibitors that act via unique mechanisms of action and possess reduced vulnerability to parasite drug resistance.

Stapled peptides are a novel class of inhibitors that can be designed to bind protein interfaces with high specificity and thereby block intra- or inter-molecular protein-protein interactions [22,23]. Unlike traditional protein therapeutics which are largely limited to extracellular targets, peptide stapling affords the ability to target a myriad of flat, elongated intracellular surfaces with high specificity due to its increased propensity for cell penetration [24]. Although many stapled peptides were originally engineered for various cancer targets [24,25], their unique potential as antimicrobial agents has recently been explored [26–28]. However, stapled peptides have not yet been tested in *Plasmodium*.

In the following study, we examined the permeability and activity of the stapled peptide, STAD-2, in *P. falciparum* infected red blood cells (iRBC) [29]. This peptide was originally designed to disrupt interaction between the regulatory subunits of human Protein Kinase A (PKA) and A Kinase Anchoring Proteins (AKAPs). PKA is a cAMP-dependent protein kinase that is critical for a wide variety of cellular processes. *HsPKA* activity is highly regulated and dependent on multiple factors including intracellular cAMP concentrations and spatial and temporal localization via AKAP interactions [30–33]. AKAPs typically bind to the docking and

dimerization domain (D/D) interface formed between two PKA regulatory (PKA-R) subunits. This docking site serves to recruit PKA to distinct subcellular locations and is a critical component of PKA regulation [29,30]. In *P. falciparum*, parasite PKA plays an important role in pathogenesis including regulation of protein phosphorylation, transport of molecules across the RBC membrane, and activation of “new permeability pathways” [34,35]. Further, RBCs release ATP in response to infection with *Plasmodium* parasites, which subsequently activates extracellular receptors to increase intracellular cAMP concentrations, thereby activating PKA. This signaling can ultimately cause deformations in the plasma membrane of both uninfected and infected RBCs [36]. While the role of AKAPs in healthy RBCs is poorly understood, recent work has shown that AKAPs play a critical role in RBC membrane stiffness and adhesion [37]. On the other hand, little is known regarding AKAPs in iRBCs; however, bioinformatics analyses have identified an ortholog of the *P. yoelii* AKAP within the *P. falciparum* genome [38]. In addition, subcellular localization of *Pf*PKA is thought to be critical for *Pf*PKA activity within iRBCs, suggesting a vital role for AKAPs in *P. falciparum* pathogenesis [39]. Much remains to be discovered regarding the roles of PKA and AKAPs in *P. falciparum* iRBCs as well as the interplay between parasite and host PKA in regulating PKA-dependent cellular processes.

Since many questions remain about the roles of *Hs*PKA and *Pf*PKA on *P. falciparum* pathogenesis and since the role of AKAPs is not well established in RBCs, we sought to explore the effects of treatment of *P. falciparum* iRBCs with the AKAP disruptor peptide STAD-2 (Stapled AKAP Disruptor 2). This work builds upon previous studies by Wang et al. which showed STAD-2 peptides were cell permeable in various mammalian cell lines and highly effective at inhibiting the intracellular interaction between *Hs*PKA-RII and AKAPs [29]. Although some important differences exist between *Pf*PKA and its human ortholog [38,40],

*Pf*PKA was previously suggested as a promising antimalarial target [34,38]. Therefore, we sought to explore whether PKA could be exploited as a potential target for inhibiting parasite pathogenesis. STAD-2 was found to be selectively permeable to iRBC and, unexpectedly, demonstrated rapid antiplasmodial activity via a PKA-independent mechanism. Furosemide-insensitive, parasite-derived permeability appears to play a significant role in iRBC import of the compound. STAD-2 localized within the intracellular parasite but was not observed within the RBC cytosol. Further, STAD-2 did not clearly associate with the regulatory subunits of PKA, indicating STAD-2 likely acts through an alternative mechanism for inhibited parasite viability. This is the first example of uptake of a stapled peptide by *P. falciparum*-iRBCs, and these findings provide important groundwork for the development of stapled peptides for malaria-specific targets.

Materials and Methods

Blood and Reagents

Human O⁺ red blood cells were either purchased from Interstate Blood Bank, Inc. or donated by healthy volunteers. This research was approved by the Institutional Review Board (IRB) at the University of Georgia (no. 2013102100); all donors signed consent forms. Unless otherwise noted, all chemicals and reagents for this study were either purchased from Sigma Aldrich or Fisher Scientific.

Parasite Culture and Synchronization

Plasmodium falciparum strains CS2, 3D7, Hb3, and Dd2 were maintained in continuous culture according to routine methods. Parasites were cultured at 4% hematocrit in O⁺ red blood cells. Cultures were maintained in 25 cm² or 75 cm² tissue culture flasks at 37°C under a gas mixture of 90% nitrogen/5% oxygen/5% carbon dioxide and in complete culture medium made up of RPMI containing 25 mM HEPES, 0.05 mg/mL hypoxanthine, 2.2 mg/mL NaHCO₃ (J.T. Baker), 0.5% Albumax (Gibco), 2 g/L glucose, and 0.01 mg/mL gentamicin. Primarily ring-stage cultures were treated routinely with 5% D-Sorbitol to achieve synchronous cultures. Unless otherwise stated, experiments were carried out using the CS2 parasite strain.

STAD-2 Synthesis and Purification

Peptides were synthesized and purified as previously described [29].

STAD-2 Permeability

Synchronous ring-stage or late-stage infected red blood cells (iRBC) and uninfected red blood cells (uRBC) were brought up to 4% hematocrit in complete culture medium. FITC-conjugated peptides were added to a final concentration of 1 μ M, and cultures were incubated for 6 hours at 37°C under standard gas conditions. Following incubation, 25 μ L cell mixture was removed and treated with 100 μ L 2 μ g/mL Hoechst 33342 for 10 minutes at 37°C. Cells were subsequently washed once in 1 mL 1X PBS, resuspended in 300 μ L 1X PBS, and analyzed for Hoechst and FITC staining on a Beckman Coulter CyAn flow cytometer. 500,000 events were collected at a rate of 15,000 – 20,000 events per second. Data was analyzed using FlowJo X single cell analysis software (FlowJo LLC).

Dose-Response Curves

Synchronous ring-stage or late-stage iRBC at <0.5% parasitemia were brought up to 4% hematocrit in complete culture medium and transferred to a 24-well tissue culture plate in 1 mL aliquots. Wells were then brought up to final concentrations of 0.5, 1, 2, or 5 μ M STAD-2 or STAD-2 scramble. 25 μ L were removed from each well at 0, 24, 48, and 72 hours, stained with 100 μ L 2 μ g/mL Hoechst 33342 for 10 minutes at 37°C, and analyzed by flow cytometry as described above. IC₅₀ values were determined according to parasitemia at 24 hours post-treatment. Parasitemia was defined as the percent of Hoechst-positive RBCs as measured by flow cytometry.

Parasite Viability Assay

Ring-stage or late-stage iRBC at <0.5% parasitemia were brought up to 4% hematocrit in complete culture medium and transferred to a 24-well tissue culture plate in 1 mL aliquots. iRBCs were then treated with 1 μ M STAD-2, 1 μ M scrambled STAD-2, or 0.001% DMSO (vehicle control). 25 μ L were removed from each well every 24 hours post-treatment, and samples were stained with Hoechst 33342 and analyzed by flow cytometry. Blood smears were made every 24 hours, fixed with methanol, and stained with Giemsa for analysis by light microscopy. Images were acquired using a Nikon Eclipse E400 microscope fitted with a Nikon Digital Sight DS-5M-L1 camera (Nikon Instruments Inc.).

Hemolysis

Synchronous late-stage iRBC were mixed with uRBC in order to achieve a series of samples with stepwise decreasing parasitemia. Samples were brought up to 4% hematocrit in complete culture medium containing 1 μ M STAD-2, 1 μ M STAD-2 scramble, or 0.001% DMSO and transferred to a 48-well tissue culture plate in 200 μ L aliquots in duplicate. The plate was incubated at 37°C under standard gas conditions for 6 hours. Following incubation, all samples were transferred to Eppendorf tubes and centrifuged at 700 rcf for 5 minutes to pellet cells. 100 μ L of supernatant was removed from each tube and transferred to a 96-well, flat-bottom tissue culture plate. Oxyhemoglobin absorbance was measured at 415 nm using a SpectraMax Plus microplate spectrophotometer with SoftMax Pro 5.4 software (Molecular Devices, LLC).

Fluorescence Microscopy

A culture of primarily late-stage 3D7 iRBC was brought up to 4% hematocrit in complete culture medium and transferred to a 24-well plate at 1 mL per well. FITC-conjugated STAD-2 or scrambled STAD-2 were added to a final concentration of 1 μ M, and cultures were incubated for 10 minutes or 3 hours at 37°C under standard gas conditions. Following incubation, 50 μ L of cell mixture was removed and immediately stained with 200 μ L 2 μ g/mL Hoechst 33342 for 10 minutes at 37°C. Cells were washed once with 1 mL 1X PBS, resuspended in 200 μ L 4% paraformaldehyde/0.0075% glutaraldehyde, and deposited on coverslips pre-treated with 0.01% poly-L-lysine (Sigma Diagnostics) for 10 minutes. Post-fixation, coverslips were washed three times with 1X PBS, mounted on a glass microscope slide (Globe Scientific Inc.) with Fluoro-Gel anti-fading solution (Electron Microscopy Sciences), and sealed. Cells were imaged with a DeltaVision II microscope system using an Olympus IX-71 inverted microscope and a CoolSnap HQ2 CCD camera. Focal planes were selected based on transmitted light images. 0.2 μ m z-stacks were acquired and deconvolved using SoftWorx 5.5 acquisition software (Applied Precision, Inc.).

Immunofluorescence Assays

A culture of primarily late-stage iRBC was incubated with STAD-2 or DMSO as described above. Following incubation, 50 μ L of cell mixture was removed and washed twice with 1 mL 1X PBS. Cells were then resuspended in 200 μ L 4% paraformaldehyde/0.0075% glutaraldehyde and transferred to a CC2 glass chamber slide (Nalge Nunc International). Cells were fixed for 30 minutes at room temperature and gently washed twice with 300 μ L 1X PBS. Fixed cells were subsequently permeabilized with 0.1% Triton X-100/PBS for 10 minutes and

washed. Cells were then treated with 0.1 µg/mL sodium borohydride/PBS for 10 minutes to reduce any free aldehyde groups, washed with 1X PBS, and blocked for 1 hour at room temperature with 3% BSA/PBS. Following blocking, cells were brought up in 200 µL primary antibody and left shaking at 4°C overnight. The following morning, cells were washed three times, for 10 minutes each, to remove excess primary antibody and brought up in 200 µL secondary antibody for 1 hour at room temperature. After washing, cells were counterstained with 200 µL 0.5 µg/mL Hoechst 33342 for 3 minutes at room temperature and washed a final time before removing slide chambers, mounting a coverslip with Fluoro-Gel, and sealing. Rat anti-*Pf*PKA-R was generously donated by Gordon Langsley (Institut Cochin) and diluted 1:300 in 3% BSA/PBS. Goat anti-*Hs*PKA-RII (Abcam) was diluted to 10 µg/mL in 3% BSA/PBS. AlexFluor647 chicken anti-rat and AlexaFluor 647 donkey anti-goat secondary antibodies were diluted 1:500 in 3% BSA/PBS.

Immunoprecipitation/Mass Spectrometry

4 X 10⁸ 3D7 parasites were lysed with cold 0.04% saponin in PBS for 10 minutes. The supernatant was, subsequently, separated from the pellet by centrifugation at 4000 rcf for 10 minutes at 4°C. This supernatant consisted of the RBC cytoplasm and parasite exported proteins (termed host supernatant). The pellet consisted of parasite cells; these were further lysed with cold 0.5% PBS. The soluble fraction (termed parasite supernatant) of the parasite cells was separated from the insoluble fraction by centrifuging the parasite lysate at 4000 rcf for 10 minutes at 4°C. The host supernatant and the parasite supernatant were each incubated with biotin-conjugated STAD-2 or STAD-2 scramble for 16 hours at 4°C. Peptide-protein complexes were precipitated using streptavidin-coupled Dynabeads (Life Technologies). Dynabeads were

subsequently washed four times with 1X PBS, and the precipitated peptide-protein complexes were solubilized in SDS-PAGE sample buffer. Proteins were, then, fractionated on 10% SDS-PAGE, excised, and identified by MS-MS (Proteomics and Mass Spectrometry Core Facility, University of Georgia).

Sequences identified by MS-MS were searched against the NCBI non-redundant protein databases for *Plasmodium falciparum* (NCBI taxonomy #5833) and human (#9606)/*Plasmodium* (#5820) and analyzed by Mascot. Results from both database searches were cross-referenced and compiled. Proteins identified for STAD-2 and STAD-2 scramble treated lysates were compared and duplicates removed to yield a final list of STAD-2-specific protein interactions. Results are ordered by Mascot ions score (http://www.matrixscience.com/help/interpretation_help.html#SCORING). Generally, scores above 40 are considered possible interactions while scores above approximately 70 are considered good matches. All identified hits with a Mascot score above 40 are included in the supplementary tables.

Coincubation Assays

Late-stage cultures were brought up to 4% hematocrit in complete culture medium and transferred to a 48-well tissue culture plate at 250 μ L per well. Plates were spun at 330 rcf for 5 minutes, the medium was aspirated, and cultures were resuspended in either 250 μ L complete culture medium or 200 μ M furosemide in complete culture medium for 10 minutes at 37°C. Plates were again spun at 330 rcf, aspirated, and resuspended in 250 μ L 1 μ M STAD-2, 5% D-Sorbitol, 200 μ M furosemide, 130 mM glycerol, 6 μ M AgNO₃, or a combination of the aforementioned for 10 minutes or 2 hours. Following incubation, 25 μ L were removed, stained,

and analyzed by flow cytometry as described above. Ten-minute time points served as controls for 5% D-Sorbitol and furosemide activities while effects on STAD-2 uptake were determined using 2-hour time points.

STAD-2 Extracellular Activity

Synchronous ring-, trophozoite-, and schizont-stage iRBC were brought up to 4% hematocrit in complete culture medium and transferred to a 48-well tissue culture plate in 225 μ L aliquots. To ensure both impermeability and fluorescence of biotin-conjugated STAD-2, biotin-conjugated STAD-2 peptides were antecedently incubated with 1.25 μ g/mL streptavidin-FITC for 20 minutes at room temperature in the dark. Following incubation, 25 μ L of peptide solutions were added to bring cells to final concentrations of 1 μ M FITC-conjugated STAD-2, 1 μ M streptavidin/FITC/biotin-conjugated STAD-2, 1 μ M streptavidin/FITC/biotin-conjugated STAD-2 scramble, 1 μ M biotin-conjugated STAD-2, or 1 μ M biotin-conjugated STAD-2 scramble. 1.25 μ g/mL streptavidin/FITC and 0.001% DMSO were included as controls. Cells were then incubated at 37 °C for 6 hours under standard gas conditions, stained with Hoechst 33342, and analyzed by flow cytometry.

Statistical Analysis

Graphing and statistical analyses were done using GraphPad Prism 5 (GraphPad Software, Inc.).

Results

STAD-2 is selectively permeable to infected red blood cells

STAD-2 was designed to target the regulatory subunit of *Hs*PKA and occlude AKAP binding interactions as previously described [29] (Figure 4.1). To study the effects of STAD-2 in *Plasmodium*-infected red blood cells (iRBC), STAD-2 permeability was first examined by incubating 1 μ M FITC-conjugated STAD-2 peptides with uninfected red blood cells (uRBC) and CS2 iRBC for 6 hours. Subsequent staining with 2 μ g/mL Hoechst 33342 enabled separation of uninfected from infected red blood cells based on their DNA content. Analysis by flow cytometry showed significant permeability of STAD-2 in iRBC while only a nominal amount was permeable to uRBC (Figure 4.2A). Cell permeability patterns were consistent across other parasite strains tested (Figure S4.1) and reached near-maximum levels by 3 hours post-treatment (Figure S4.2).

P. falciparum has a blood stage life cycle of 44-48 hours wherein parasites upregulate new permeability pathways during the later stages of development. These pathways serve to facilitate uptake of solutes that are essential for parasite growth and division and are marked by the upregulation of a unique *Plasmodium* surface anion channel (PSAC) [41]. In order to examine the influence of parasite stage on uptake of STAD-2, iRBC were synchronized using 5% D-Sorbitol, and peptide permeability was measured in ring- and late-stage parasites. Late-stage iRBC demonstrated significantly increased uptake of STAD-2 relative to ring-stage parasites, consistent with the increased permeability of late-stage iRBC (Figures 4.2B and 4.2C). As controls, iRBC were also treated with the unstapled STAD-2 parent peptide as well as a scrambled version of STAD-2 possessing identical chemical composition but a scrambled amino acid sequence (Figure 4.1A). Permeability of these controls was almost negligible as measured

by flow cytometry (Figures 4.2B and 4.2C), demonstrating selective uptake of STAD-2 by iRBC.

STAD-2 reduces parasite viability

Since STAD-2 was selectively permeable to iRBC, we wanted to determine whether STAD-2 treatment had an effect on parasite viability *in vitro*. We first treated ring- and late-stage iRBC with 0, 0.5, 1, 2, and 5 μM STAD-2 or STAD-2 scramble for 24 hours and subsequently determined parasitemia relative to DMSO-treated controls. While treatment with the scramble control had negligible effects on parasite viability at all concentrations tested, a concentration-dependent decrease in parasitemia was observed in STAD-2-treated iRBC 24 hour post-treatment (Figure 4.3A). Consistent with increased STAD-2 permeability in late-stage iRBC (Figures 4.2B and 4.2C), late-stage parasites were slightly more susceptible to STAD-2 inhibition ($\text{IC}_{50} \approx 1 \mu\text{M}$) than ring-stage parasites ($\text{IC}_{50} \approx 1.5 \mu\text{M}$).

To further explore the effects of STAD-2 on parasite viability *in vitro*, synchronous ring- and late-stage iRBC were treated with 1 μM STAD-2 or scrambled STAD-2, and parasitemia was determined by flow cytometry in conjunction with light microscopy every 24 hours for 72 hours post-treatment. Again, STAD-2 scramble had no effect on parasite viability whereas both late- and ring-stage iRBC had significantly decreased parasitemias relative to their DMSO controls by 48 hours post-STAD-2 treatment (Figures 4.3B, $p < 0.001$). STAD-2, likewise, inhibited several other parasite strains tested (Figure S4.3). Interestingly, the morphology of STAD-2-treated iRBC did not differ from DMSO controls (Figure 4.3B).

Throughout the previous experiments, it was noticed that parasitemia was decreased as early as 6 hours post-treatment as detected by flow cytometry (Figure S4.4). This, combined with

the lack of morphological effects following STAD-2 treatment (Figure 4.3B), led us to explore whether STAD-2 was inducing lysis of iRBC. To test this hypothesis, we prepared serial dilutions of late-stage iRBC in uRBC in order to achieve a series of samples ranging from 0 to 8% parasitemia. We then treated the samples with 1 μ M STAD-2 or STAD-2 scramble for 6 hours and quantified cell lysis by measuring the absorbance of oxyhemoglobin in the sample medium (A_{415}). While levels of lysis induced by STAD-2 scramble were essentially identical to DMSO controls, STAD-2-induced lysis was significantly greater than controls and directly correlated with increasing parasitemia (Figure 4.3D). Hence, we propose that STAD-2-induced cell lysis is specific to *P. falciparum* infected cells.

STAD-2 traffics to the intracellular parasite

Currently, there is nothing known concerning AKAPs in relation to *P. falciparum* iRBC. Thus, we wanted to probe whether STAD-2 localized within the host red blood cell or within the parasite. In order to determine intracellular localization of FITC-conjugated STAD-2, iRBC were treated and stained as before and analyzed by fluorescence microscopy. Repeated analyses found that STAD-2 consistently localized within the parasite but rarely within the parasite digestive vacuole (Figure 4.4A). At no point was STAD-2 observed within the red blood cell cytosol. This pattern of peptide localization was consistent in both fixed and unfixed cells as well as both undivided (trophozoite) and divided (schizont) late-stage parasites. In addition, we found that STAD-2 quickly reached intracellular parasites, localizing within parasites as early as 20 minutes post-treatment, and maintained an identical pattern of localization as late as 6 hours post-treatment (Figure 4.4B.). Thus, selective uptake and localization of STAD-2 seems independent of any changes in parasite morphology during late-stage development.

STAD-2 does not associate with PKA

Since STAD-2 localizes within the parasite and not within the cytoplasm of the red blood cell, we wanted to determine if STAD-2 targets PKA within the parasite. We first addressed this question using immunofluorescence assays of iRBC treated with FITC-conjugated STAD-2 and probed with either anti-*Pf*PKA R or anti-*Hs*PKA RII antibodies. STAD-2 did not definitively colocalize with either of the regulatory subunits tested in iRBC (Figure 4.5A), although lack of colocalization with *Hs*PKA can likely be attributed to the compound's inability to accumulate in the RBC cytoplasm. Likewise, coimmunoprecipitation experiments using biotin-conjugated STAD-2 did not yield detectable levels of the probed PKA subunits by western blotting (data not shown) nor were they evident as interacting partners when analyzed by mass spectrometry (Tables S4.1 and S4.2). Finally, we compared the effects of treatment with STAD-2 to those of the PKA small molecule inhibitor, H89. Both STAD-2 and H89 were applied at their relative IC₅₀ values (1 μ M and 30 μ M, Figure S4.5) and analyzed by blood smears at 48 hours post-treatment. Although STAD-2-treated iRBC did not differ morphologically from DMSO controls, H89-treated iRBC consistently showed clear morphological changes including the notable absence of a digestive vacuole (Figure 4.5B). Thus, we suggest that STAD-2 may act via an alternate mechanism that does not involve disruption of PKA signaling.

STAD-2 is internalized via unknown parasite permeability pathways

Although it is well established that *Plasmodium* parasites have increased permeability to extracellular solutes during the latter half of the blood-stage life cycle, many questions remain regarding the mechanisms of permeability. It is generally accepted that smaller solutes are imported via a PSAC that is upregulated by the parasite throughout the course of development;

however considerably less is understood regarding uptake of larger solutes. In order to better understand how the relatively large ~2.5 kDa peptide, STAD-2, gains intracellular access to iRBC, we measured uptake of 1 μ M STAD-2 in the presence of the PSAC inhibitor furosemide. Although STAD-2/furosemide co-treatment alone had no discernible effect on STAD-2 uptake, pre-incubation of iRBC with 200 μ M furosemide followed by a 2-hour co-treatment showed a consistent but statistically insignificant decrease in STAD-2 uptake (Figure 4.6A). Thus, it appears that STAD-2 import does not heavily rely on the PSAC.

Recent studies have shown that some AKAPs associate with membrane aquaporins and play a role in aquaporin phosphorylation and channel regulation within various cell types [42,43]. Although evidence suggests the presence of both aquaporin 1 (AQP1) and aquaporin 3 (AQP3) on the surface of healthy red blood cells [44], few studies have examined the role of membrane aquaporins in *P. falciparum* iRBC. However, AQP3 is thought to be the major glycerol channel in human erythrocytes and may play a role in the virulence of intraerythrocytic parasites [45]. To further explore the role of membrane transport mechanisms in STAD-2 uptake, we performed co-incubation experiments similar to those above using D-Sorbitol (PSAC solute), glycerol (AQP3 solute [46,47]), or AgNO₃ (AQP1 inhibitor [48]). Co-incubation of iRBC with 1 μ M STAD-2 and 130 mM glycerol or 6 μ M AgNO₃ yielded no apparent change in STAD-2 uptake; however, co-incubation with 5% D-Sorbitol resulted in a slight reduction of STAD-2 uptake that was comparable to that seen with furosemide (Figure 4.6B). Thus, although AQP1 and AQP3 are unlikely to play a role in STAD-2 uptake or activity, the PSAC may be responsible for a fraction of STAD-2 import. Nevertheless, we propose that none of the assessed means of transport greatly contribute to the uptake of STAD-2 by iRBC.

STAD-2 permeability is peptide-specific

Since none of the examined membrane channels contributed substantially to the uptake of STAD-2, we further explored the requirements of iRBC permeability by testing for uptake of a variety of different stapled, FITC-conjugated peptides. All peptides were applied at a concentration of 1 μ M for 6 hours and analyzed by flow cytometry as previously described. The overall net charge and amino acid sequence of all peptides tested are shown in Table 4.1. The first series of peptides analyzed explored the influence of peptide charge on iRBC uptake (Figure 4.7A) while the second series examined uptake of other STAD peptides that were developed previously (Figure 4.7B) [29]. Unexpectedly, STAD-2 was the only peptide that demonstrated clear permeability to iRBC (Figure 4.7C) providing further evidence that iRBC uptake of STAD-2 is highly specific.

STAD-2 displays increased activity at the erythrocyte membrane

Given the evidence that STAD-2 treatment induces iRBC lysis, we next considered whether the highly specific uptake observed with STAD-2 was essential for its lytic activity. To examine this, biotin-conjugated STAD-2 peptides were preincubated with streptavidin/FITC. Streptavidin is a large, ~60 kDA protein with an extraordinarily high affinity for biotin ($K_D \approx 4 \times 10^{-14}$ M) [49]. Preincubation of biotin-conjugated STAD-2 with streptavidin/FITC served to ensure both impermeability as well as fluorescence of the biotin/STAD-2 conjugate. Following incubation of biotin-conjugated STAD-2 with streptavidin/FITC, synchronous iRBC were treated with 1 μ M FITC-conjugated, streptavidin/FITC/biotin-conjugated, or biotin-conjugated STAD-2 peptides, as well as their scrambled controls, for 6 hours before analysis by flow cytometry. Interestingly, treatment with streptavidin/FITC/biotin-conjugated STAD-2 caused a significant decrease in parasitemia in both trophozoite (~30% reduction) and schizont (~60% reduction)

iRBC at 6 hours post-treatment (Figure 4.8, $p < 0.05$ and $p < 0.001$, respectively). In contrast, FITC-conjugated STAD-2 induced an insignificant reduction in parasitemia only in late schizonts (~10% reduction). As no shift in FITC was observed following streptavidin/FITC/biotin-conjugated STAD-2 treatment, these results indicate that STAD-2 uptake is not required for peptide-mediated lysis and, rather, that peptide activity is elevated at the erythrocyte membrane. Unexpectedly, biotin-conjugated STAD-2 peptides alone also induced a similar reduction in parasitemia (Figure 4.8). Since these peptide conjugates lack a fluorescent tag, it is not possible to discern whether biotin-conjugated STAD-2 is internalized by iRBC. However, the similar increase in STAD-2-mediated lysis would suggest that either the altered structure or the different charge of biotin-conjugated STAD-2 inhibits peptide uptake.

Discussion

With *Plasmodium* drug resistance on the rise, malaria control efforts are in desperate need of new antimalarials that are highly efficacious and largely refractory to parasite mechanisms of drug resistance. For the time being, artemisinin combination therapy (ACT) remains the WHO-recommended first line treatment for *P. falciparum* malaria. And, although resistance in the Greater Mekong Subregion has hampered the efficacy of artemisinin monotherapies, ACT currently remains highly effective at curing malaria provided it is paired with an efficacious partner drug [50]. However, mounting evidence of delayed clearance times places even ACTs in jeopardy and further underscores the need for new antimalarials [51].

In 2009, a high throughput phenotypic screen of nearly 2 million compounds from GlaxoSmithKline identified 13,533 compounds that inhibited growth of *P. falciparum* by greater than 80% at 2 μ M concentration [52]. Of the compounds identified and validated in the study, a large majority were protein kinase inhibitors. Although *P. falciparum* has a relatively small kinome, composed of less than 100 identified kinases, many are highly divergent from those within the human host [40,53]. Furthermore, since many kinase signaling pathways are evolutionarily conserved, it has been suggested that a single kinase inhibitor might exhibit pluripotency and, therefore, reduced vulnerability to drug resistant mutations [53]. Thus, protein kinases represent promising candidates as future antimalarial targets.

In the present study, we explored the effects of the human AKAP disruptor peptide STAD-2 on *P. falciparum* iRBC. We demonstrated STAD-2 to be highly and selectively permeable to iRBC. In addition, STAD-2 effectively inhibited parasite viability at $IC_{50} \approx 1 \mu$ M. Surprisingly, analyses using antibodies specific to both *P. falciparum* and *H. sapiens* PKA regulatory subunits found no evidence of association of STAD-2 with human or parasite PKA

within the iRBC. Likewise, parasite responses to treatment with the PKA small molecule inhibitor H89 differed considerably from treatment with STAD-2, providing further evidence that STAD-2 may not inhibit PKA regulation in iRBC. This is most likely due to the fact that STAD-2 does not accumulate in the RBC cytosol, yielding the human PKA-R target inaccessible, and *Pf*PKA-R does not contain the conserved D/D domain that is targeted by STAD-2. However, since *Hs*PKA-R is known to play a critical role in membrane stiffness and adhesion [37], it will be interesting to study the role of human AKAPs on *Plasmodium*-iRBCs through selective delivery of STAD-2 into the RBC cytoplasm. In an effort to dissect the mechanism of iRBC import of STAD-2, we found that intake was largely independent of the PSAC. In addition, import was highly sequence-specific since other stapled peptides, even some bearing very similar composition to STAD-2, were largely impermeable to iRBC.

This research provides the first support for the use of stapled peptides as potential candidates for exploring malaria-specific signaling and inhibition in RBCs. Although further study will be necessary to dissect the highly specific mechanisms of uptake seen with STAD-2, the selective permeability of stapled peptides to *P. falciparum* iRBC may ensure low cytotoxicity of future antimalarial stapled peptides.

As experiments examining the mechanism of peptide uptake did not show significant contributions by neither the PSAC nor resident RBC aquaporins, it remains unclear exactly how STAD-2 is imported into the parasite. Aside from the PSAC, permeability of iRBC is poorly understood. Various studies have shown high permeability of positively charged cell-penetrating peptides in *P. falciparum*-iRBC. These peptides typically possess octaarginine or octalysine structures and are thought to be taken up by endocytic mechanisms [54–56]. Also, like STAD-2, cell-penetrating peptides demonstrate selective permeability to iRBC relative to healthy uRBC

[57]. However, the lack of permeability of control positively charged peptides in this study, particularly STAD-2 scramble and STAD-3, suggests that there may be more at play here than non-selective endocytosis. Therefore, it is possible that STAD-2 may be imported through a specific protein interaction that dictates permeability.

Although efforts to identify the mechanism of action of STAD-2 peptides within iRBC were inconclusive, it is interesting to consider the observed lytic activity of STAD-2 within iRBC. This activity may have important implications regarding STAD-2 function in *P. falciparum*. Previous studies have demonstrated a role for *Pf*PKA in regulation of parasite permeability such that overexpression of *Pf*PKA-R led to inhibition of anionic channel conductance [35]. In addition, characterization of *Pf*PKA-C from iRBC found highest activity of *Pf*PKA-C in schizont-infected cells, consistent with our observed STAD-2 activity in late-stage parasites [58]. Therefore, although we found no definitive association of STAD-2 with PKA-R, it is possible that STAD-2-induced iRBC lysis results from altered activity of PKA. Alternatively, our IP/MS experiments showed association of STAD-2 with cytoadherence linked asexual protein 3.1, or CLAG3, in the parasite supernatant (Table S4.2). Recent studies have shown CLAG3 to be associated with the PSAC such that CLAG3 alters erythrocyte permeability [59,60], raising the possibility that STAD-2 may interfere with CLAG3 function and/or PSAC activity, thereby leading to iRBC lysis. The increase in iRBC lysis observed with extracellularly restricted STAD-2 may provide further support for this proposed interaction.

Conclusions

Parasite drug resistance poses a serious threat to ongoing malaria control and elimination efforts. Development of new antimalarials targeting essential parasite components, such as kinases, or utilizing novel mechanisms of action may prevent devastating losses in our advancement toward malaria elimination. Here, we provide important groundwork for the use of stapled peptides as a novel class of antimalarials. Our data demonstrate the stapled AKAP disruptor, STAD-2, to be selectively permeable to iRBC. Furthermore, iRBC uptake of STAD-2 is highly specific and not reliant on known parasite permeability pathways. Notably, iRBC lysis triggered by STAD-2 appears to occur through a yet unknown, PKA-independent mechanism. Future research will explore the efficacy of stapled peptides designed to specifically inhibit protein-protein interactions unique to kinase targets in *P. falciparum*. We believe that the high specificity and unique mechanism of action of stapled peptides may yield promising new antimalarials with reduced vulnerability to parasite drug resistance.

References

1. WHO (2014) World Malaria Report 2014. doi:10.1007/s00108-013-3390-9.
2. Shretta R, Yadav P (2012) Stabilizing supply of artemisinin and artemisinin-based combination therapy in an era of wide-spread scale-up. *Malar J* 11: 399. doi:10.1186/1475-2875-11-399.
3. Ashley EA, Dhorda M, Fairhurst RM, Amaratunga C, Lim P, et al. (2014) Spread of Artemisinin Resistance in *Plasmodium falciparum* Malaria. *N Engl J Med* 371: 411–423. doi:10.1056/NEJMoa1314981.
4. Dondrop AM, Nosten F, Yi P, Das D, Phyo AP, et al. (2009) Artemisinin Resistance in *Plasmodium falciparum* Malaria. *N Engl J Med* 361: 455–467.
5. Dondorp AM, Yeung S, White L, Nguon C, Day NPJ, et al. (2010) Artemisinin resistance: current status and scenarios for containment. *Nat Rev Microbiol* 8: 272–280. doi:10.1038/nrmicro2331.
6. Harikishore A, Niang M, Rajan S, Preiser PR, Yoon HS (2013) Small molecule *Plasmodium* FKBP35 inhibitor as a potential antimalaria agent. *Sci Rep* 3: 2501. doi:10.1038/srep02501.
7. White NJ, Pukrittayakamee S, Phyo AP, Rueangweerayut R, Nosten F, et al. (2014) Spiroindolone KAE609 for *falciparum* and *vivax* malaria. *N Engl J Med* 371: 403–410. doi:10.1056/NEJMoa1315860.
8. Bowman JD, Merino EF, Brooks CF, Striepen B, Carlier PR, et al. (2014) Antiapicoplast and gametocytocidal screening to identify the mechanisms of action of compounds within the malaria box. *Antimicrob Agents Chemother* 58: 811–819. doi:10.1128/AAC.01500-13.
9. Srinivasan P, Yasgar A, Luci DK, Beatty WL, Hu X, et al. (2013) Disrupting malaria parasite AMA1-RON2 interaction with a small molecule prevents erythrocyte invasion. *Nat Commun* 4: 2261. doi:10.1038/ncomms3261.
10. Yeung BKS, Zou B, Rottmann M, Lakshminarayana SB, Ang SH, et al. (2010) Spirotetrahydro beta-carbolines (spiroindolones): a new class of potent and orally efficacious compounds for the treatment of malaria. *J Med Chem* 53: 5155–5164. doi:10.1021/jm100410f.
11. Petersen I, Eastman R, Lanzer M (2011) Drug-resistant malaria: molecular mechanisms and implications for public health. *FEBS Lett* 585: 1551–1562. doi:10.1016/j.febslet.2011.04.042.
12. Delfino RT, Santos-Filho OA, Figueroa-Villar JD (2002) Molecular modeling of wild-type and antifolate resistant mutant *Plasmodium falciparum* DHFR. *Biophys Chem* 98: 287–300.

13. Mharakurwa S, Kumwenda T, Mkulama MAP, Musapa M, Chishimba S, et al. (2011) Malaria antifolate resistance with contrasting *Plasmodium falciparum* dihydrofolate reductase (DHFR) polymorphisms in humans and *Anopheles* mosquitoes. PNAS 108: 18796–18801.
14. Akhoun B a, Singh KP, Varshney M, Gupta SK, Shukla Y, et al. (2014) Understanding the mechanism of atovaquone drug resistance in *Plasmodium falciparum* cytochrome b mutation Y268S using computational methods. PLoS One 9: e110041. doi:10.1371/journal.pone.0110041.
15. Fisher N, Abd Majid R, Antoine T, Al-Helal M, Warman AJ, et al. (2012) Cytochrome b mutation Y268S conferring atovaquone resistance phenotype in malaria parasite results in reduced parasite bc1 catalytic turnover and protein expression. J Biol Chem 287: 9731–9741. doi:10.1074/jbc.M111.324319.
16. Schwöbel B, Alifrangis M, Salanti A, Jelinek T (2003) Different mutation patterns of atovaquone resistance to *Plasmodium falciparum* in vitro and in vivo : rapid detection of codon 268 polymorphisms in the cytochrome b as potential in vivo. Malar J 2.
17. Chinappi M, Via A, Marcatili P, Tramontano A (2010) On the mechanism of chloroquine resistance in *Plasmodium falciparum*. PLoS One 5: e14064. doi:10.1371/journal.pone.0014064.
18. Ferreira PE, Holmgren G, Veiga MI, Uhlén P, Kaneko A, et al. (2011) PfMDR1: mechanisms of transport modulation by functional polymorphisms. PLoS One 6: e23875. doi:10.1371/journal.pone.0023875.
19. Arieu F, Witkowski B, Amaratunga C, Beghain J, Langlois A-C, et al. (2014) A molecular marker of artemisinin-resistant *Plasmodium falciparum* malaria. Nature 505: 50–55. doi:10.1038/nature12876.
20. Ghorbal M, Gorman M, Macpherson CR, Martins RM, Scherf A, et al. (2014) Genome editing in the human malaria parasite *Plasmodium falciparum* using the CRISPR-Cas9 system. Nat Biotechnol 32. doi:10.1038/nbt.2925.
21. Winzeler E a, Manary MJ (2014) Drug resistance genomics of the antimalarial drug artemisinin. Genome Biol 15: 544. doi:10.1186/s13059-014-0544-6.
22. Walensky LD, Bird GH (2014) Hydrocarbon-stapled peptides: principles, practice, and progress. J Med Chem 57: 6275–6288. doi:10.1021/jm4011675.
23. Verdine GL, Hilinski GJ (2012) All-hydrocarbon stapled peptides as Synthetic Cell-Accessible Mini-Proteins. Drug Discov Today Technol 9: e41–e47. doi:10.1016/j.ddtec.2012.01.004.
24. Verdine GL, Walensky LD (2007) The challenge of drugging undruggable targets in cancer: lessons learned from targeting BCL-2 family members. Clin cancer Res 13: 7264–7270. doi:10.1158/1078-0432.CCR-07-2184.

25. Walensky LD, Kung AL, Escher I, Malia TJ, Barbuto S, et al. (2004) Activation of apoptosis in vivo by a hydrocarbon-stapled BH3 helix. *Science* (80-) 305: 1466–1470. doi:10.1126/science.1099191.
26. Nomura W, Aikawa H, Ohashi N, Urano E, Métifiot M, et al. (2013) Cell-permeable stapled peptides based on HIV-1 integrase inhibitors derived from HIV-1 gene products. *ACS Chem Biol* 8: 2235–2244. doi:10.1021/cb400495h.
27. Cui H-K, Qing J, Guo Y, Wang Y-J, Cui L-J, et al. (2013) Stapled peptide-based membrane fusion inhibitors of hepatitis C virus. *Bioorg Med Chem* 21: 3547–3554. doi:10.1016/j.bmc.2013.02.011.
28. Chapuis H, Slaninová J, Bednářová L, Monincová L, Buděšínský M, et al. (2012) Effect of hydrocarbon stapling on the properties of α -helical antimicrobial peptides isolated from the venom of hymenoptera. *Amino Acids* 43: 2047–2058. doi:10.1007/s00726-012-1283-1.
29. Wang Y, Ho TG, Bertinetti D, Neddermann M, Franz E, et al. (2014) Isoform-Selective Disruption of AKAP-Localized PKA Using Hydrocarbon Stapled Peptides. *ACS Chem Biol* 9: 635–642. doi:10.1021/cb500329z.
30. Wong W, Scott JD (2004) AKAP signalling complexes: focal points in space and time. *Nat Rev Mol Cell Biol* 5: 959–970. doi:10.1038/nrm1527.
31. Edwards AS, Scott JD (2000) A-kinase anchoring proteins: protein kinase A and beyond. *Curr Opin Cell Biol* 12: 217–221.
32. Langeberg LK, Scott JD (2005) A-kinase-anchoring proteins. *J Cell Sci* 118: 3217–3220. doi:10.1242/jcs.02416.
33. Scott JD, Dessauer CW, Taskén K (2013) Creating order from chaos: cellular regulation by kinase anchoring. *Annu Rev Pharmacol Toxicol* 53: 187–210. doi:10.1146/annurev-pharmtox-011112-140204.
34. Haste NM, Talabani H, Doo A, Merckx A, Langsley G, et al. (2012) Exploring the *Plasmodium falciparum* cyclic-adenosine monophosphate (cAMP)-dependent protein kinase (PfPKA) as a therapeutic target. *Microbes Infect* 14: 838–850. doi:10.1016/j.micinf.2012.05.004.
35. Merckx A, Nivez M-P, Bouyer G, Alano P, Langsley G, et al. (2008) *Plasmodium falciparum* regulatory subunit of cAMP-dependent PKA and anion channel conductance. *PLoS Pathog* 4: e19. doi:10.1371/journal.ppat.0040019.
36. Ramdani G, Langsley G (2014) ATP, an extracellular signaling molecule in red blood cells: a messenger for malaria? *Biomed J* 37: 284–292.

37. Maciaszek JL, Andemariam B, Abiraman K, Lykotrafitis G (2014) AKAP-dependent modulation of BCAM/Lu adhesion on normal and sickle cell disease RBCs revealed by force nanoscopy. *Biophys J* 106: 1258–1267. doi:10.1016/j.bpj.2014.02.001.
38. Wurtz N, Chapus C, Desplans J, Parzy D (2011) cAMP-dependent protein kinase from *Plasmodium falciparum*: an update. *Parasitology* 138: 1–25. doi:10.1017/S003118201000096X.
39. Merckx A, Bouyer G, Thomas SLY, Langsley G, Egée S (2009) Anion channels in *Plasmodium-falciparum*-infected erythrocytes and protein kinase A. *Trends Parasitol* 25: 139–144. doi:10.1016/j.pt.2008.12.005.
40. Doerig C (2004) Protein kinases as targets for anti-parasitic chemotherapy. *Biochim Biophys Acta* 1697: 155–168. doi:10.1016/j.bbapap.2003.11.021.
41. Desai S (2014) Why do malaria parasites increase host erythrocyte permeability? *Trends Parasitol* 30: 151–159. doi:10.1016/j.pt.2014.01.003.
42. Okutsu R, Rai T, Kikuchi A, Ohno M, Uchida K, et al. (2008) AKAP220 colocalizes with AQP2 in the inner medullary collecting ducts. *Kidney Int* 74: 1429–1433. doi:10.1038/ki.2008.402.
43. Gold MG, Reichow SL, O'Neill SE, Weisbrod CR, Langeberg LK, et al. (2011) AKAP2 anchors PKA with aquaporin-0 to support ocular lens transparency. *EMBO Mol Med* 4: 15–26. doi:10.1002/emmm.201100184.
44. Roudier N, Verbavatz J, Maurel C, Ripoche P, Frederique T (1998) Evidence for the Presence of Aquaporin-3 in Human Red Blood Cells*. *J Biol Chem* 273: 8407–8412.
45. Liu Y, Promeneur D, Rojek A, Kumar N, Frøkiær J, et al. (2007) Aquaporin 9 is the major pathway for glycerol uptake by mouse erythrocytes , with implications for malarial virulence. *PNAS* 104: 12560–12564.
46. Pavlovic-Djuranovic S, Schultz JE, Beitz E (2003) A single aquaporin gene encodes a water/glycerol/urea facilitator in *Toxoplasma gondii* with similarity to plant tonoplast intrinsic proteins. *FEBS Lett* 555: 500–504. doi:10.1016/S0014-5793(03)01313-9.
47. Beitz E, Pavlovic-Djuranovic S, Yasui M, Agre P, Schultz JE (2004) Molecular dissection of water and glycerol permeability of the aquaglyceroporin from *Plasmodium falciparum* by mutational analysis. *PNAS* 101: 1153–1158. doi:10.1073/pnas.0307295101.
48. Yang B, Kim JK, Verkman AS (2006) Comparative efficacy of HgCl with candidate aquaporin-1 inhibitors DMSO, gold, TEA, and acetazolamide. *FEBS Lett* 580: 6679–6684. doi:10.1016/j.febslet.2006.11.025.Comparative.
49. Holmberg A, Blomstergren A, Nord O, Lukacs M, Lundeberg J, et al. (2005) The biotin-streptavidin interaction can be reversibly broken using water at elevated temperatures. *Electrophoresis* 26: 501–510. doi:10.1002/elps.200410070.

50. WHO (2013) Emergency response to artemisinin resistance in the Greater Mekong subregion.
51. WHO (2012) Update on artemisinin resistance - April 2012.
52. Gamo F-J, Sanz LM, Vidal J, De Cozar C, Alvarez E, et al. (2010) Thousands of chemical starting points for antimalarial lead identification. *Nature* 465: 305–310. doi:10.1038/nature09107.
53. Lucet IS, Tobin A, Drewry D, Wilks AF, Doerig C (2012) Plasmodium kinases as targets for new-generation antimalarials. *Future Med Chem* 4: 2295–2310. doi:10.4155/fmc.12.183.
54. Kolevzon N, Nasereddin A, Naik S, Yavin E, Dzikowski R (2014) Use of peptide nucleic acids to manipulate gene expression in the malaria parasite *Plasmodium falciparum*. *PLoS One* 9: e86802. doi:10.1371/journal.pone.0086802.
55. Copolovici DM, Langel K, Eriste E, Langel Ü (2014) Cell-penetrating peptides: Design, synthesis, and applications. *ACS Nano* 8: 1972–1994. doi:10.1021/nn4057269.
56. Sparr C, Purkayastha N, Kolesinska B, Gengenbacher M, Amulic B, et al. (2013) Improved efficacy of fosmidomycin against plasmodium and mycobacterium species by combination with the cell-penetrating peptide octaarginine. *Antimicrob Agents Chemother* 57: 4689–4698. doi:10.1128/AAC.00427-13.
57. Kamena F, Monnanda B, Makou D (2011) On the mechanism of eukaryotic cell penetration by α - and β -oligoarginines--targeting infected erythrocytes. *Chem Biodivers* 8: 1–12. doi:10.1002/cbdv.201000318.
58. Li J, Cox LS (2000) Isolation and characterisation of a cAMP-dependent protein kinase catalytic subunit gene from *Plasmodium falciparum*. *Mol Biochem Parasitol* 109: 157–163.
59. Nguitragool W, Bokhari AAB, Pillai AD, Rayavara K, Sharma P, et al. (2011) Malaria parasite clag3 genes determine channel-mediated nutrient uptake by infected red blood cells. *Cell* 145: 665–677. doi:10.1016/j.cell.2011.05.002.
60. Nguitragool W, Rayavara K, Desai SA (2014) Proteolysis at a specific extracellular residue implicates integral membrane CLAG3 in malaria parasite nutrient channels. *PLoS One* 9: e93759. doi:10.1371/journal.pone.0093759.
61. Kinderman FS, Kim C, von Daake S, Ma Y, Pham BQ, et al. (2006) A dynamic mechanism for AKAP binding to RII isoforms of cAMP-dependent protein kinase. *Mol Cell* 24: 397–408. doi:10.1016/j.molcel.2006.09.015.

Figures

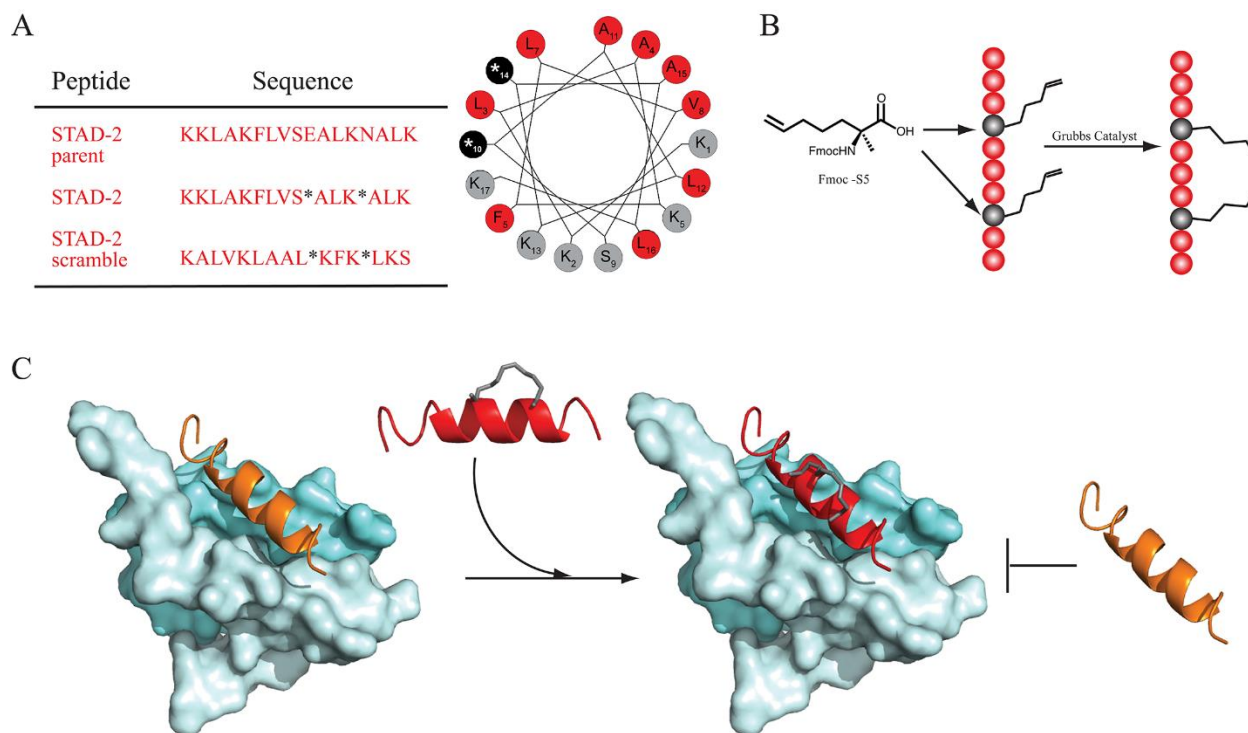


Figure 4.1. STAD-2 synthesis and function. (A) STAD-2 and STAD-2 scramble were synthesized by substituting S-pentenyl alanine (S_5 , shown as *) into positions that are opposite to the binding surface targeting PKA-R. A helical wheel represents the STAD-2 secondary structure wherein hydrophobic residues are shown in red, S_5 in black, and other residues in grey. (B) Fmoc chemistry was used to synthesize STAD-2 peptides containing the non-natural S_5 residues at $i, i+4$ positions. Ring-closing metathesis was performed using Grubbs I catalyst to generate the hydrocarbon staple. (C) The interaction between the *Hs*PKA D/D domain (pale cyan) and the docking sequence of an AKAP (orange) can be inhibited by the stapled disruptor peptide STAD-2 (red). STAD-2 mimics the docking sequence of an AKAP and disrupts binding to the regulatory subunit of PKA. Images were created using the crystal structure of PKA-RII (PDB access code: 2HWN [61]).

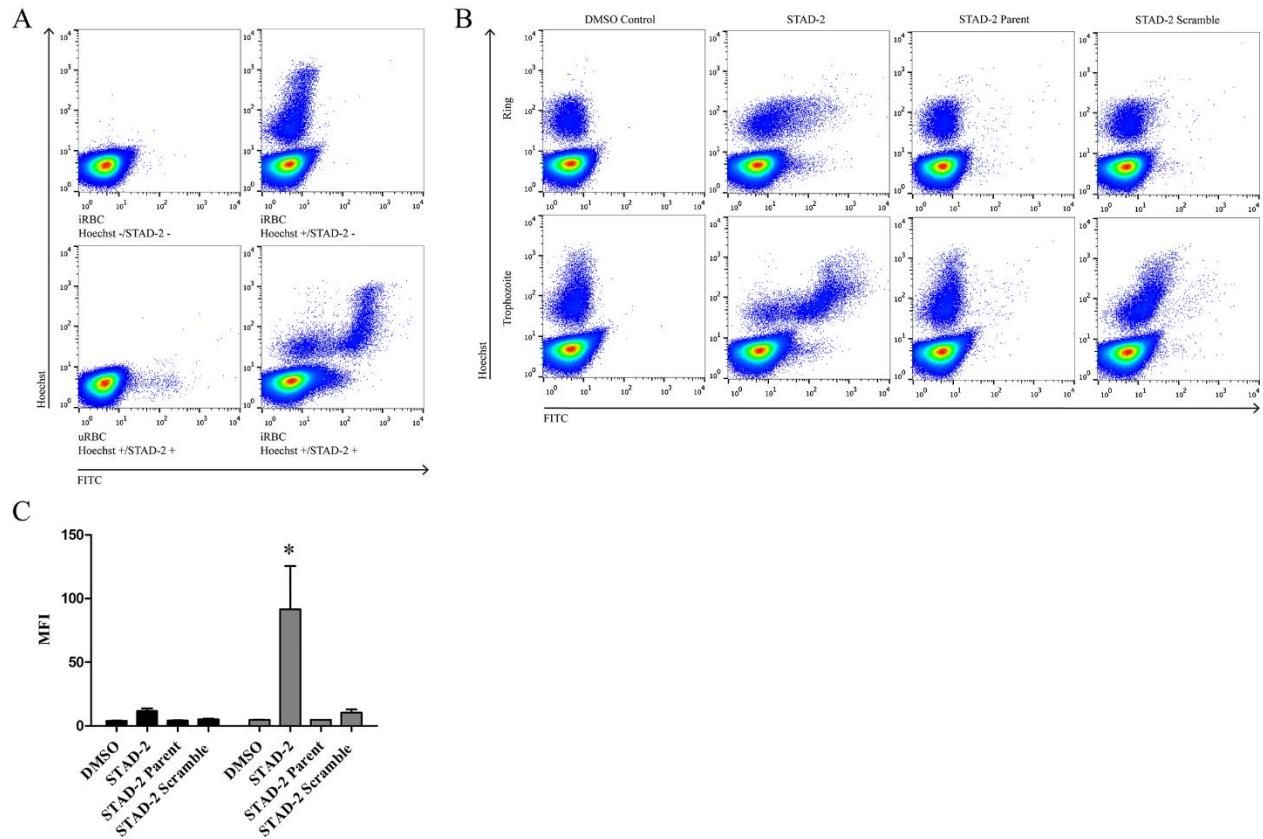


Fig 4.2. STAD-2 peptides are selectively permeable to *Plasmodium*-infected red blood cells.

(A) *Plasmodium*-iRBC were treated for 6 hours with 1 μ M FITC-conjugated STAD-2 and analyzed by flow cytometry. iRBC showed selective permeability to STAD-2 relative to uRBC.

(B, C) Treatment of synchronous ring-stage (black bars) or late-stage (grey bars) cultures with 1 μ M FITC-conjugated STAD-2, unstapled STAD-2 parent, or STAD-2 scramble demonstrated significantly increased uptake of STAD-2 by late-stage relative to ring-stage iRBC. However, both ring-stage and late-stage iRBC were minimally permeable to STAD-2 parent and STAD-2 scramble controls (2way ANOVA with Bonferroni posttest, $p < 0.001$, $n = 3-6$, mean \pm S.E.).

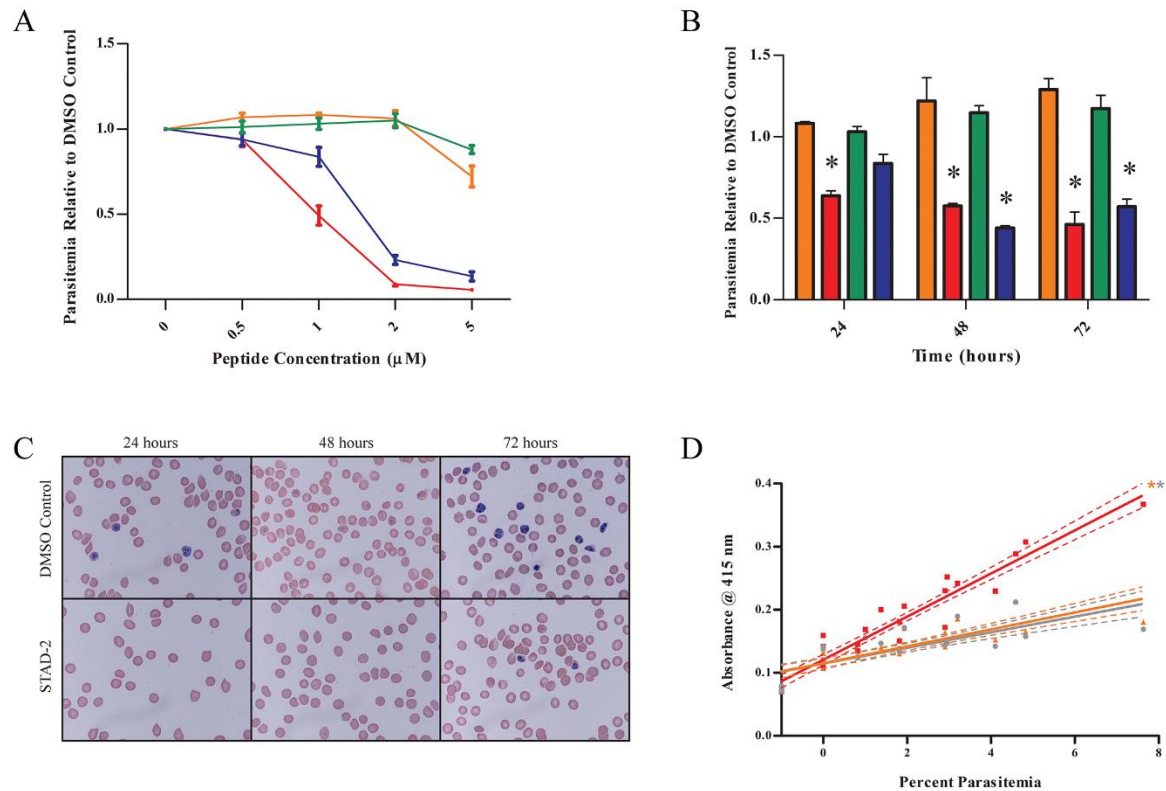


Fig 4.3. STAD-2 reduces viability of *P. falciparum* in vitro. (A) Synchronous ring- or late-stage iRBC were treated with 0, 0.5, 1, 2, or 5 μ M STAD-2 or its scramble control, and parasitemia was determined by flow cytometry at 24-hours post-treatment. STAD-2 $IC_{50} \approx 1$ μ M for late-stage and 1.5 μ M for ring-stage parasites (n=3, mean \pm S.E., red = STAD-2/late, blue = STAD-2/ring, orange = STAD-2 scramble/late, green = STAD-2 scramble/ring). (B) Synchronous iRBC were treated with 1 μ M STAD-2 or STAD-2 scramble, and parasitemia was determined by flow cytometry at 24, 48 and 72 hours post-treatment. A significant decrease in parasitemia was seen with STAD-2 treatment of both ring- and late-stage iRBC (2way ANOVA, $p < 0.001$, n=3, mean \pm S.E., red = STAD-2/late, blue = STAD-2/ring, orange = STAD-2 scramble/late, green = STAD-2 scramble/ring). (C) Analysis of cells from (B) by light microscopy showed STAD-2 treated iRBC to be morphologically indistinguishable from untreated controls. (D) Late-stage iRBC of

increasing parasitemia were treated with 1 μ M STAD-2, 1 μ M STAD-2 scramble, or DMSO control for 6 hours. Since the presence of oxyhemoglobin is indicative of red blood cell lysis, culture medium was removed and analyzed for evidence of oxyhemoglobin (A_{415}) by UV-Vis spectroscopy. Linear regression demonstrates positive correlation of cell lysis with increasing parasitemia and significantly increased lysis in STAD-2 treated cells relative to STAD-2 scramble and DMSO controls ($p < 0.0001$, $n=4$).

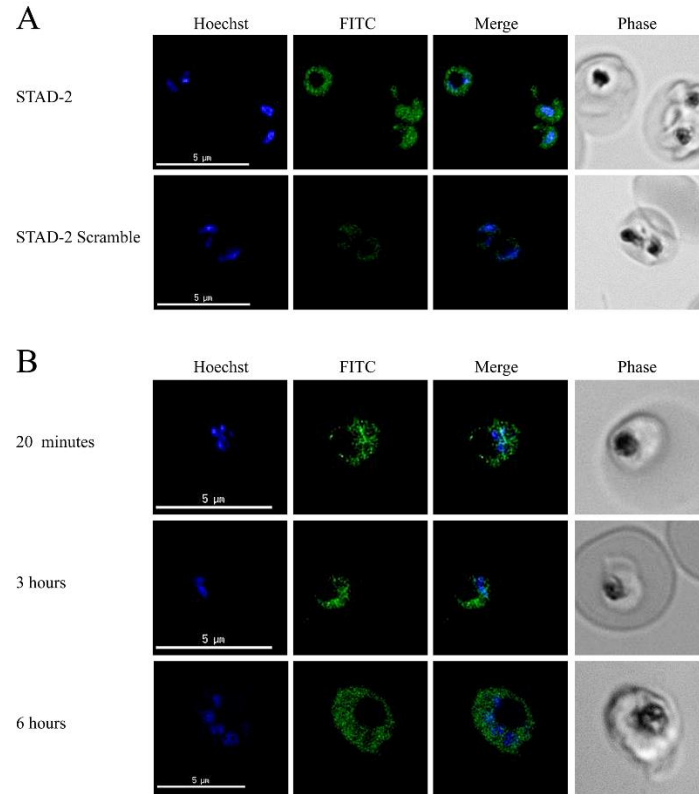


Fig 4.4. STAD-2 rapidly localizes within the parasitophorous vacuole. (A) 3D7 iRBC were treated with 1 μ M STAD-2 or STAD-2 scramble, stained with 2 μ g/mL Hoechst 33342, and analyzed by fluorescence microscopy. STAD-2 peptides consistently localized within the intracellular parasite and at much higher levels than its scrambled control. (B) iRBC treated for 20 minutes, 3 hours, or 6 hours with 1 μ M STAD-2 showed that STAD-2 traffics to the parasitophorous vacuole by 20 minutes post-treatment.

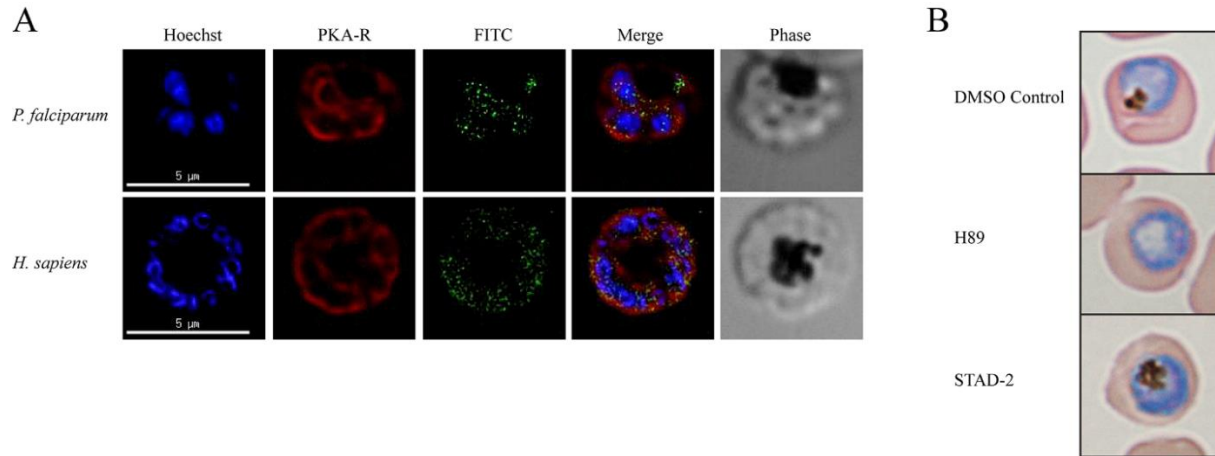


Fig 4.5. STAD-2 does not associate with PKA. (A) Late-stage iRBC were treated with 1 μ M FITC-conjugated STAD-2 for 2 hours and probed for *P. falciparum* PKA-R (top panel) or *H. sapiens* PKA-RII (bottom panel). STAD-2 did not show clear colocalization with either of the regulatory subunits. (B) Late-stage iRBC were treated with 1 μ M STAD-2, 30 μ M H89 (small molecule inhibitor of PKA), or 0.001% DMSO and analyzed by light microscopy at 48 hours post-treatment. H89-treated iRBC demonstrated clear absence of parasite digestive vacuoles while STAD-2 treated iRBC were indistinguishable from DMSO controls.

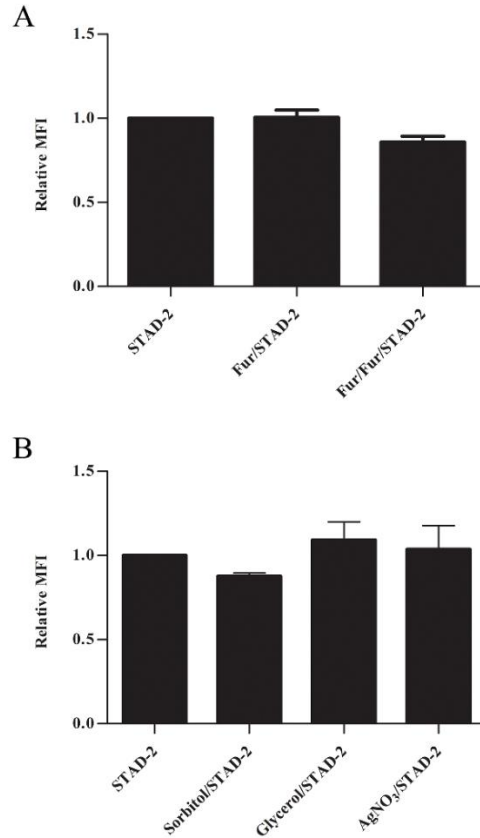


Fig 4.6. STAD-2 uptake is largely independent of the PSAC. (A) Late-stage iRBC were treated with 1 μ M STAD-2 in the presence of 200 μ M furosemide following pre-treatment with complete culture medium (Fur/STAD-2) or 200 μ M furosemide (Fur/Fur/STAD-2). Treatment of late-stage iRBC with STAD-2 in the presence of furosemide demonstrated a visible, yet insignificant, decrease in STAD-2 uptake only when iRBC were pre-treated with furosemide (two-tailed t test, $p=0.0557$, $n=3$, mean \pm S.E.). (B) Late-stage iRBC were treated with 1 μ M STAD-2 in the presence of 5% D-Sorbitol (PSAC solute), 130 mM glycerol (AQP3 solute), or 6 μ M AgNO₃ (AQP1 inhibitor). Treatment with STAD-2 in the presence of 5% D-Sorbitol yielded a decrease in STAD-2 uptake similar to that seen in (A) while treatment in the presence of glycerol or AgNO₃ did not differ from STAD-2 alone ($n=2$, mean \pm S.E.).

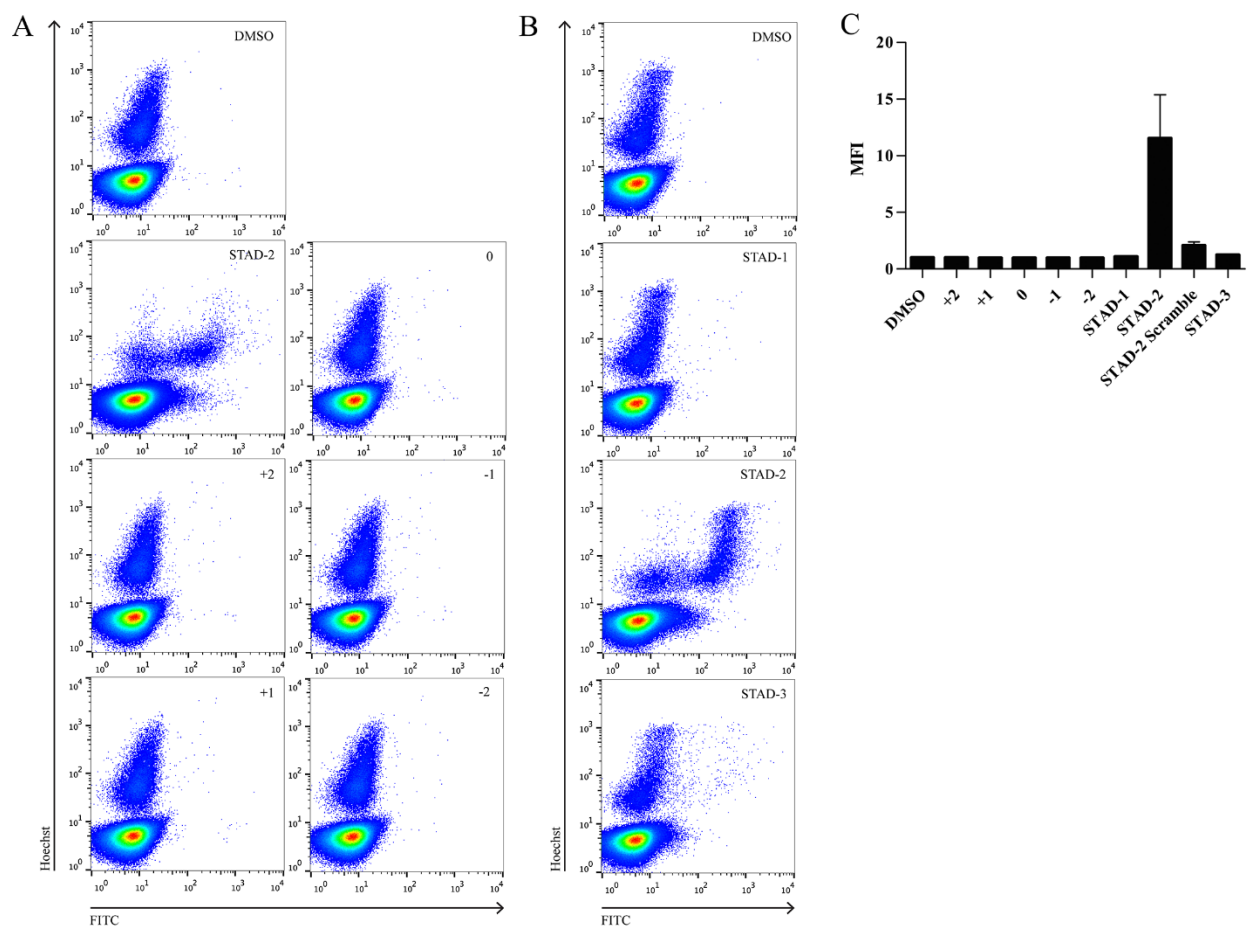


Fig 4.7. STAD-2 is uniquely permeable to iRBC. iRBC were treated for 6 hours with 1 μ M stapled peptides of varying charges (A) or variants of STAD-2 (B), analyzed by flow cytometry, and reported as median fluorescence intensity (C, n=2-6, mean \pm S.E.). Of the various stapled peptides analyzed, only STAD-2 was clearly permeable to iRBC.

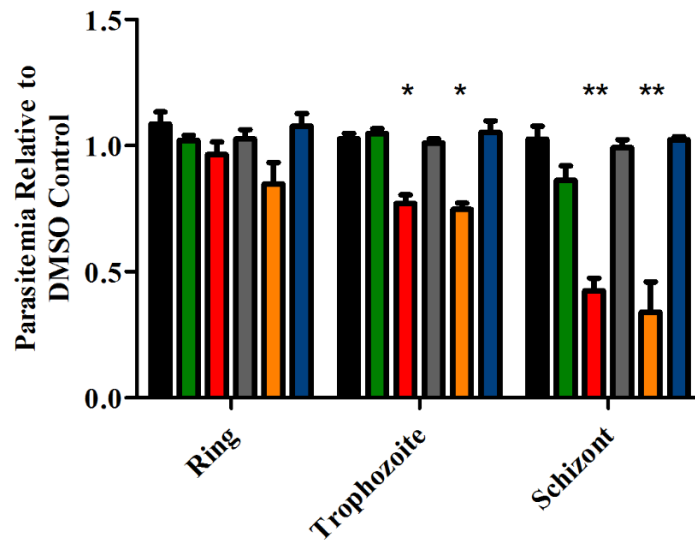


Figure 4.8. STAD-2 activity is elevated at the erythrocyte membrane. Synchronous ring, trophozoite, or schizont iRBC were treated with 1 uM FITC-conjugated STAD-2 (green), strep/biotin-conjugated STAD-2 (red), strep/biotin-conjugated STAD-2 scramble (grey), biotin-conjugated STAD-2 (orange), or biotin-conjugated STAD-2 scramble (blue) for 6 hours and analyzed by flow cytometry. Streptavidin (black) and DMSO controls were included for reference. Both strep/biotin-conjugated and biotin-conjugated STAD-2 treatments caused a significant decrease in parasitemia 6 hours post-treatment (2way ANOVA with Bonferroni posttest, * $p < 0.05$, ** $p < 0.001$, $n = 2-6$, mean \pm S.E.).

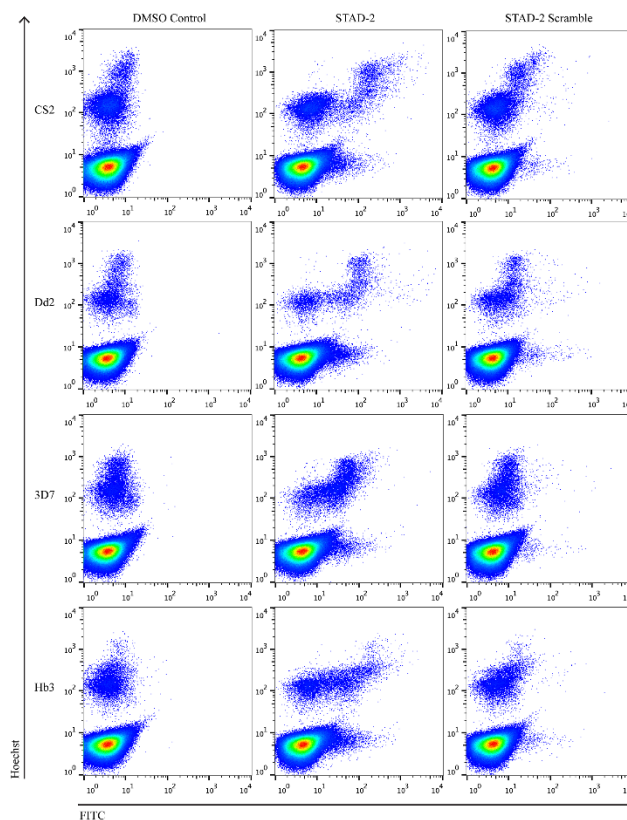


Figure S4.1. STAD-2 is permeable to *P. falciparum* strains *in vitro*. Late-stage iRBC were treated with 1 μ M FITC-conjugated STAD-2 for 2 hours, stained with 2 μ g/mL Hoechst 33342, and analyzed for STAD-2 uptake by flow cytometry. CS2, Dd2, 3D7, and Hb3 parasite strains demonstrate comparable levels of permeability to STAD-2 peptides (n=2).

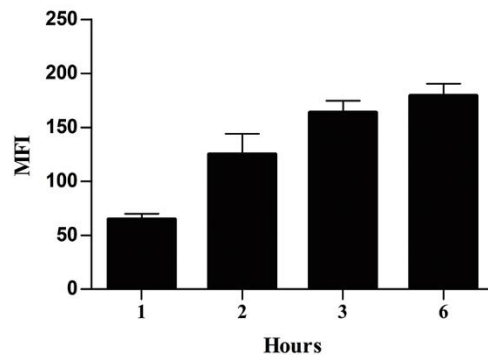


Figure S4.2. STAD-2 permeability increases with time. Late-stage iRBC were treated with 1 μ M FITC-conjugated STAD-2 for 1, 2, 3, or 6 hours and subsequently stained with 2 μ g/mL Hoechst 33342 before analysis by flow cytometry. Near-maximum levels of STAD-2 uptake are evident by 3 hours post-treatment (n=3, mean \pm S.E.).

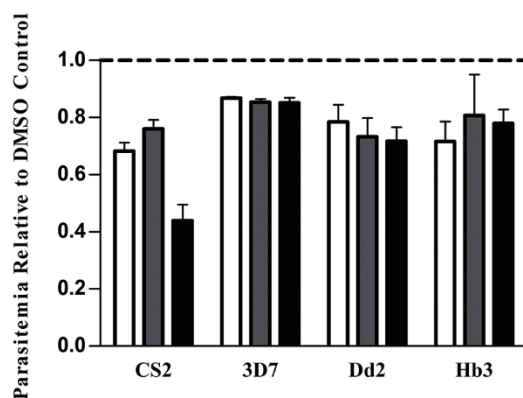


Figure S4.3. STAD-2 reduces viability of *P. falciparum* strains *in vitro*. Late-stage CS2, 3D7, Dd2, and Hb3 parasite strains were treated with 1 μ M FITC-conjugated STAD-2, and parasitemia was determined by flow cytometry at 24, 48 and 72 hours post-treatment. STAD-2 demonstrated variable antimalarial activity between strains and reduced viability in CS2, Dd2, and Hb3 strains (n=3, mean \pm S.E.).

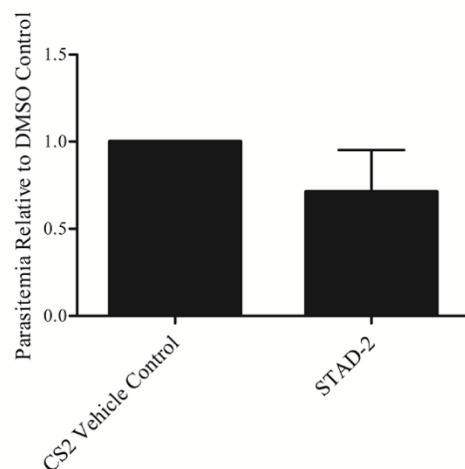


Figure S4.4. STAD-2 reduces parasitemia 6 hours post-treatment. Late-stage iRBC were treated with 1 μ M FITC-conjugated STAD-2 for 6 hours, stained with 2 μ g/mL Hoechst 33342, and analyzed by flow cytometry. Reduction in parasitemia was evident as early as 6 hour post-treatment (n=7, mean \pm S.E.).

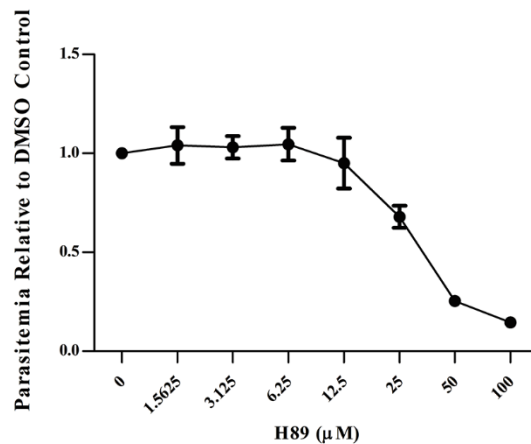


Figure S4.5. H89 Dose-Response Curve. Late-stage iRBC were treated with serial dilutions (100, 50, 25, 12.5, 6.24, 3.13, 1.56, 0.78, and 0 μM) of the small molecule PKA inhibitor, H89, for 24 hours and stained with 2 μg/mL Hoechst 33342 for parasitemia analysis by flow cytometry. H89 *in vitro* IC₅₀ ≈ 30 μM in late-stage CS2 parasites (n=2, mean ± S.E.).

Tables

Table 4.1. Stapled Peptides

Peptide	Sequence (Positive, Negative, Polar)	Charge	Length*
+2 Charged	Beta-Ala S ₅ K K L S ₅ T T	+2	8
+1 Charged	Beta-Ala S ₅ K G L S ₅ T T	+1	8
Neutral Charged	Beta-Ala S ₅ G G L S ₅ T T	0	8
-1 Charged	Beta-Ala S ₅ E G L S ₅ T T	-1	8
-2 Charged	Beta-Ala S ₅ E E L S ₅ T T	-2	8
STAD-1	Beta-Ala K K Y A K Q L A D S ₅ I I K S ₅ A T E	+2	18
STAD-2	Beta-Ala K K L A K F L V S ₅ A L K S ₅ A L K	+5	18
STAD-2 Scramble	Beta-Ala K A L V K L A A L S ₅ K F K S ₅ L K S	+5	18
STAD-3	Beta-Ala K K Y A Q R L S K K I V R A V S ₅ Q W A S ₅	+6	21

*Length in amino acids

Table S4.1. Top hits from Host Supernatant.

Accession Number	Description	Score
169791771	Chain B, Human Hemoglobin D Los Angeles: Crystal Structure	3025.79
149243188	Chain A, Structure Of A Complex Between The A Subunit Of Protein Phosphatase 2a And The Small T Antigen Of Sv40	2429.13
66731527	hemoglobin beta chain [Homo sapiens]	2181.17
528081985	Chain A, Crystal Structure Of The Nuclear Export Receptor Crm1 (exportin-1) Lacking The C-terminal Helical Extension At 4.5a	1954.79
1136741	KIAA0002 [Homo sapiens]	1862.54
36796	t-complex polypeptide 1 [Homo sapiens]	1549.23
194373691	unnamed protein product [Homo sapiens]	1146.61
32455246	serine/threonine-protein phosphatase 2A 65 kDa regulatory subunit A beta isoform isoform a [Homo sapiens]	1106.41
262118263	55 kDa erythrocyte membrane protein isoform 4 [Homo sapiens]	1052.54
540344569	protein phosphatase 1 regulatory subunit 7 isoform 5 [Homo sapiens]	1014.8
19482174	cullin-2 isoform c [Homo sapiens]	952.17
194390984	unnamed protein product [Homo sapiens]	942.14
34193885	UBE2O protein [Homo sapiens]	796.07
194386886	unnamed protein product [Homo sapiens]	754.45
574451196	Chain A, Crystal Structure Of The Fp Domain Of Human F-box Protein Fbxo7(semet)	699.22
578801114	PREDICTED: pyruvate kinase PKLR isoform X2 [Homo sapiens]	540.51
189069189	unnamed protein product [Homo sapiens]	518.92
578835639	PREDICTED: proteasome inhibitor PI31 subunit isoform X3 [Homo sapiens]	472.06
16359158	Actin, beta [Homo sapiens]	457.33
194388336	unnamed protein product [Homo sapiens]	427.41
119581650	resistance to inhibitors of cholinesterase 8 homolog A (C. elegans), isoform CRA_c [Homo sapiens]	413.5
62955833	protein DDII1 homolog 2 [Homo sapiens]	362.26
119582323	diaphanous homolog 1 (Drosophila), isoform CRA_a [Homo sapiens]	336.09
556503347	vacuolar protein sorting-associated protein VTA1 homolog isoform c [Homo sapiens]	308.47
29029559	exportin-2 isoform 1 [Homo sapiens]	305.89
119610151	fatty acid synthase [Homo sapiens]	299.31
304571975	L-xylulose reductase isoform 2 [Homo sapiens]	299.08
530390698	PREDICTED: adenylate kinase isoenzyme 1 isoform X3 [Homo sapiens]	290.76
111306542	Tubulin folding cofactor E-like [Homo sapiens]	282.2
194387314	unnamed protein product [Homo sapiens]	241.18
196049606	Chain A, Pcbp2 Kh1-Kh2 Domains	231.99
119607136	ATPase, H ⁺ transporting, lysosomal 50/57kDa, V1 subunit H, isoform CRA_c [Homo sapiens]	207.08

119607136	ATPase, H ⁺ transporting, lysosomal 50/57kDa, V1 subunit H, isoform CRA_c [Homo sapiens]	207.08
4506411	ran GTPase-activating protein 1 [Homo sapiens]	204.67
574968841	Ras-like GTP-binding protein YPT1 [Plasmodium falciparum FCH/4]	177.59
1060903	phosphatidylinositol transfer protein [Homo sapiens]	173.34
14715077	Stomatin [Homo sapiens]	171.69
41393545	ras-related protein Rab-5C isoform a [Homo sapiens]	165.64
4557361	BH3-interacting domain death agonist isoform 2 [Homo sapiens]	150.02
7710086	ras-related protein Rab-10 [Mus musculus]	147.48
193785071	unnamed protein product [Homo sapiens]	144.43
221045874	unnamed protein product [Homo sapiens]	138.51
73536070	Chain A, Crystal Structure Of The Human Protein Tyrosine Phosphatase, Ptpn7 (Heptp, Hematopoietic Protein Tyrosine Phosphatase)	137.03
7022606	unnamed protein product [Homo sapiens]	132.25
560936937	PREDICTED: ribose-phosphate pyrophosphokinase 1 [Camelus ferus]	130.55
574999933	hypothetical protein PFMC_03692 [Plasmodium falciparum CAMP/Malaysia]	122.87
193787853	unnamed protein product [Homo sapiens]	107.32
221045312	unnamed protein product [Homo sapiens]	104.83
158430541	Chain A, Crystal Structure Of The Putative Ubiquitin Conjugating Enzyme, Pfe1350c, From Plasmodium Falciparum	99.65
119595803	hCG41772, isoform CRA_a [Homo sapiens]	96.4
315259111	NEDD8-MDP1 protein [Homo sapiens]	94.05
300934782	transportin-3 isoform 2 [Homo sapiens]	92.54
193785311	unnamed protein product [Homo sapiens]	92.08
574966533	V-type proton ATPase catalytic subunit A [Plasmodium falciparum FCH/4]	84.31
119627243	Fas (TNFRSF6) associated factor 1, isoform CRA_b [Homo sapiens]	80.76
225891	theta1 globin	80.7
194328762	dnaJ homolog subfamily A member 4 isoform 3 [Homo sapiens]	79.21
436432388	cullin-5, partial [Homo sapiens]	78.18
984305	hPAK65, partial [Homo sapiens]	67.72
361132517	Chain A, Structure Of Ddb1-Ddb2-Cul4a-Rbx1 Bound To A 12 Bp Abasic Site Containing Dna-Duplex	65.94
193786136	unnamed protein product [Homo sapiens]	65.62
13528771	Ubiquitin-fold modifier conjugating enzyme 1 [Homo sapiens]	61.48
48257132	GLRX3 protein [Homo sapiens]	60.79
763431	albumin-like [Homo sapiens]	45.38

Table S4.2. Top hits from Parasite Supernatant.

Accession Number	Description	Score
583224913	hypothetical protein PFNF54_03521 [Plasmodium falciparum NF54]	960.04
124806612	conserved Plasmodium membrane protein [Plasmodium falciparum 3D7]	706.63
124506661	RhopH3 [Plasmodium falciparum 3D7]	596.65
124808276	rhoptry-associated protein 1, RAP1 [Plasmodium falciparum 3D7]	546.56
4758274	protein 4.1 isoform 6 [Homo sapiens]	509.66
641579788	elongation factor 1-alpha [Plasmodium reichenowi]	484.46
583222626	hypothetical protein PFNF54_05344 [Plasmodium falciparum NF54]	443.26
124504715	Cytoadherence linked asexual protein 3.1 [Plasmodium falciparum 3D7]	423.89
124808177	plasmepsin II [Plasmodium falciparum 3D7]	410.19
457870788	casein kinase II alpha subunit, partial [Plasmodium cynomolgi strain B]	365.36
124513506	60S ribosomal protein L6-2, putative [Plasmodium falciparum 3D7]	316.67
564281666	40S ribosomal protein S3 [Plasmodium yoelii 17X]	310.35
340523183	Rhesus blood group CE antigen [Homo sapiens]	305.65
124513388	60S ribosomal protein L23, putative [Plasmodium falciparum 3D7]	303.05
297343011	Chain A, Crystal Structure Of Nucleosome Assembly Protein S (Pfnaps) Plasmodium Falciparum	275.1
574968899	hypothetical protein PFFCH_00706 [Plasmodium falciparum FCH/4]	273.07
583225203	GTP-binding nuclear protein Ran [Plasmodium falciparum NF54]	243.31
124505571	40S ribosomal protein S19, putative [Plasmodium falciparum 3D7]	240.77
124809020	60S ribosomal protein L14, putative [Plasmodium falciparum 3D7]	240.23
1942549	Chain A, Plasmepsin Ii, A Hemoglobin-Degrading Enzyme From Plasmodium Falciparum, In Complex With Pepstatin A	239.90
332639841	Chain A, Crystal Structure Of Plasmepsin I (Pmi) From Plasmodium Falciparum	221.95
574965060	elongation factor 1-alpha [Plasmodium falciparum FCH/4]	211.68
574752876	hypothetical protein PFFVO_00444 [Plasmodium falciparum Vietnam Oak-Knoll (FVO)]	209.68
579103850	hypothetical protein PFBG_06095, partial [Plasmodium falciparum 7G8]	208.58
124810024	conserved Plasmodium protein, unknown function [Plasmodium falciparum 3D7]	193.07
194390580	unnamed protein product [Homo sapiens]	187.88
583213539	hypothetical protein C923_04268 [Plasmodium falciparum UGT5.1]	183.69
574751535	hypothetical protein PFFVO_01548 [Plasmodium falciparum Vietnam Oak-Knoll (FVO)]	178.77
579333288	hypothetical protein PFAG_03260 [Plasmodium falciparum Santa Lucia]	157.25
574987819	hypothetical protein PFMALIP_02788 [Plasmodium falciparum MaliPS096_E11]	150.15
574965565	hypothetical protein PFFCH_03788 [Plasmodium falciparum FCH/4]	143.7
124803615	casein kinase II, alpha subunit [Plasmodium falciparum 3D7]	140.99
70940074	40S ribosomal subunit protein S9 [Plasmodium chabaudi chabaudi]	138.68
194389302	unnamed protein product [Homo sapiens]	133.97

583215234	hypothetical protein C923_02904 [Plasmodium falciparum UGT5.1]	118.56
237640627	Chain A, Crystal Structure Of Nucleosome Assembly Protein From Plasmodium Falciparum	116.97
82595793	ribosomal protein L1p [Plasmodium yoelii yoelii 17XNL]	107.92
258597720	60S ribosomal protein L7-3, putative [Plasmodium falciparum 3D7]	106.81
574999933	hypothetical protein PFMC_03692 [Plasmodium falciparum CAMP/Malaysia]	103.75
579122813	hypothetical protein PFBG_03161 [Plasmodium falciparum 7G8]	102.25
258597165	Antigen UB05 [Plasmodium falciparum 3D7]	97.55
124506321	40S ribosomal protein S9, putative [Plasmodium falciparum 3D7]	91.03
579338554	hypothetical protein PFAG_01516 [Plasmodium falciparum Santa Lucia]	82.59
583224413	hypothetical protein PFNF54_04037 [Plasmodium falciparum NF54]	74.87
37777724	exported protein 1 [Plasmodium falciparum]	74.12
574976683	hypothetical protein, variant [Plasmodium falciparum Tanzania (2000708)]	72
124513900	40S ribosomal protein S13, putative [Plasmodium falciparum 3D7]	55.49
296005391	40S ribosomal protein S15/S19, putative [Plasmodium falciparum 3D7]	51.78
124802054	DNA/RNA-binding protein, putative [Plasmodium falciparum 3D7]	51.29
70935336	hypothetical protein [Plasmodium chabaudi chabaudi]	49.33
574996133	40S ribosomal protein S5 [Plasmodium falciparum Palo Alto/Uganda]	49.29
574974561	hypothetical protein PFTANZ_02640 [Plasmodium falciparum Tanzania (2000708)]	46.23

CHAPTER 5

TARGETED INHIBITION OF *PLASMODIUM FALCIPARUM* CALCIUM DEPENDENT PRTOEIN KINASE-1 WITH A STAPLED J DOMAIN DISRUPTOR PEPTIDE ³

³ Flaherty, B.R., Wang, Y., Ho, T.G., Kennedy, E.J., and Peterson, D.S. To be submitted to ACS Chemical Biology.

Abstract

Calcium-dependent protein kinases (CDPK) are a unique family of protein kinases found in plants and apicomplexan parasites. Reverse genetic analyses have demonstrated CDPK1 to be essential during both *Plasmodium* sexual and asexual development. During the asexual blood-stage life cycle, CDPK1 phosphorylates key members of the glideosome, thereby controlling parasite motility and erythrocyte egress and invasion. CDPK1 is composed of a calmodulin-like domain, a kinase domain, and an autoinhibitory J domain. We synthesized hydrocarbon stapled peptides designed to mimic the J domain and inhibit *Pf*CDPK1 kinase activity. J domain disruptor (JDD) peptides were selectively permeable to late schizonts and colocalized with dividing daughter cells in these very late-stage parasites. Treatment of late-stage parasites with $\geq 5 \mu\text{M}$ JDD resulted in a significant decrease in parasite viability mediated by a blockage of merozoite invasion of erythrocytes. This marks the first use of stapled peptides designed to specifically target essential *P. falciparum* proteins. The study validates *Pf*CDPK1 as a potential antimalarial target and provides further support for stapled peptides as future antimalarial agents.

Introduction

Plasmodium falciparum is an intracellular protozoan parasite endemic to 87 countries across the globe [1]. Its continued transmission placed approximately 3.2 billion individuals at risk of malaria and led to an estimated 584,000 deaths in 2013 alone [2]. Contrary to what such estimates might suggest, the global health community has made significant advances in malaria control over recent years, effectively reducing malaria mortality rates by 47% worldwide since 2000. Such advances have been achieved, primarily, through increased access to vector control measures, diagnostic testing, and efficacious antimalarial drugs. However, evidence of spreading resistance to both insecticides and antimalarial drugs places ongoing control efforts in serious jeopardy [3,4].

The development of drug resistance in *Plasmodium* depends on a variety of factors including (a) the mutation rate of the parasite, (b) the fitness cost associated with drug-resistant mutations, (c) the magnitude of drug selection pressure, and (d) the level of treatment compliance within the community [5]. Under standard conditions, the highly plastic *Plasmodium* genome readily undergoes mitotic recombination events that generate the single nucleotide variants and copy number variants that contribute to the evolution of drug resistance [6]. With the addition of drug pressure, mutant parasites gain a selective advantage that can overcome mutation-associated fitness costs and enable the spread of drug resistant clones. While some regions of the genome are more refractory to recombination events, others localize near “recombination hotspots” and are, therefore, more prone to accumulating mutations [7]. Nevertheless, resistance to all antimalarial monotherapies, including the most recently employed artemisinin-based drugs, has developed in at least one part of the world and currently places critical malaria control efforts at serious risk [4,5]. While a combinatorial approach – applying

multiple drugs with varying mechanisms of action – has delayed the spread of resistance, future control efforts will rely on the discovery and development of new and novel antimalarial drugs.

All existing antimalarial drugs, as well as many of those currently under development, are small molecule inhibitors [8–12]. These drugs act by binding within confined hydrophobic pockets of target proteins and, either directly or allosterically, inhibiting protein activity.

Unfortunately, the rigid specificity of these small molecule inhibitors renders them inherently vulnerable to the development of resistance, particularly in a genetically plastic organism like *Plasmodium*. Time to resistance can vary and depends both on the biological and community factors listed above as well as the mechanism of action of the drug of interest. While highly effective drugs, like chloroquine, maintained efficacy for as many as 40 years [4], others, like atovaquone, can establish resistance within a single infection [13]. Future antimalarials should seek to target immutable components of the *Plasmodium* genome and/or employ unique mechanisms of action that present reduced susceptibility to parasite mechanisms of resistance.

Recent work in our lab proposed the use of chemically stabilized peptides as potential antimalarial agents that may be uniquely refractory to *Plasmodium* mechanisms of drug resistance [14]. Chemically stabilized, or stapled, peptides are a novel class of inhibitors composed of a polypeptide sequence locked into an α -helical conformation by a hydrocarbon staple [15]. These non-traditional protein therapeutics can be designed to bind protein interfaces with high specificity and thereby block intra- or inter-molecular protein-protein interactions [16,17]. Helix stabilization via the hydrocarbon staple affords increased cell permeability relative to traditional protein therapeutics and, therefore, expands the list of potential protein targets [18]. We propose that targeting stapled peptides to flat, elongated surfaces of proteins unique to

Plasmodium may offer a novel method of parasite inhibition with reduced propensity for escape mutations.

Previous studies in our lab examining the permeability of the *Hs*PKA-targeting Stapled AKAP Disruptor-2 (STAD-2) found this stapled peptide to be selectively permeable to *P. falciparum*-infected red blood cells (iRBC) *in vitro* [14]. Unexpectedly, STAD-2 demonstrated rapid antiparasmodial activity via a PKA-independent mechanism. Further analysis suggested that STAD-2 activity is mediated by iRBC-specific lysis. Peptide permeability was shown to be highly specific to STAD-2 and mediated via a *Plasmodium* surface anion channel (PSAC)-independent pathway.

While studies with STAD-2 established important groundwork for the use of stapled peptides in *Plasmodium*, STAD-2's undefined mechanism of action in *P. falciparum*, as well as its potent activity against *Hs*PKA, renders it a poor candidate antimalarial. However, since stapled peptides can be designed to target any accessible protein interface, we considered that stapled peptides could be designed to inhibit *Plasmodium*-specific protein targets. Herein, we explore the use of a *P. falciparum*-specific stapled peptide kinase inhibitor *in vitro*.

In 2009, a high throughput analysis of nearly 2 million GlaxoSmithKline compounds identified 13,533 candidates that inhibited *P. falciparum* growth by greater than 80% at 2 μ M concentration [19]. Of those compounds identified and validated, a large majority were protein kinase inhibitors. Although *P. falciparum* has a relatively small kinome, composed of less than 100 identified kinases, a significant proportion of those have no ortholog in the mammalian genome [20,21]. For example, the calcium dependent protein kinases (CDPKs) can be found in plants and alveolates but are altogether absent from metazoans; meanwhile the FIKKs, which are characterized by a Phe-Ile-Lys-Lys sequence in the N-terminal region of their kinase domain, do

not cluster with any known eukaryotic kinase group [20]. It has, therefore, been suggested that such *Plasmodium* kinases may be ideal targets for antimalarial drug development. In the following, we explore the antimalarial potential of a stapled peptide designed to target the *P. falciparum* calcium dependent protein kinase, CDPK1.

The CDPKs are a family of serine/threonine kinases that are found in plants and many apicomplexan parasites such as *Toxoplasma gondii*, *Cryptosporidium parvum*, and multiple species of *Plasmodium* [22]. They are generally characterized by a S/T kinase domain linked to four EF-hand domains that function analogously to calmodulin [23]. Between the catalytic and calmodulin-like domains (CLD) lies an autoinhibitory junction domain, sometimes referred to as the J domain. At basal Ca^{2+} levels, the J domain is thought to serve as a pseudosubstrate, blocking the active site of the enzyme and inhibiting kinase activity. Following a tightly regulated increase in intracellular Ca^{2+} , binding of Ca^{2+} to the CLD triggers a conformational change characterized by increased intramolecular interactions between the CLD and the autoinhibitor and subsequent enzyme activation [22,24].

In plants, CDPKs serve essential roles in a diverse array of functions ranging from biotic and abiotic stress signaling to vacuolar biogenesis and pollen development [24,25]. As such, plant CDPK families are generally large, reaching up to as many as 34 members in some organisms such as *Arabidopsis* [24]. In Apicomplexans, CDPKs play a similarly wide range of roles throughout parasite development despite possessing fewer family members. Phylogenetic analyses indicate that *T. gondii* contains 11 CDPK-like genes while *P. falciparum* contains 8 and *C. parvum* contains only 7 [22]. Of these, six have been confirmed to be expressed and conserved in nearly all apicomplexan parasites – CDPK1, CDPK3, CDPK4, CDPK5, CDPK6, and CDPK7 [26]. Studies in *Plasmodium* and *T. gondii* have established functions for many of

these kinases. For example, CDPK1 has been repeatedly shown to play a role in microneme secretion, parasite motility, host cell egress, and host cell invasion in both *T. gondii* and *Plasmodium* [27–29]. Reverse genetic analyses in *P. berghei* demonstrated CDPK3 to play an essential role in ookinete motility and invasion of the peritrophic membrane in the mosquito midgut [30,31]. Gene knockout studies of *P. berghei* CDPK4 implicated this kinase as a critical regulator of microgametocyte exflagellation [32]. Disruption of *PbCDPK6* revealed this kinase to be the key mediator of the sporozoite transition from a migratory to an invasive phenotype [33]. Finally, genetic knockdown of *TgCDPK7* pointed to its essential role in positioning and partitioning of the centrosomes during parasite division [26].

In this study, we explore the permeability and activity of a chemically stapled peptide designed to mimic the autoinhibitory J domain of *PfCDPK1*. This work was inspired by previous studies which demonstrated inhibition of *PfCDPK1* activity by J domain-associated peptides [27,28]. For example, Bansal et al. achieved inhibition of rCDPK1 as well as inhibition of merozoite invasion with partial peptides designed to simulate portions of the *PfCDPK1* J domain [28]. Similarly, after validating *in vitro* inhibition of rCDPK1 by both full-length and partial J domain, Azevedo et al. demonstrated CDPK1-dependent parasite arrest following transfection with a conditionally expressed J-GFP fusion protein [27]. Although maximal recombinant kinase inhibition was attained with full-length J domain, both studies found that C-terminal partial peptides demonstrated high binding affinity and significant inhibition of rCDPK1. As a result, we chose to model our J domain disruptor (JDD) stapled peptide after the C-terminal region of *PfCDPK1*.

Flow cytometric analyses demonstrated JDD to be selectively permeable to late, schizogenic infected red blood cells (iRBC). This pattern of uptake was consistent with previous

studies showing upregulated expression of *Pf*CDPK1 throughout erythrocyte schizogeny [28,34]. Analysis of peptide localization by fluorescence microscopy found JDD to localize to dividing daughter cells within late schizonts, again consistent with studies demonstrating *Pf*CDPK1 localization to the merozoite plasma membrane [27,34]. Finally, JDD exhibited clear antiplasmodial activity at concentrations $\geq 5 \mu\text{M}$. This inhibition was characterized by a defect in erythrocyte invasion and was consistent with previous studies showing blockage of invasion by both J domain-associated peptides as well as the CDPK1 small molecule inhibitor, K252a [28,34]. The following work validates JDD as a *Pf*CDPK1 inhibitor and supports the use of chemically stapled peptides as novel antimalarial agents.

Materials and Methods

Blood and Reagents

Human O⁺ red blood cells were either purchased from Interstate Blood Bank, Inc. or donated by healthy volunteers. This research was approved by the Institutional Review Board (IRB) at the University of Georgia (no. 2013102100); all donors signed consent forms. Unless otherwise noted, all chemicals and reagents for this study were either purchased from Sigma Aldrich or Fisher Scientific.

Parasite Culture and Synchronization

Plasmodium falciparum CS2 parasites were maintained in continuous culture according to routine methods. Parasites were cultured at 4% hematocrit in O⁺ red blood cells. Cultures were maintained in 25 cm² or 75 cm² tissue culture flasks at 37°C under a gas mixture of 90% nitrogen/5% oxygen/5% carbon dioxide and in complete culture medium made up of RPMI containing 25 mM HEPES, 0.05 mg/mL hypoxanthine, 2.2 mg/mL NaHCO₃ (J.T. Baker), 0.5% Albumax (Gibco), 2 g/L glucose, and 0.01 mg/mL gentamicin. Primarily ring-stage cultures were treated routinely with 5% D-Sorbitol to achieve synchronous cultures.

JDD Synthesis and Purification

Peptides were synthesized and purified as previously described [35]. JDD design was based off multiple sequence alignment of the J domain regions from various species of *Plasmodium*. Alignments were conducted using Geneious software (version 7.0).

JDD Permeability

Synchronous ring-stage or late-stage infected red blood cells (iRBC) and uninfected red blood cells (uRBC) were brought up to 4% hematocrit in complete culture medium. FITC-conjugated peptides were added to a final concentration of 1 μ M, and cultures were incubated for 6 hours at 37°C under standard gas conditions. Following incubation, 25 μ L cell mixture was removed and treated with 100 μ L 2 μ g/mL Hoechst 33342 for 10 minutes at 37°C. Cells were subsequently washed once in 1 mL 1X PBS, resuspended in 300 μ L 1X PBS, and analyzed for Hoechst and FITC staining on a Beckman Coulter CyAn flow cytometer. 500,000 events were collected at a rate of 15,000 – 20,000 events per second. Data was analyzed using FlowJo X single cell analysis software (FlowJo LLC).

Fluorescence Microscopy

A 5 mL culture of primarily late-stage iRBC was brought up to 4% hematocrit in complete culture medium and transferred to a T25 tissue culture flask. FITC-conjugated JDD was added to a final concentration of 1 μ M after which the culture was incubated for 6 hours at 37°C under standard gas conditions. Following incubation, 50 μ L of cell mixture was removed and washed twice with 1 mL 1X PBS. Cells were subsequently stained with 200 μ L 2 μ g/mL Hoechst 33342 for 10 minutes at 37°C. After staining, cells were washed twice with 1X PBS, deposited on a glass microscope slide, covered with a glass coverslip, and sealed. Live cells were immediately imaged with a DeltaVision II microscope system using an Olympus IX-71 inverted microscope and a CoolSnap HQ2 CCD camera. 0.2 μ m z-stacks were acquired and deconvolved using SoftWorx 5.5 acquisition software (Applied Precision, Inc.).

JDD-Induced Hemolysis

Synchronous late-stage iRBC were mixed with uRBC in order to achieve a series of samples with stepwise decreasing parasitemia. Samples were brought up to 4% hematocrit in complete culture medium containing 1 μ M JDD, 1 μ M JDD scramble, or 0.001% DMSO and transferred to a 48-well tissue culture plate in 200 μ L aliquots in duplicate. The plate was incubated at 37°C under standard gas conditions for 6 hours. Following incubation, all samples were transferred to microcentrifuge tubes and centrifuged at 700 rcf for 5 minutes to pellet cells. 100 μ L of supernatant was removed from each tube and transferred to a 96-well, flat-bottom tissue culture plate. Oxyhemoglobin absorbance was measured at 415 nm using a SpectraMax Plus microplate spectrophotometer with SoftMax Pro 5.4 software (Molecular Devices, LLC).

JDD Dosing Assay

Ring-stage or late-stage iRBC at <0.5% parasitemia were brought up to 4% hematocrit in complete culture medium and transferred to a 24-well tissue culture plate in 1 mL aliquots. iRBCs were then treated with 1 μ M JDD or 0.001% DMSO (vehicle control) once at assay initiation, once every 24 hours, or once every 12 hours for 72 hours. Cultures were stored at 37°C under standard gas conditions. 25 μ L were removed from each well every 24 hours post-assay initiation, and samples were stained with Hoechst 33342 for parasitemia analysis via flow cytometry.

JDD Dose-Response

Synchronous, late-stage iRBC at approximately 0.5% parasitemia were brought up to 4% hematocrit in complete culture medium and transferred to a 24-well tissue culture plate in 1 mL

aliquots. Plates containing uRBC or iRBC were supplemented with JDD or JDD scramble peptides to final concentrations of 1, 2.5, or 10 μ M and subsequently stored at 37°C under standard gas conditions. At 24 hours post-treatment, 25 μ L were removed from each well and treated with 2 μ g/mL Hoechst 33342 for parasitemia analysis by flow cytometry. Giemsa-stained blood smears were also prepared at 24 hours post-treatment.

Statistical Analysis

Graphing and statistical analyses were done using GraphPad Prism 5 (GraphPad Software, Inc.).

Results

JDD mimics the autoinhibitory J domain of PfCDPK1

JDD was designed to mimic the autoinhibitory J domain of *Pf*CDPK1. In the absence of Ca^{2+} , native CDPK1 exists in an inactive state wherein the J domain is bound to the protein kinase domain and inhibits kinase activity (Figure 5.1.A). Binding of Ca^{2+} to the calmodulin-like domain (CLD) of inactive CDPK1 induces a conformational change that ultimately results in displacement of the J domain and subsequent activation of the CDPK1 kinase domain. In order to inhibit *Pf*CDPK1 activity, we designed JDD to simulate the autoinhibitory region of the J domain and bind to the CDPK1 kinase domain thereby displacing the native J domain and inhibiting CDPK1 activity (Figure 5.1B). Multiple sequence alignment of the J domains of various species of *Plasmodium* demonstrate the *Plasmodium* J domain to be highly conserved between species (Figure 5.1C). Based off this alignment, as well as previous studies demonstrating that the C-terminal region of the J domain most strongly binds and inhibits the CDPK1 kinase domain [27,28], we chose to model our J domain disruptor peptide after the C-terminal helical region located between amino acids 352 and 370 of the native J domain (red, Figure 5.1C).

JDD is selectively permeable to schizogenic iRBC

In order for JDD peptides to contact their CDPK1 target, JDD must first gain access to the intracellular parasite. Although the full details of cell permeability in iRBC remain poorly understood, most solutes are thought to be taken up via a *Plasmodium* Surface Anion Channel (PSAC) that is expressed by the parasite on the erythrocyte membrane during the latter stages of the blood-stage life cycle. This non-specific channel provides the intracellular parasite with

essential nutrients such as amino acids, sugars, anions, purines, and vitamins [36]. Despite the broad spectrum of PSAC-permeable solutes, most research has demonstrated channel permeability to be limited to low molecular weight molecules [37]. Therefore, our initial studies sought to explore whether the ~2 kDa JDD peptide was permeable to iRBC.

Permeability was first examined by incubating 1 μ M FITC-conjugated JDD peptides with uninfected red blood cells (uRBC) and CS2 iRBC for 6 hours. Following incubation, cells were stained with 2 μ g/mL Hoechst 33342 and analyzed by flow cytometry. As an increase in Hoechst signaling indicates higher quantities of DNA, cells with higher levels of Hoechst staining represent those infected with schizogenic parasites, or parasites undergoing DNA replication, while cells with baseline Hoechst staining represent anucleate, uninfected red blood cells. JDD peptides demonstrated moderate, but selective, permeability to schizogenic iRBC, as evidenced by high levels of Hoechst staining in the FITC-positive iRBC population (Figure 5.2A). In order to further confirm the influence of parasite stage on JDD uptake, iRBC were synchronized using 5% D-Sorbitol, and peptide permeability was measured in ring- versus late-stage parasites. Again, schizogenic iRBC demonstrated increased JDD uptake relative to ring and early-trophozoite iRBC (Figure 6.2B). This pattern of staining is consistent with previous studies showing increased expression of *Pf*CDPK1 in late schizonts [28,34]. As a control, ring- and late-stage iRBC were also treated with scrambled JDD peptides possessing identical chemical composition to JDD but a scrambled amino acid sequence. JDD scramble peptides demonstrated no permeability to iRBC regardless of parasites stage. These results may suggest a role for intracellular binding in intraerythrocytic peptide retention.

Previous studies exploring the use of stapled peptides in *P. falciparum* found high permeability of PKA-targeting STAD-2 stapled peptides in late-stage iRBC [14]. STAD-2

peptides were modified by addition of a polyethylene glycol (PEG) group, which imparts increased solubility to the polypeptide chain. Since JDD achieves only moderate permeability in very late-stage iRBC, we sought to explore if PEGylation, and its resultant increase in solubility, would influence JDD permeability to iRBC. However, analysis by flow cytometry demonstrated permeability patterns of JDD-PEG to be identical to those of the unmodified JDD peptide (Figure 5.2C). Comparison of the median FITC intensity of iRBC treated with these various stapled compounds clearly demonstrates negligible permeability of JDD scramble peptides, modest permeability of JDD and JDD-PEG, and significant permeability of STAD-2 stapled peptides (Figure 5.2D).

JDD colocalizes with daughter cells in segmented parasites

Since JDD demonstrated increased permeability in schizogenic parasites, we next wanted to explore the localization of JDD in late-stage iRBC. To do this, synchronous iRBC were treated with 1 μ M FITC-conjugated JDD peptides for 6 hours and subsequently stained with 2 μ g/mL Hoechst 33342. Live cells were then mounted on a cover slip and examined by fluorescence microscopy. While JDD fluorescence was most evident in very late, divided schizonts, faint staining could also be seen in early late-stage (trophozoite) iRBC (Figure 5.3). In these early late-stage iRBC, JDD appeared to traffic to the intracellular parasite but was not seen within the parasite digestive vacuole. Meanwhile, in very late, segmented iRBC, JDD brightly colocalized with dividing daughter cells. This pattern of localization is, again, consistent with previous data showing that *Pf*CDPK1 localizes to the merozoite plasma membrane and plays an essential role in merozoite motility and microneme secretion [34]. The high permeability and

clear localization of JDD peptides in these late schizonts would suggest that JDD peptides may, indeed, be reaching their intended CDPK1 target.

JDD is not hemolytic

Given that previous studies with STAD-2 peptides found that STAD-2 demonstrated PKA-independent hemolytic activity in iRBC [14], we wondered if such lytic activity was specific to STAD-2 or if it was simply a byproduct of stapled peptide uptake. If the latter, such nonspecific lytic activity might hinder JDD from reaching its intended intracellular target. Since JDD, like STAD-2, demonstrates selective permeability to iRBC, we chose to explore whether JDD peptides were also capable of inducing iRBC lysis. To address this question, serial dilutions of synchronous, late-stage iRBC were prepared in order to yield a series of samples ranging from 0% to 8% parasitemia. Samples were then treated with 1 μ M JDD or JDD scramble for 6 hours, after which the extent of cell lysis was determined by measuring the absorbance of oxyhemoglobin in the sample medium at $\lambda = 415$ nm. Unlike STAD-2, JDD-induced lysis of iRBC was minimal at all parasitemias tested and identical to both JDD scramble-treated and untreated iRBC controls (Figure 5.4). These results indicate that JDD displays no hemolytic activity in iRBC, and, rather, that STAD-2 hemolytic activity is specific to its yet unknown mechanism of action.

1 μ M JDD demonstrates poor antiplasmodial activity

Our studies thus far have shown that JDD is selectively permeable to schizogenic iRBC and localizes to the dividing daughter cells in segmented schizonts. These observations are consistent with previous studies of *Pf*CDPK1 and suggest that the synthetic JDD stapled peptides

may, indeed, be binding to their intended CDPK1 target. Since previous analyses of J domain inhibitors found that binding of synthetic J domain constructs to *Pf*CDPK1 effectively arrested parasite development [27,28], we set out to determine if treatment of late-stage iRBC with JDD stapled peptides would yield similar antiparasmodial activity. In order to test this, we first treated late-stage iRBC with 1 μ M JDD and analyzed changes in parasitemia by flow cytometry at 24, 48, and 72 hours post-treatment. Since previous studies found that STAD-2 displayed antimalarial activity with an IC_{50} of 1 μ M, we chose to begin our analysis of JDD peptides at this same concentration. Unfortunately, treatment of iRBC with 1 μ M JDD peptides produced no change in parasitemia relative to DMSO controls. These results can be explained by a variety of scenarios. First, although previous studies demonstrated hydrocarbon stabilized peptides to possess a serum half-life on the range of ~30 hours [18], stapled peptides do not remain stable indefinitely in solution. It is possible that JDD peptides lose stability in solution over time such that single treatment with JDD is insufficient to attain inhibition of CDPK1. If that is the case, especially considering the short time window of CDPK1 activity, periodic supplementation with JDD peptides may be necessary. Alternatively, 1 μ M concentration might be too low to achieve effective CDPK1 inhibition. Finally, despite evidence suggesting otherwise, perhaps our JDD peptides are not reaching their intended target.

In an effort to further explore JDD antiparasmodial activity, we first considered multiple treatments with JDD over time, maintaining sufficiently high levels of JDD to achieve *Pf*CDPK1-associated inhibition of parasite growth. To test this, synchronous late-stage iRBC were treated with 1 μ M JDD once at assay initiation, once every 24 hours, or once every 12 hours for 72 hours. Parasitemia was determined by flow cytometry at 24, 48, and 72 hours post-assay initiation. Although multiple JDD treatments had a more pronounced effect on parasite

viability over time, reductions in parasite density remained moderate, dropping by only 5-25% at 48 and 72 hours post-assay initiation (Figure 5.5A, grey and white striped bars). However, reductions in parasitemia of up to 20% were also observed in the DMSO negative control populations, particularly those controlling for 12 hour JDD treatments (Figure 5.5A, solid bars). With DMSO toxicity taken into account, changes in parasite viability achieved using periodic supplementation with 1 μ M JDD were insignificant. Therefore, repeated dosing with JDD peptides does not effectively achieve *Pf*CDPK1-mediated inhibition of parasite growth.

High dose JDD displays clear antimalarial activity

Since repeated dosing did not significantly increase JDD's antiparasmodial activity, we next explored if increasing JDD concentration would yield a more significant reduction in parasite viability. Late-stage iRBC were treated with 1, 2, 5, or 10 μ M JDD or JDD scramble, and parasitemia was determined by flow cytometry at 24 hours post-treatment. Although treatment with JDD scramble had no effect on parasite viability at any concentration tested, treatment with 5 and 10 μ M JDD yielded significant reductions in parasitemia by 24 hours post-treatment (~10% and ~50%, $p < 0.01$ and $p < 0.001$, Figure 5.5B). Analysis of Giemsa-stained blood smears showed a clear drop in the presence of ring-stage parasites following 10 μ M JDD treatment, suggesting that JDD-treated parasites are defective in their ability to invade healthy erythrocytes. Given the established role of *Pf*CDPK1 in merozoite invasion [28,34], these results indicate that JDD peptides effectively inhibit *Pf*CDPK1.

Discussion

*Pf*CDPK1 was first identified by Zhao et al. in 1993 [38]. Since then, numerous studies have examined the role of CDPK1 in *Plasmodium* parasites. Genetic disruption of this calcium-dependent kinase in blood-stage *P. falciparum* has been unsuccessful, suggesting that CDPK1 is essential to parasite asexual development [27,39]. In addition, genetic knockdown of *Pb*CDPK1 found the kinase to be indispensable during sexual development within the mosquito [40], indicating that CDPK1 may be essential throughout all stages of parasite development.

During the asexual life cycle, *Pf*CDPK1 has been shown to phosphorylate two key proteins: glideosome associated protein 45 (GAP45) and myosin A tail domain-interacting protein (MTIP) [34,41]. These proteins are members of the *Plasmodium* glideosome, an actin- and myosin-based motor complex that is anchored to the Inner Membrane Complex (IMC) of the zoite pellicle and is essential for parasite gliding, invasion, and egress [42]. Inhibition of *Pf*CDPK1 by small molecule inhibitors or peptides simulating regions of the J domain led to defects in microneme discharge and blockage in host cell invasion [28,34] while inhibition with a full-length transgenic J domain arrested parasites in early schizogony [27].

In this study, we have shown *in vitro* inhibition of *Pf*CDPK1 by the J domain disrupting stapled peptide, JDD. JDD was designed to mimic the C-terminal region of the autoinhibitory J domain of *Pf*CDPK1. The peptide was selectively permeable to schizogenic iRBC and colocalized with dividing daughter cells in the replicating parasite. Treatment of late-stage iRBC with $\geq 5 \mu\text{M}$ JDD resulted in blockage of merozoite invasion, providing evidence that JDD peptides effectively inhibit their *Pf*CDPK1 target.

This work marks the first use of hydrocarbon stapled peptides designed to target an essential *Plasmodium* protein. Our results are consistent with previous CDPK1 literature and

indicate that JDD effectively inhibits parasite growth via a CDPK1-mediated blockage in merozoite invasion. In addition, the concentration of JDD peptides necessary to achieve this inhibition was significantly reduced relative to previous studies, which required as high as 120 μ M treatment with C-terminal partial peptides to achieve ~42% inhibition of invasion [28]. This enhanced efficacy is likely due to both the increased cellular permeability afforded by the hydrocarbon staple as well as the more specific binding interaction of the helical peptide relative to a disordered partial peptide. Future studies in our lab will seek to further increase JDD efficacy *in vitro* by exploring inhibition by different regions of the *Pf*CDPK1 J domain. In addition, since the *Plasmodium* J domain is conserved between species, we will examine the activity of JDD against *P. berghei* *in vivo*.

This is the second example of a chemically stabilized peptide with sufficient permeability to access intracellular *Plasmodium* parasites. Ongoing work in our lab is examining the mechanism of iRBC uptake of stapled peptides like STAD-2 and JDD in order to further develop these compounds as promising antimalarial agents. Although broad use of peptide therapeutics has generally been limited by poor bioavailability, addition of the hydrocarbon staple confers strong protease resistance and enhanced oral availability of stapled peptide therapeutics [43]. Such evidence provides further support for this rising class of peptide therapeutics as promising future antimalarials.

Conclusions

This study is the first to utilize hydrocarbon stapled peptides designed to specifically target proteins unique to *P. falciparum*. JDD peptides were designed to mimic the *Pf*CDPK1 autoinhibitory J domain. JDD was selectively permeable to late schizonts. Analysis by fluorescence microscopy demonstrated JDD colocalization with dividing daughter cells in these late, dividing parasites. At $\geq 5 \mu\text{M}$ concentration, JDD significantly reduced parasite viability via blockage of erythrocyte invasion. Given CDPK1's established role in microneme secretion, parasite motility, and host cell invasion, our results demonstrate successful inhibition of *Pf*CDPK1 by JDD stapled peptides. This work both provides support for the use of stapled peptides as antimalarial agents and validates CDPK1 as a target for antimalarial drug development.

References

1. Guerra C a., Gikandi PW, Tatem AJ, Noor AM, Smith DL, et al. (2008) The limits and intensity of *Plasmodium falciparum* transmission: Implications for malaria control and elimination worldwide. *PLoS Med* 5: 0300–0311. doi:10.1371/journal.pmed.0050038.
2. WHO (2014) World Malaria Report 2014.
3. Mnzava AP, Knox TB, Temu E a, Trett A, Fornadel C, et al. (2015) Implementation of the global plan for insecticide resistance management in malaria vectors: progress, challenges and the way forward. *Malar J* 14: 1–9. doi:10.1186/s12936-015-0693-4.
4. Packard RM (2014) The Origins of Antimalarial-Drug Resistance. *N Engl J Med* 371: 397–399. doi:10.1056/NEJMp1403340.
5. Petersen I, Eastman R, Lanzer M (2011) Drug-resistant malaria: molecular mechanisms and implications for public health. *FEBS Lett* 585: 1551–1562. doi:10.1016/j.febslet.2011.04.042.
6. Bopp SER, Manary MJ, Bright a T, Johnston GL, Dharia N V, et al. (2013) Mitotic evolution of *Plasmodium falciparum* shows a stable core genome but recombination in antigen families. *PLoS Genet* 9: e1003293. doi:10.1371/journal.pgen.1003293.
7. Eklund EH, Fidock D a (2007) Advances in understanding the genetic basis of antimalarial drug resistance. *Curr Opin Microbiol* 10: 363–370. doi:10.1016/j.mib.2007.07.007.
8. Harikishore A, Niang M, Rajan S, Preiser PR, Yoon HS (2013) Small molecule *Plasmodium* FKBP35 inhibitor as a potential antimalaria agent. *Sci Rep* 3: 2501. doi:10.1038/srep02501.
9. White NJ, Pukrittayakamee S, Phyo AP, Rueangweerayut R, Nosten F, et al. (2014) Spiroindolone KAE609 for *falciparum* and *vivax* malaria. *N Engl J Med* 371: 403–410. doi:10.1056/NEJMoA1315860.
10. Bowman JD, Merino EF, Brooks CF, Striepen B, Carlier PR, et al. (2014) Antiapicoplast and gametocytocidal screening to identify the mechanisms of action of compounds within the malaria box. *Antimicrob Agents Chemother* 58: 811–819. doi:10.1128/AAC.01500-13.
11. Srinivasan P, Yasgar A, Luci DK, Beatty WL, Hu X, et al. (2013) Disrupting malaria parasite AMA1-RON2 interaction with a small molecule prevents erythrocyte invasion. *Nat Commun* 4: 2261. doi:10.1038/ncomms3261.

12. Yeung BKS, Zou B, Rottmann M, Lakshminarayana SB, Ang SH, et al. (2010) Spirotetrahydro beta-carbolines (spiroindolones): a new class of potent and orally efficacious compounds for the treatment of malaria. *J Med Chem* 53: 5155–5164. doi:10.1021/jm100410f.
13. Vaidya AB, Vaidya AB, Mather MW, Mather MW (2000) Atovaquone resistance in malaria parasites. *Drug Resist Updat* 3: 283–287. doi:10.1054/drup.2000.0157.
14. Flaherty BR, Wang Y, Trope EC, Ho TG, Muralidharan V, et al. (2015) The Stapled AKAP Disruptor Peptide STAD-2 Displays Antimalarial Activity through a PKA-Independent Mechanism. *PLoS One* 10: e0129239. doi:10.1371/journal.pone.0129239.
15. Schafmeister CE, Po J, Verdine GL (2000) An All-Hydrocarbon Cross-Linking System for Enhancing the Helicity and Metabolic Stability of Peptides. *J Am Chem Soc* 122: 5891–5892. doi:10.1021/ja000563a.
16. Walensky LD, Bird GH (2014) Hydrocarbon-stapled peptides: principles, practice, and progress. *J Med Chem* 57: 6275–6288. doi:10.1021/jm4011675.
17. Verdine GL, Hilinski GJ (2012) All-hydrocarbon stapled peptides as Synthetic Cell-Accessible Mini-Proteins. *Drug Discov Today Technol* 9: e41–e47. doi:10.1016/j.ddtec.2012.01.004.
18. Verdine GL, Walensky LD (2007) The challenge of drugging undruggable targets in cancer: lessons learned from targeting BCL-2 family members. *Clin cancer Res* 13: 7264–7270. doi:10.1158/1078-0432.CCR-07-2184.
19. Gamo F-J, Sanz LM, Vidal J, De Cozar C, Alvarez E, et al. (2010) Thousands of chemical starting points for antimalarial lead identification. *Nature* 465: 305–310. doi:10.1038/nature09107.
20. Lucet IS, Tobin A, Drewry D, Wilks AF, Doerig C (2012) Plasmodium kinases as targets for new-generation antimalarials. *Future Med Chem* 4: 2295–2310. doi:10.4155/fmc.12.183.
21. Doerig C (2004) Protein kinases as targets for anti-parasitic chemotherapy. *Biochim Biophys Acta* 1697: 155–168. doi:10.1016/j.bbapap.2003.11.021.
22. Nagamune K, Sibley LD (2006) Comparative genomic and phylogenetic analyses of calcium ATPases and calcium-regulated proteins in the Apicomplexa. *Mol Biol Evol* 23: 1613–1627. doi:10.1093/molbev/msl026.
23. Harmon AC, Gribskov M, Harper JF (2000) CDPKs—a kinase for every Ca²⁺ signal? *Trends Plant Sci* 5: 154–159.

24. Harper JF, Harmon A (2005) Plants, symbiosis and parasites: a calcium signalling connection. *Nat Rev Mol Cell Biol* 6: 555–566. doi:10.1038/nrm1679.
25. Schulz P, Herde M, Romeis T (2013) Calcium-Dependent Protein Kinases: Hubs in Plant Stress Signaling and Development. *Plant Physiol* 163: 523–530. doi:10.1104/pp.113.222539.
26. Morlon-Guyot J, Berry L, Chen CT, Gubbels MJ, Lebrun M, et al. (2014) The *Toxoplasma gondii* calcium-dependent protein kinase 7 is involved in early steps of parasite division and is crucial for parasite survival. *Cell Microbiol* 16: 95–114. doi:10.1111/cmi.12186.
27. Azevedo, Mauro F., Sanders, Paul R., Krejany, Efrosinia, Nie, Catherine Q., Fu, Ping, Bach, Leon A., Wunderlich, Gerhard, Crabb, Brendan S., Gilson PR (2013) Inhibition of *Plasmodium falciparum* CDPK1 by conditional expression of its J-domain demonstrates a key role in schizont development. *Biochem J*.
28. Bansal A, Singh S, More KR, Hans D, Nangalia K, et al. (2013) Characterization of *Plasmodium falciparum* calcium-dependent protein kinase 1 (PfCDPK1) and its role in microneme secretion during erythrocyte invasion. *J Biol Chem* 288: 1590–1602. doi:10.1074/jbc.M112.411934.
29. Lourido S, Shuman J, Zhang C, Shokat KM, Hui R, et al. (2010) Calcium-dependent protein kinase 1 is an essential regulator of exocytosis in *Toxoplasma*. *Nature* 465: 359–362. doi:10.1038/nature09022.
30. Ishino T, Orito Y, Chinzei Y, Yuda M (2006) A calcium-dependent protein kinase regulates *Plasmodium* ookinete access to the midgut epithelial cell. *Mol Microbiol* 59: 1175–1184. doi:10.1111/j.1365-2958.2005.05014.x.
31. Siden-Kiamos I, Ecker A, Nybäck S, Louis C, Sinden RE, et al. (2006) *Plasmodium berghei* calcium-dependent protein kinase 3 is required for ookinete gliding motility and mosquito midgut invasion. *Mol Microbiol* 60: 1355–1363. doi:10.1111/j.1365-2958.2006.05189.x.
32. Billker O, Dechamps S, Tewari R, Wenig G, Franke-Fayard B, et al. (2004) Calcium and a calcium-dependent protein kinase regulate gamete formation and mosquito transmission in a malaria parasite. *Cell* 117: 503–514. doi:10.1016/S0092-8674(04)00449-0.
33. Coppi A, Tewari R, Bishop JR, Bennett BL, Lawrence R, et al. (2007) Heparan Sulfate Proteoglycans Provide a Signal to *Plasmodium* Sporozoites to Stop Migrating and Productively Invade Host Cells. *Cell Host Microbe* 2: 316–327. doi:10.1016/j.chom.2007.10.002.

34. Green JL, Rees-Channer RR, Howell SA, Martin SR, Knuepfer E, et al. (2008) The motor complex of *Plasmodium falciparum*: phosphorylation by a calcium-dependent protein kinase. *J Biol Chem* 283: 30980–30989. doi:10.1074/jbc.M803129200.
35. Wang Y, Ho TG, Bertinetti D, Neddermann M, Franz E, et al. (2014) Isoform-Selective Disruption of AKAP-Localized PKA Using Hydrocarbon Stapled Peptides. *ACS Chem Biol* 9: 635–642. doi:10.1021/cb500329z.
36. Lisk G, Desai S a (2005) The plasmodial surface anion channel is functionally conserved in divergent malaria parasites. *Eukaryot Cell* 4: 2153–2159. doi:10.1128/EC.4.12.2153-2159.2005.
37. Desai S (2014) Why do malaria parasites increase host erythrocyte permeability? *Trends Parasitol* 30: 151–159. doi:10.1016/j.pt.2014.01.003.
38. Zhao Y, Kappes B, Franklin RM (1993) Gene structure and expression of an unusual protein kinase from *Plasmodium falciparum* homologous at its carboxyl terminus with the EF hand calcium-binding proteins. *J Biol Chem* 268: 4347–4354.
39. Kato N, Sakata T, Breton G, Le Roch KG, Nagle A, et al. (2008) Gene expression signatures and small-molecule compounds link a protein kinase to *Plasmodium falciparum* motility. *Nat Chem Biol* 4: 347–356. doi:10.1038/nchembio.87.
40. Sebastian S, Brochet M, Collins MO, Schwach F, Jones ML, et al. (2012) A *Plasmodium* calcium-dependent protein kinase controls zygote development and transmission by translationally activating repressed mRNAs. *Cell Host Microbe* 12: 9–19. doi:10.1016/j.chom.2012.05.014.
41. Thomas DC, Ahmed A, Gilberger TW, Sharma P (2012) Regulation of *Plasmodium falciparum* glideosome associated protein 45 (PfGAP45) phosphorylation. *PLoS One* 7: e35855. doi:10.1371/journal.pone.0035855.
42. Frénal K, Polonais V, Marq JB, Stratmann R, Limenitakis J, et al. (2010) Functional dissection of the apicomplexan glideosome molecular architecture. *Cell Host Microbe* 8: 343–357. doi:10.1016/j.chom.2010.09.002.
43. Bird GH, Irimia A, Ofek G, Kwong PD, Wilson I a, et al. (2014) Stapled HIV-1 peptides recapitulate antigenic structures and engage broadly neutralizing antibodies. *Nat Struct Mol Biol* 21: 1058–1067. doi:10.1038/nsmb.2922.

Figures

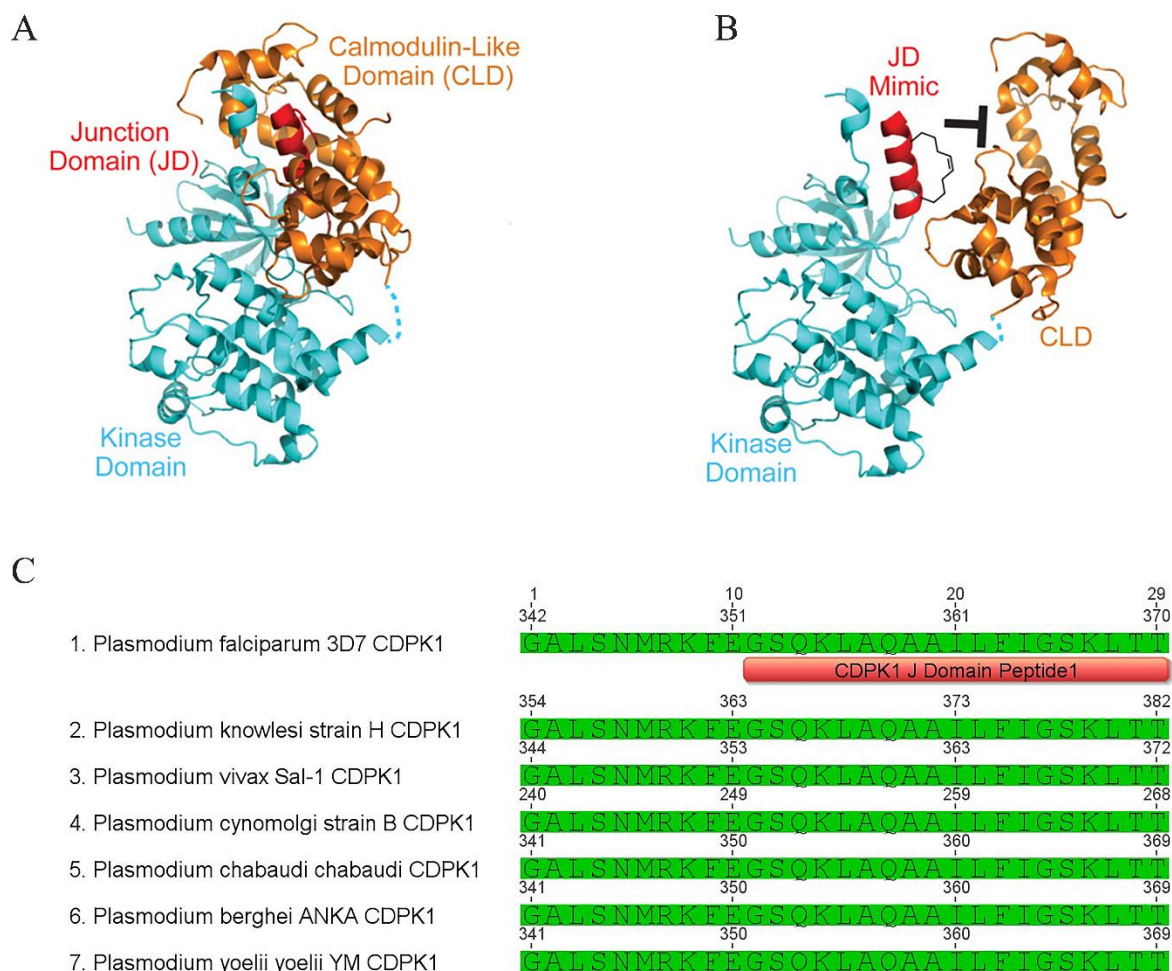


Figure 5.1. JDD synthesis and function. (A) A model of *Pf*CDPK1 demonstrates binding of the autoinhibitory J domain between the Calmodulin-like Domain (CLD) and the Kinase Domain of CDPK1. (B) JDD was designed to mimic the autoinhibitory J domain of native *Pf*CDPK1 and lock the enzyme in its inactive state. (C) Multiple sequence alignment of the J domain region from several *Plasmodium* species demonstrates high conservation of the J domain between species.

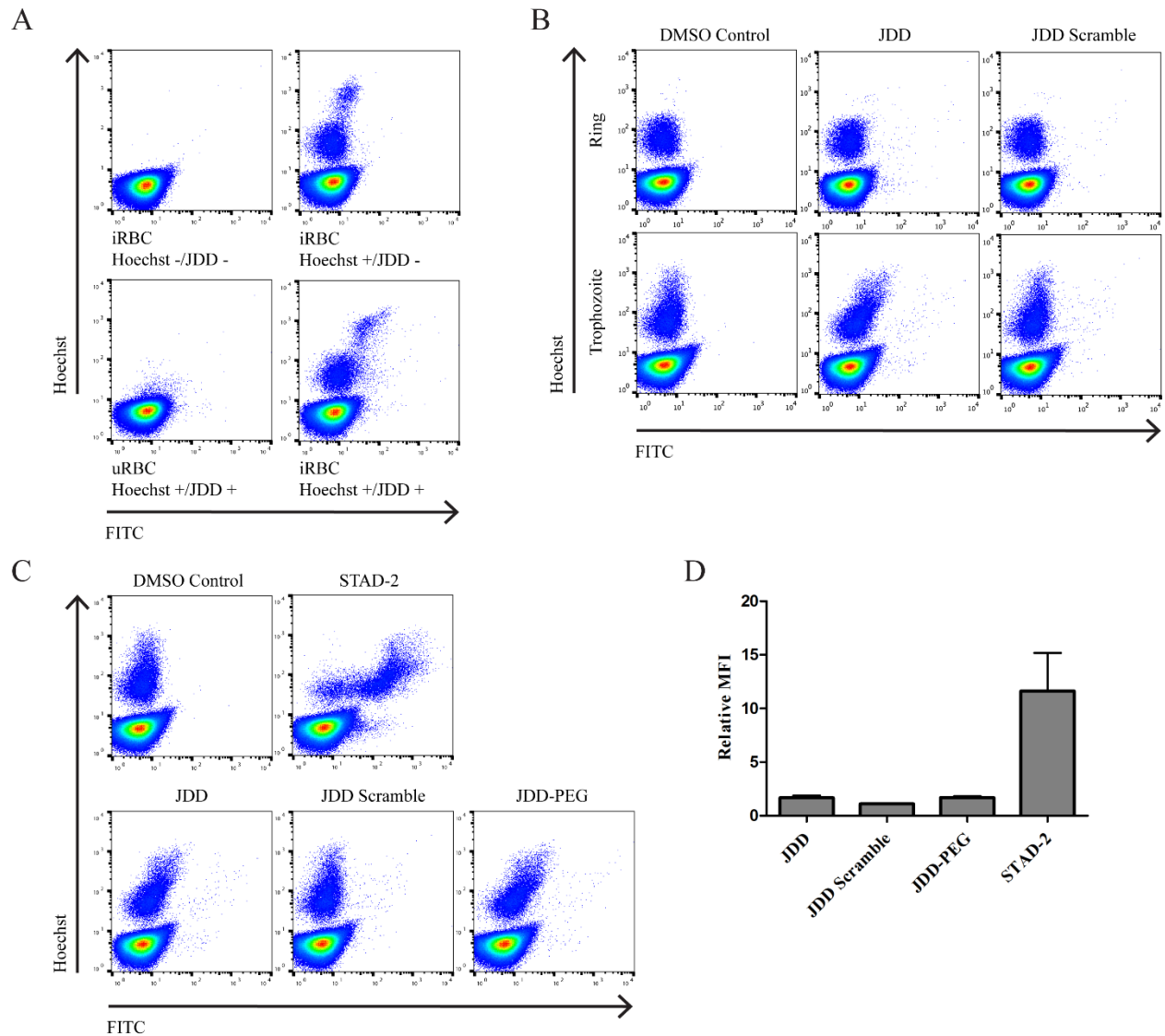


Figure 5.2. JDD is selectively permeable to schizonts. (A) iRBC were treated for 6 hours with 1 μ M FITC-conjugated JDD, stained with 2 μ g/mL Hoechst 33342 DNA stain, and analyzed by flow cytometry. JDD demonstrated selective permeability to late, schizogenic parasites, as evidenced by high Hoechst staining in the FITC-positive population. JDD uptake was negligible in early parasites and uRBC. (B) Treatment of synchronous ring-stage or late-stage (trophozoite) cultures with 1 μ M FITC-conjugated JDD or JDD scramble demonstrated increased uptake of JDD by late, replicating schizonts relative to ring-stage or early trophozoite iRBC. Neither ring- nor late-stage iRBC were permeable to the JDD scramble control. (C, D) Treatment of late-stage

iRBC with STAD-2, JDD, JDD scramble, or PEGylated JDD (JDD-PEG) demonstrated a modest, but insignificant, increase in uptake of JDD and JDD-PEG relative to the JDD scramble control. Permeability of all JDD peptides was considerably reduced when compared to iRBC uptake of STAD-2 (median fluorescence intensity relative to DMSO control, $n=6$, mean \pm S.E., 1way ANOVA followed by Dunn's Multiple Comparison Test).

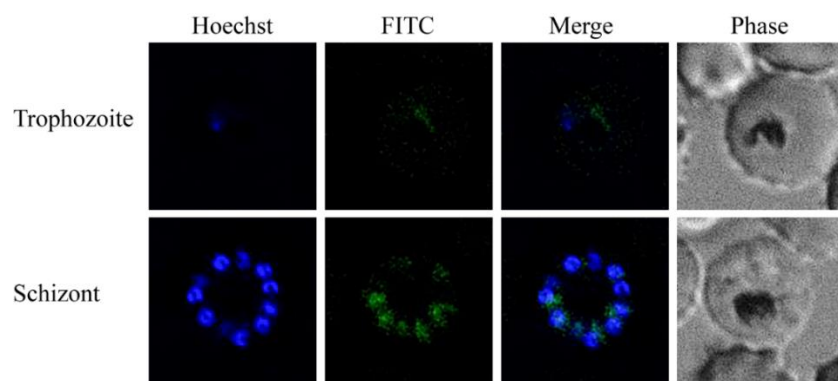


Figure 5.3. JDD colocalizes with late, segmented schizonts. Synchronous late-stage CS2 iRBC were treated with 1 μ M FITC-conjugated JDD for 6 hours, stained with 2 μ g/mL Hoechst 33342, and analyzed by fluorescence microscopy. JDD demonstrated no colocalization with ring-stage parasites; weak colocalization with later, pre-schizogenic parasites (trophozoite); and strong colocalization with segmented schizonts.

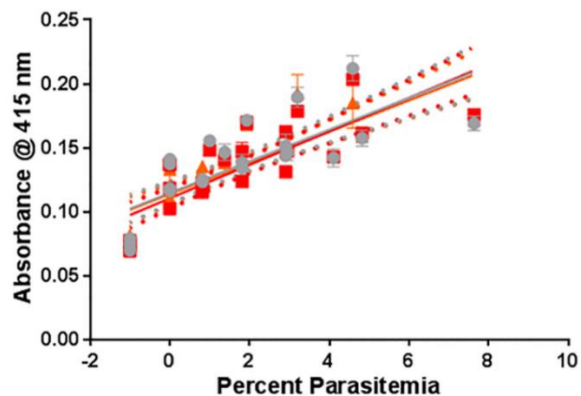
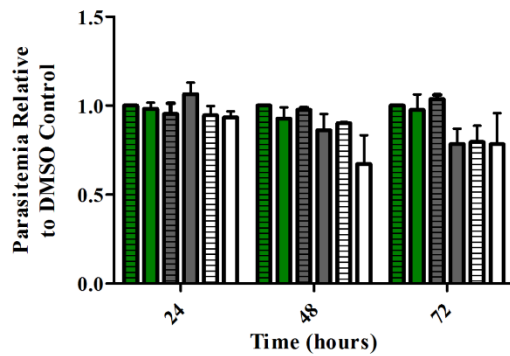


Figure 5.4. JDD is not hemolytic. Synchronous late-stage iRBC of increasing parasitemia were treated with 1 μ M JDD (red), 1 μ M JDD Scramble (orange), or vehicle control (grey) for 6 hours. Culture medium from each well was analyzed for evidence of RBC lysis by measuring oxyhemoglobin absorbance (A_{415}) by UV-Vis spectroscopy. Linear regression demonstrates no significant difference in cell lysis between treatment conditions (n=4, mean \pm S.E.).

A



B

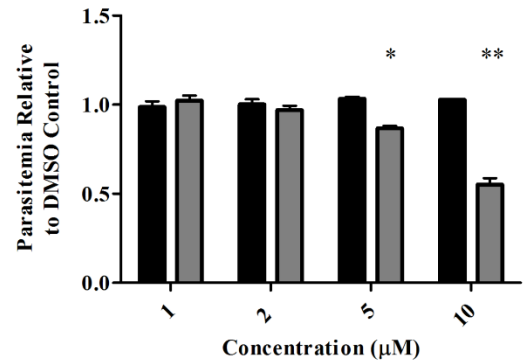


Figure 5.5. JDD displays antimalarial activity. (A) Synchronous ring-stage iRBC were treated with 1 μ M JDD once at assay initiation (green bars), every 24 hours (grey bars), or every 12 hours (white bars). Parasitemia was determined by flow cytometry at 24, 48 and 72 hours post-assay initiation. DMSO controls (striped bars) were included for reference. (B) Synchronous late-stage iRBC were treated with 1, 2, 5, or 10 μ M JDD (grey bars) or JDD scramble (black bars), and parasitemia was determined by flow cytometry at 24 hours post-treatment. Treatment with ≥ 5 μ M JDD caused a significant drop in parasite viability (2way ANOVA with Bonferroni posttests, * p < 0.01, ** p < 0.001, n=2-5, mean \pm S.E.).